Smart Material Design, Inc.
980 Half Day Road
Highland Part, IL 60035

Quantitative Nondestructive Evaluation and Reliability Assessment of the Aging Aircraft Structure Components

Final report developed under STTR contract
F49620-99-C-0038
Dates covered: 08/01/99 – 01/31/2000

Prepared by :

Alexander Sutin

Chicago, IL
April 2000

AFRL-SR-BL-TR-00-

0188

REPORT DOCUMENTATION PAGE

1. AGENCY USE ONLY (Leave blank)	2. REPORT DATE	3. REPORT TYPE AND DATES COVERED
	April 30, 2000	Final 08/01/99 – 01/31/2000

4. TITLE AND SUBTITLE
Quantitative Nondestructive Evaluation and Reliability Assessment of the Aging Aircraft Structure Components

5. FUNDING NUMBERS
F49620-99-C-0038

6. AUTHOR(S)
Alexander Sutin, Principal Investigator

7. PERFORMING ORGANIZATION NAME(S) AND ADDRESS(ES)

Smart Material Design, Inc.
980 Half Day Road
Highland Part, IL 60035

Department of Civil and Materials Engineering, University Illinois at Chicago,
842 West Taylor St.,
Chicago, Illinois 606607-7023

8. PERFORMING ORGANIZATION REPORT NUMBER

9. SPONSORING / MONITORING AGENCY NAME(S) AND ADDRESS(ES)

USAF, AFMC
Air Force Office of Scientific Research
801 North Randolph St., room 732
Arlington VA 22203-1977

10. SPONSORING / MONITORING AGENCY REPORT NUMBER

11. SUPPLEMENTARY NOTES

12a. DISTRIBUTION / AVAILABILITY STATEMENT
Approved for public release; distribution is unlimited

12b. DISTRIBUTION CODE

13. ABSTRACT ***(Maximum 200 Words)***

The report developed under STTR contract presents the results of work performed on development of a new probabilistic model for reliability assessment of the aging aircraft structural components and nonlinear acoustic instrumentation for collecting the input data for reliability model. The reliability of aging components is estimated on the basis of crack propagator concept CP (probability of crack extension from one position to the next during specified time interval). Monte Carlo Simulation is employed for numerical realization. Parameters of CP can be evaluated and experimentally verified by nonlinear acoustic technique and instrumentation. This instrumentation uses the interaction of ultrasonic waves with vibration (Nonlinear Elastic Wave Spectroscopy – NEWS). High sensitivity of nonlinear acoustic technique for crack detection and location was demonstrated for different class of materials: polycarbonate, steel, aluminum, adhesive bonded aluminum plates. This technique allows to estimate crack size and location that are the input parameters for the reliability model. Draft design of the instrumentation has been also developed.

Phase II will pursuer advanced development of reliability model. The stationary and in-field usage nonlinear instrumentation prototypes and software will be developed for lifetime and quantitative reliability assessment of the aging structure components

14. SUBJECT TERMS
STTR Report, Reliability Assessment, Aging Aircraft,
Nonlinear Elastic Wave Spectroscopy, Probabilistic Crack Model.

15. NUMBER OF PAGES
100

16. PRICE CODE

17. SECURITY CLASSIFICATION OF REPORT	18. SECURITY CLASSIFICATION OF THIS PAGE	19. SECURITY CLASSIFICATION OF ABSTRACT	20. LIMITATION OF ABSTRACT
Unclassified	Unclassified	Unclassified	Unlimited

Table of Contents

1. Introduction

Non-destructive evaluation of remaining life and reliability of structure components in case of aging, cyclic damage and cumulative damage is critical to the assessment of reliability of the entire aging aircraft. Reliability of aging components can be estimated with the help of probabilistic model developed on the basis of crack propagator concept CP (probability of crack formation between any two point) and Monte Carlo Simulation. Parameters of CP can be evaluated and experimentally verified with the high level of precision by nonlinear acoustic technique and instrumentation. This instrumentation uses the interaction of ultrasonic waves with vibration (Nonlinear Elastic Wave Spectroscopy – NEWS) to collect data for reliability assessment based on probabilistic model of crack. In Phase I principals of nonlinear acoustic approach were demonstrated and draft design of the instrumentation was developed.

The overall objective of the Phase I proposal was to develop nonlinear acoustic instrumentation for estimations of the crack parameters and to use date, received by with this instrumentation, in a new probabilistic fracture model for the aging aircraft structural component. The specific objectives of the program were formulated as follows:

1. Propose fracture mechanism model for the materials or part in question.
2. Develop nonlinear acoustic instrumentation for the control of initiation phase of fatigue damage. Determination of correlation between nonlinear acoustic response and crack parameters.
3. Develop the theoretical model describing the modulation of acoustical signal by vibration due to crack and relationship between the level of modulation and the crack parameters.
4. Investigate the application of the "crack propagator" approach for estimation of remain time life of aircraft structural component.
5. Verify the proposed probabilistic fracture mechanics model for the material or parts in questions.

The brief results of phase I project can be formulated as followed:

1.1. Probabilistic approach to reliability assessment of aging aircraft structural component in question

The probabilistic approach to reliability assessment of aging aircraft structural component in question have been developed. The concept of Crack Propagator has been extended into the time domain by incorporating the Crack Layer kinetic theory into a probabilistic framework of Statistical Fracture Mechanics. This model allows to provide numerical simulation of Crack Layer growth from an initial small defect to the ultimate failure. Such stimulation provides functional relation between the time to failure and the initial defect size for different applied load and structural element considered. The suggested model is used for calculation of conditional reliability function that provides useful information in evaluation the life expectance of structural component with required level

of reliability. Calculations of the lifetime expectance as a function of normalized applied stress have been conducted.

1.2. Development of the Nonlinear Elastic Wave Spectroscopy (NEWS) instrumentation

The experimental setup to observe nonlinear acoustic interaction between ultrasound and vibration was mounted. The instrumentation provides the excitation of high-frequency ultrasonic wave and the low-frequency vibration in the material under investigation, and measurement of the interaction product -- modulation of sound by vibration. This modulation manifests itself as a sideband component in the spectrum of the received ultrasound signal. The instrumentation consists of:

1. The low-frequency excitation part is an instrumental hammer with attached piezoelectric sensor for triggering of recording signal. The several instrumentals hammers for various condition of vibration excitation were build and tested.
2. The high-frequency ultrasound part includes high frequency generator, power and piezoelectric sensors attached to the investigated part.
3. The registration part consist of piezoelectric sensor to transfer acoustical signal to electrical signal and LeCroy digital oscilloscope. The primary processing was conducted by oscilloscope. The signal was also transferred to computer for secondary processing.

1.3. Software for NEWS signal processing

The software for signal processing has been developed. The software is written using MatLab and allows to conduct the following operation with the received signals:

a. Spectral analysis
b. Averaging of the signal due to impact variation.
c. Calculation of suggested criteria of modulation such as the Nonlinear Index (NI). The modulation criteria in the frequency domain is calculated by summation, normalization and averaging of the modulation spectra for the certain range of ultrasonic frequencies.

1.4. NEWS testing of different materials

The preliminary testing was conducted for different kinds of materials used in airspace industry. The following materials were investigated:

a. Polycarbonate plates

Several polycarbonate plates used in F16 canopy were tested. The crack growing was initiated under cyclic loading .The large difference in the modulation signals was observed for samples with small cracks in comparison with samples without cracks. The dependence of the nonlinear index on the crack size was also observed and investigated.

b. Aluminum strain hardening components

The aluminum strain hardening components (47x45x5 $mm^{3)}$ were tested by NEWS. The modulations were observed in samples with different crack lengths. The nonlinear acoustic signatures for different samples having different crack size were obtained.

c. Adhesive bounded aluminum plates

The nonlinear acoustic technique was applied to aluminum bounded plates supplied by Boeing. The samples were heat treated to produce some kind of damage and reduce the strength of bonded joints. The experiments had shown higher level of modulation for the samples having the low level of strength compare to normal samples that were not acted by treatment.

d. High pressure pipelines

NEWS was applied to thin high pressure pipelines used in different control systems. The damage was caused by multiple tube bending. NEWS registered appearance of nonlinearity (accumulated damage) in spite of no visible crack was observed.

1.5. Theoretical model describing the modulation of ultrasound by vibration due to cracks

The two theoretical model describing nonlinear acoustic effects produced by a single crack as well as a cluster of microcracks have been developed.

a. A single crack model considers a crack as a domain of contact between two rough surfaces. The applied vibration varies surface contact area within the domain due to deformation of asperities in contact, leading to a nonlinear elastic response. The suggested acoustical crack model takes into account the resonance properties of the investigated specimens, crack size and crack position. The expression for the level of side components in a spectra of the simple geometry specimen has been obtained. The theoretical model predicts the amplitude and frequency dependencies of the side components on the amplitude levels of the applied signals and on frequencies of excitation. The linear dependence of side component on the level of low frequency vibration was determined. This dependence allows to use a certain modulation criterion that is independent on the level of excitation, i.e., Nonlinearity Index. This method is especially impotent for impact produced vibration since it is almost impossible to provide the constant parameters of every impact. The predicted dependencies of side components on the frequency of ultrasonic waves demonstrate the necessity for frequency averaging of the side components. The program calculated NEWS output data for parts having simple geometry have been developed and the model calculations have been conducted. They demonstrated the dependencies of the side band components on interaction frequencies and crack position.

b. Model of multicrack cluster. This model considers the variation of the nonlinear acoustic parameters in the material with microcracks. The suggested approach is based on Prof. Chudnovsky's work, on the foundations of Statistics of Fracture Statistic. The developed theory connects the nonlinear signature of the material with the crack distribution characteristics . This information will serve as a basis for detection of the distributed damage.

1.6. Crack location by NEWS.

NEWS pulse location method is based on the radiation and reception of ultrasonic pulses. The difference from common ultrasonic pulses scanning method is an application of the low frequency vibration to the tested component. This vibration produces the modulation of the signal reflected from cracks. Experimental verification of the method has been done on steel plates having different kinds of defects (a hole, an open crack, a close crack). The high frequency impulse had a frequency more higher than 1MHz, and the modulating vibration frequency was about 10 Hz. It was demonstrated that this method can distinguish a crack on the background of strong reflection from other inhomogeneities (open holes and holes with bolts).

1.7. Mechanical Design of the Instrumentation

Different design options of the instrumentation were considered. Kinematics analysis was performed and parameters of the instrumental hammer were defined. Production drawings of the instrumentation are under consideration. The design and manufacture of the instrumentation will be completed in Phase II of this project.

2. Probabilistic approach to reliability assessment of aging aircraft structural component in question

2.1. Fundamentals of probabilistic approach.

The primary objective of our efforts is the development of a computerized system for remaining life and reliability assessment **of the aircraft structural components** on the basis of a new probabilistic approach combined with nonlinear acoustic characterization of the current state.

The aircraft aging phenomena usually consists of three stages:

1. Submicro- and microdefect accumulation (incubation) leading to crack inaction.

2. Slow crack growth (fatigue, creep, stress-corrosion crack).

3. Dynamic (unstable) crack propagation leading to a catastrophic fracture.

The useful lifetime of an aircraft structure is determined by the first two stages, since the third one is very short. The formation of a set of cracks manifests the end of the first stage and the beginning of the second stage. It is our intention to utilize a nonlinear acoustic technique for determination of the beginning of the second stage and to correlate the basic parameters of the set of cracks (the distribution of crack size, number, mutual position) with nonlinear acoustic response of the structural element.

The duration of the second stage is determined by fatigue and /or corrosion crack growth rate that will be estimated on the basis of Crack Propagator (CP) concept. CP concept, recently developed within Statistical Fracture Mechanics, will be employed for evaluation of the remaining lifetime. The Crack Propagator, i.e., the probability of crack front extension from one position to another during a specified time interval, depends on the load, structural elements geometry, crack size and fracture surface roughness. Reliability of aging components will be then evaluated with the help of probabilistic model developed on the basis of crack propagator concept. To fulfill this task statistical distribution and failure rates will be experimentally determined for different environmental condition of crack propagation. Probability density function for the stress and strength variation over the time will be evaluated and reliability of aging components that accounts for strength and toughness deterioration will be estimated.

Statistical characterization of the current crack population (size, number and locations) by nonlinear acoustics NDE technique is one of the challenges of the proposed method. This technique is based on nonlinear acoustic principles and is much more sensitive to fatigue damage than the **commonly used ultrasonic NDE technique.** The foundation for the new nonlinear acoustic NDE method is the significant change in nonlinear elastic response of the structural element resulting from crack(s) initiation and growth. The

sensitivity of nonlinear elastic spectroscopy (NEWS) to the initiation and propagation of cracks is orders of magnitude higher than that of conventional NDE methods.

The nonlinear acoustic NDE results combined with the information regarding geometry and service conditions of a particular structural element will provide a sufficient input data for evaluation of remaining lifetime and reliability by Statistical Fracture Mechanics techniques.

Basic Concepts and Assumption

Several natural assumptions regarding the propagation stage of fracture process underlie the probabilistic model:

1. The crack path is randomly selected from a set of all possible (virtual) crack paths Ω (The set of experimentally observed trajectories depicted in Fig. 2.1 is a pictorial representation of a sample set of Ω). Statistical characterization of this set is based on: a) fractographic analysis of observed crack trajectories for the material or part in question, b) stress analysis and c) the nonlinear acoustic determination of the size, orientation and location of the most dangerous defect (crack).

2. Crack advance along a particular path is characterized by the Crack Layer kinetic equations, that represent a mathematical model of evolution of a system consisting of a crack and a process zone (PZ), formed in front of the crack tip.

3. Crack advance consists of a sequence of elementary steps, controlled by Grifith criterion $G_1 \geq 2\,\gamma$, where G_1 stands for the energy release rate (ERR) due to crack extension into the PZ, and $\gamma = \gamma(t)$ is the specific fracture energy, that decreases with time, reflecting material degradation within the process zone.

One of the main building blocks of the formalism is the crack propagator. Let us consider a component under a load containing a crack ω_0 with its tip as x (Fig.2.2). First we define a conditional propagator, $P(x,t;X,T \,/\, \omega)$, as the probability that the crack tip advances from position x at the time t through position X at the time $T > t$ along the path ω , i.e. the condition $G_1 \geq 2\,\gamma(t)$ is met at every point of the crack trajectory ω.

If one assumes that the crack trajectories are mutually exclusive (only one trajectory is observed in every individual specimen, then the probability , $P(x,t;X,T)$ of crack extension from x through X during the time interval $T - t$ can be written as total probability.

$$P(x,t;X,T) = \sum P(x,t;X,T / \omega_\kappa)\, P(\omega_k)$$

Here $P(\omega_k)$ stands for the probability that the crack "chooses" a path ω_κ among all virtual paths extended from x to X. $P(x,t;X,T)$ is called the crack propagator (CP). In other

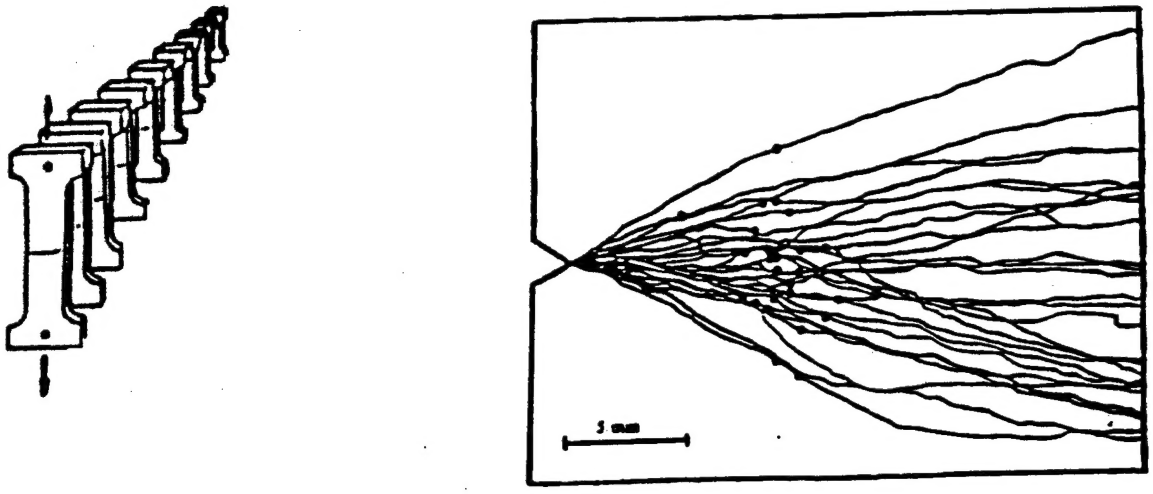

Fig. 2.1. The ensemble of 27 macroscopically identical SEEN specimens (fatigue to failure under identical condition). Dots indicate the points of transition to unstable propagation (critical points)

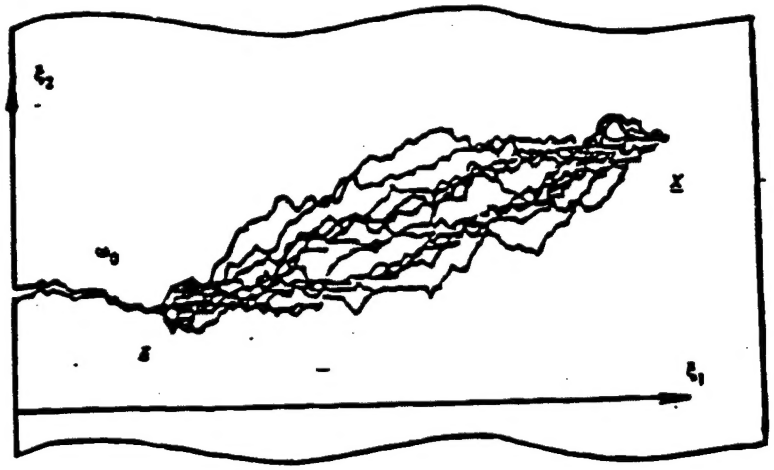

Fig.2.2. A sample set of virtual paths leading from point x to point X

words, CP is the average over all virtual trajectories of the conditional probability of crack formation between the points x and X along a particular trajectory ω_κ during the time interval $T-t$.

Once the CP has been evaluated for a particular aircraft structural component, the probabilities of crack propagation to the certain depth, crack arrest, distribution of critical load, toughness parameter, time to failure, and reliability function can be readily computed.

Evaluation of the CP results from three major tasks:

1. Selection of a set of virtual crack trajectories Ω possessing a prescribed roughness characterized by crack diffusion coefficient and the fractal dimension of crack trajectories.

2. Determination of the conditional propagator $P(x,t;X,T / \omega_\kappa)$

3. Computation of the average $P(x,t;X,T / \omega_\kappa)$ over Ω by means of a functional integration.

Monte-Carlo stimulation

A numerical approach, most convenient for development of a software for reliability analysis, is Monte-Carlo technique [9]. It allows one to combine the physical insight and understanding of the Statistical Fracture Mechanisms with the flexibility of Monte-Carlo method. In particular, it allows one to perform parametric studies, necessary for calibration of the proposed method.

Following the spirit of Monte-Carlo technique, the functional integration, i.e. the averaging over the set of virtual crack trajectories Ω is substituted by a computer stimulation of a large number of virtual crack paths followed by an estimation of the frequencies of various fracture events among the set of trajectories Ω. The approach was successfully applied to the modeling of fracture test in various materials, including different composites [10-14].

The tasks discusses in the previous section can be reformulated for the Monte-Carlo method as follows:

1. Computer simulation of the fracture paths with a prescribed roughness, i.e., the crack diffusion coefficient and fractal dimension.

2. Numerical solution of Crack Layer kinetic equations along the simulated trajectories ω_κ . The output characteristics for each trajectory ω_κ from the set of $\{\omega_\kappa\}$ are: the probability distribution of the depth of crack penetration during time interval $T-t$; the critical crack length; the time $t^*(\omega_\kappa)$ of crack instability, i.e., the conditional time of ultimate failure along the particular crack trajectory ω_κ,

conditional reliability $R(t / \omega_\kappa)$, i.e., the probability of "no failure" along the particular crack trajectory ω_κ prior the time t; etc.

3. Statistical averaging of the output characteristics. Specifically, the reliability function $R(t)$ of structural component in question is defined as the conditional reliability $R(t / \omega_\kappa)$ averaged over Ω :

$$R(t) = < R(t / \omega_\kappa) >_\Omega$$

for the Here the angle brackets $<\ldots>_\Omega$ stand for the procedure of statistical averaging over Ω.

Some illustrative examples of the proposed probabilistic model are given in details in [1,8,33] and will serve as the basis for the reliability assessment particular structural elements under specified loading and environmental conditions.

2.2. The development of probabilistic approach for reliability assessment.

Kinetics of Fracture Propagation.

The concept of Crack Propagator discussed in Phase I proposal has been extended into the time domain by incorporating the Crack Layer kinetic theory into a probabilistic framework of Statistical Fracture Mechanics. The fundamentals of Crack Layer theory and it implementation in probabilistic setting are briefly presented below.

The crack and the process (damage) zone (PZ), commonly observed in front of the crack tip, are together considered as a system called the Crack Layer (CL) [7-14, 33]. Since the size of PZ in most of engineering materials is much smaller than the crack size, the CL can be characterized by two parameters, i.e., the crack and PZ sizes, l and L (Fig.2.3). Following the basic principle of Thermodynamics of Irreversible Processes, the driving forces of the crack and PZ growth are determined as derivative of Gibbs potential G with respect to the crack and CL size l and L respectively:

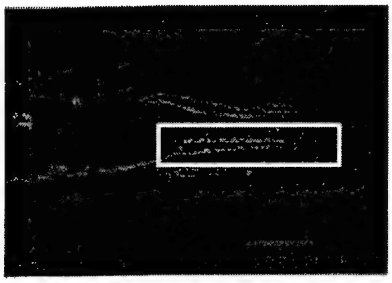

Crack and process zone in PE

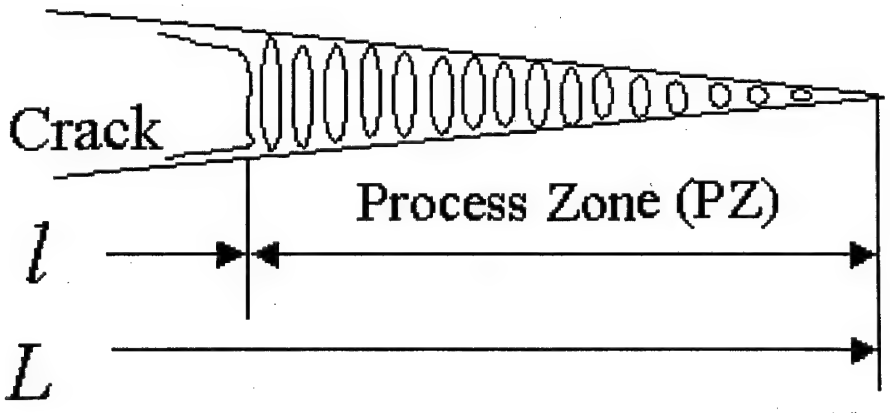

Figure 2.3. Illustration and schematics of the Crack Layer

$$X_{CR} = -\frac{\partial G}{\partial l}, \quad X_{PZ} = -\frac{\partial G}{\partial L}$$

The driving forces depend on properties of the original and damaged (within PZ) materials, and account for the energy absorbed within the PZ during its formation, as well as on specimen geometry and loading conditions. The kinetics of CL propagation is governed by the following equations:

$$d/dt\,l = k_1 X_{CR}, \quad d/dt\,L = k_2 X_{PZ} \tag{2.1}$$

with the initial conditions

$$l = l_0 \text{ and } L = L_0 \text{ at the time of inspection } t = t_0$$

An equilibrium size of the PZ, L_{eq}, is determined by $X_{PZ} = 0$.

The material within the PZ degrades with time leading to a decrease of specific fracture energy γ in Grifith condition, i.e., $\gamma = \gamma_0 f(t)$, where γ_0 is the specific fracture energy at the time t_0, and f(t) is a decreasing function of time, that reflects particular mechanisms of material degradation such as mechanical fatigue, electro-chemical corrosion or thermal fluctuations, to name a few. Kinetic equations (1) together with the PZ material degradation law form a strongly nonlinear system of equations. The numerical solution of this system (the fourth order Runge-Kutta method) reveals two basic scenarios of CL behavior shown in Figs.2.4. The CL grows continuously (Fig. 6a), when during the thermodynamic forces X_l, and X_L are positive during the entire process. The discontinuity of the CL growth (Fig. 6b) appears when the crack driving force $X_l < 0$, so that the crack is arrested. Crack reinitiation then takes certain time during which $2\gamma(\tau)$ decreases to the level of G_1. Than the crack starts to propagate through PZ until it reaches an undegraded material, becomes arrested and stays stationary until this material degrades to the level of G_1 to allow further crack advance. Thus the next cycle begins. Therefore, a discontinuous CL growth is a sequence of CL stationary states and relatively fast transitions from one state to another.

Numerous observations of various authors suggest that the step-wise discontinuous CL growth is the dominant mode of crack propagation under both creep and fatigue loading. The average rate of discontinuous crack growth and the lifetime are mostly determined by the duration of CL stationary configurations. That, in turn, depends on how big is the gap between $2\gamma_0$ and the ERR G_1.The same time, the lifetime weakly depends on the values of kinetic coefficients k_l, and k_L that affect only the transition time from one stationary configuration to another. This time interval is found to be noticeably shorter than the CL stationary states (see Fig.2.4b).

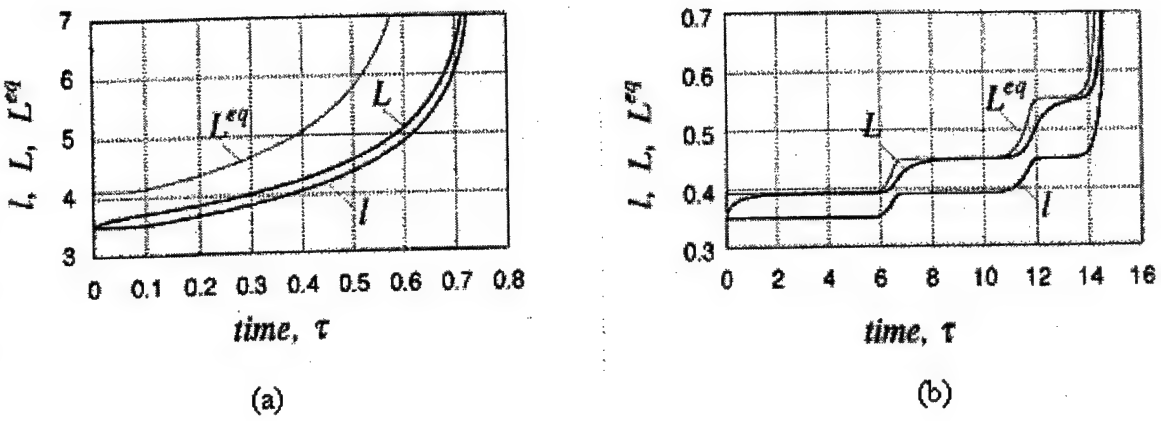

Figure 2.4. Two basic scenarios of CL growth

Reliability Function.

Let consider an acoustic interrogation of the structural component at time t_o, that results in detection of a microcrack(s). Apparently, there is an uncertainty in the size, location and orientation of the cracks. Here, for an illustrative purpose only, we assume the location and orientation of the crack are well defined and only the size is uncertain. A distribution of maximal values from the families of the distribution of extremes is the distribution of choice, since the largest microcrack is most likely to trigger the fracture process. The most general cumulative distribution function $F(l_0)$ for maximal values of initial crack size l_0 can be presented as follows [8]:

$$\left\{\begin{array}{ll} l_0 < l_0^{\min} & : F(l_0) \equiv 0 \\ l_0^{\min} \le l_0 \le l_0^{\max} & : F(l_0) \equiv \exp(-\alpha(\frac{l_0^{\max} - l_0}{l_0 - l_0^{\min}})^{\beta}) : (\alpha > 0, \beta > 0) \\ l_0^{\max} < l_0 & : F(l_0) \equiv 1 \end{array}\right\}$$

The range of possible initial crack length $[l_0^{min}, l_0^{max}]$ is determine from the acoustic data and the scale and shape parameters α and β are chosen to mach as close as possible the histogram of the experimentally measured crack size.

Numerical simulation of CL growth in single edge notch specimen from an initial crack l_o to the ultimate failure provides a simple functional relation between the time to failure t_f and the initial crack size l_o:

$$t_f(l_0) = A + B \cdot \log(l_0)$$

Here the coefficients A and B are the functions of applied load and the size of the structural element considered [27]. Thus the cumulative distribution function of time to failure along a random crack trajectory ω_κ, $F(t_f / \omega_\kappa)$, results from strait forward calculations of the single valued function $t(l_o)$ of the random variable l_o. Therefore the conditional reliability function $R(t / \omega_\kappa)$ is also determine, since

$$R(t / \omega_\kappa) = 1 - F(t_f / \omega_\kappa) .$$

Finally, after averaging over the set of virtual trajectories Ω illustrated on Fig.2.1, one finds the reliability function $R(t) = < R(t / \omega_\kappa) > \Omega$ for various level of applied stresses depicted on Fig. 2.5. The calculations have been performed for transparence grade Polycarbonate under mechanical stress only (aging, temperature variation or chemical aggression have not been considered). However, the outlined method allows to account for material aging, chemical aggression etc. as soon as the kinetic equations for the corresponding processes are reported.

The reliability function thus determined provides also useful information in evaluation the life expectance of structural component with required level of reliability. This suggestion is illustrated in Figure 2.6 that shows the lifetime expectance as a function of normalized applied stress. It shows, for example, the lifetime at 0.1 normalized stress is reduced from about 20 years to 12 years, i.e., by 40% when the required reliability increases from 0.8 to 0.999.

The algorithms of these types of computations have been validated on various examples.

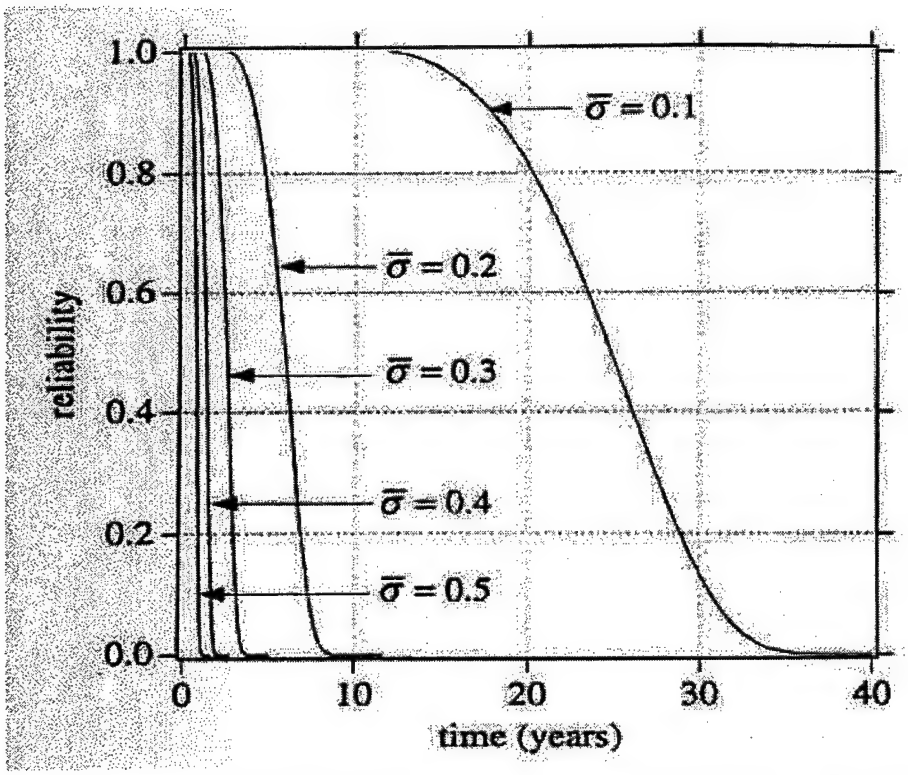

Figure 2.5. The reliability function for various level of normalized applied stress σ/σ_ψ

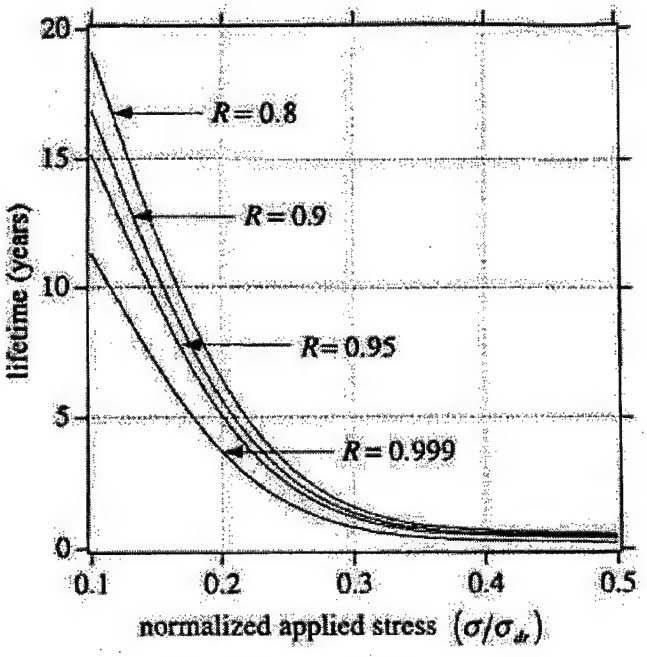

Figure 2.6. The lifetime dependence on the normalized stress and required reliability R value.

3. Nonlinear Acoustic Technique Principles

There are several nonlinear effects that are used for Nonlinear Elastic Wave Modulation Spectroscopy (NEWS), i.e. second harmonic generation, modulation of sound by vibration, amplitude-dependent internal friction and resonance frequency shift with amplitude.

Historically, the first applications of the nonlinear technique were performed using the second harmonic method. This method involves measurement of the second harmonic generated by the nonlinear distortion of a sinusoidal acoustic signal due to defects. The first test of this method in the United States was made as early as in 1979 when the second harmonics of high frequency ultrasonic waves propagating through contact was observed by Buck et al. [2] and Richardson et al. [3]. Another modification of the second harmonic method was developed for the quality control of the attachment of thermal protecting tiles for the Soviet spaceship "Buran", Sutin et al. [4]. One more example of the application of the second harmonic method is the detection of cracks in large (over 3 meter long, 0.65 x 0.45 m^2 cross-section) graphite electrodes used in aluminum production line, Sutin et al. [5].

The team from Los Alamos National Laboratory has developed NDE method based on the measurements of the resonance frequency shifts and damping characteristics as a function of the resonance peak acceleration amplitude [15,16]. This method is called *nonlinear resonant ultrasound spectroscopy* (NRUS) and its application is illustrated in Figure 3.1.

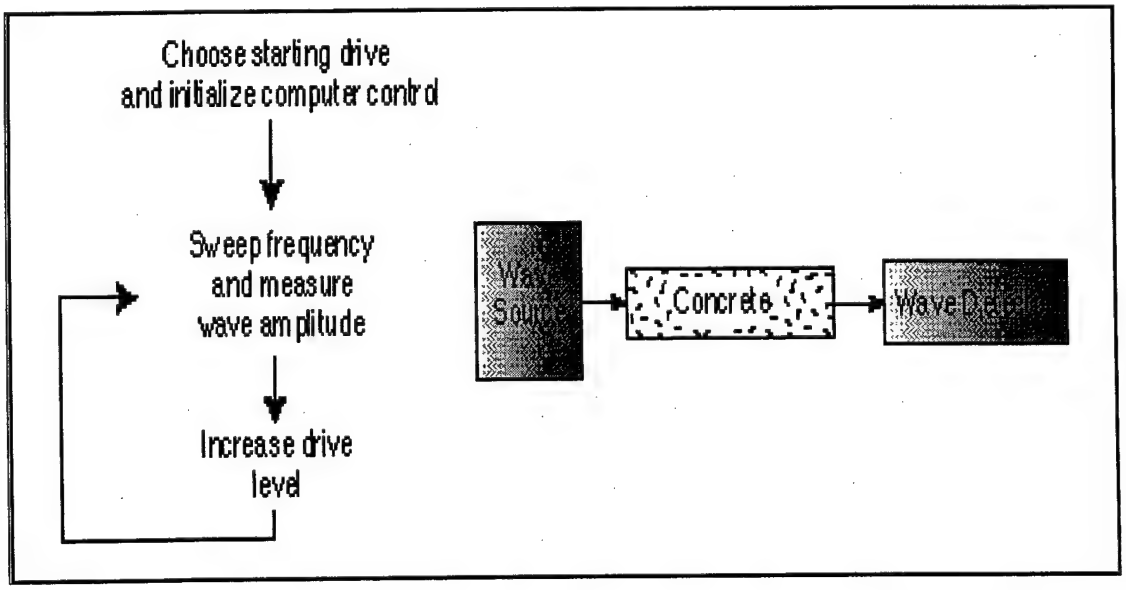

Figure 3.1. Experimental procedure for *nonlinear resonant ultrasound spectroscopy.*

A rod of concrete or other material is resonated at a fixed input wave volume from frequency a to frequency b. The resonance mode lies between frequencies a and b. The input wave volume is increased and the frequency is swept from a to b again, etc. A non-contact laser or contact accelerometer is used to detect the wave. As an example, an experiment was conducted with the help of nonlinear resonance ultrasound spectroscopy on two concrete samples, one undamaged and one damaged by the alkali-silica gel reaction (ASR). The resonance curves show a significant change in resonant frequency as drive level is increased. This is due to the material nonlinearity. Other nonlinear effects including harmonics and nonlinear wave dissipation are also produced (not illustrated). Suffice it to say that the we can use the frequency shift to characterize the damage in the material using the "signature" shown in the figure.

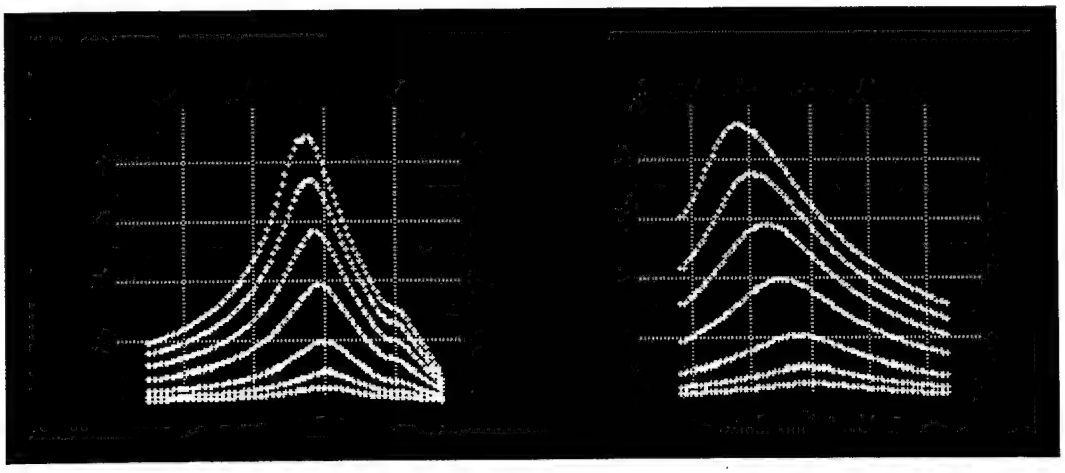

Undamaged Damaged

Figure 3.2. Application of *NRUS* to differentiate undamaged and ASR damaged samples of concrete.

The illustrations show fundamental-mode resonance of concrete bars for seven progressively increasing volumes. Note the very different nature of the damaged sample curves. The peaks are broader and the shift in the peak with volume is significantly higher than that for the undamaged sample. The peak shift and the peak width are the nonlinear diagnostics, or signatures.

Another approach to evaluate the nonlinear acoustic parameters of the material is to measure ultrasonic waves modulation by vibration, [6, 21-28]. This method is known as nonlinear wave modulation spectroscopy (NWMS), another subset of NEWS. The physical nature of this modulation can be explained with a simple crack model. Consider the sample in Figure 3.3 with the single crack shown as the only flaw. The method uses the interaction of a high-frequency ultrasonic signal with low-frequency vibration. The low-frequency vibration signal alternates between shrinkage and dilation of the flaw. Consider the case when the amplitude of the vibration during the compression phase is sufficient to close the crack (Figure 3.3a), and the subsequent tension opens the crack

(Figure 3.3b). Suppose the ultrasonic signal has a frequency at least an order of magnitude larger than the low-frequency signal. During the dilation phase of the low-frequency cycle, the high-frequency signal is partially decoupled by the opened crack. This reduces the amplitude of the high-frequency signal passed through the crack. In the other half of the low-frequency cycle, the signal produces compression and the crack is closed. The closed crack does not decouple the ultrasonic signal and the amplitude of the transmitted signal increases. This results in an amplitude modulation of the ultrasonic signal as shown in Figure 3.4; i.e., low amplitude during the dilation part of the vibration signal and high amplitude during the compressive phase. Fourier transformation of this signal reveals sideband frequencies that are the sum and difference of the frequencies of the ultrasonic probe and vibration signals. These new frequency components are the sign that a flaw or crack is present.

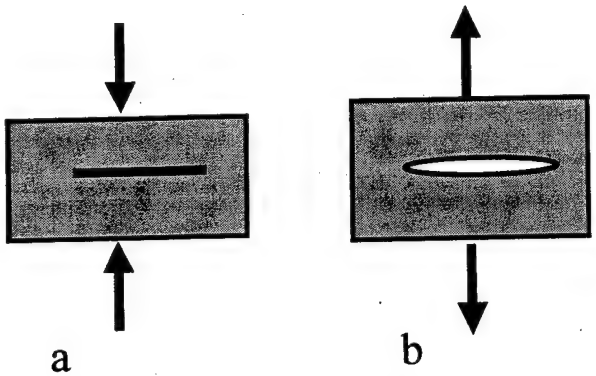

Figure 3.3. Sample with flaw
a. closed by compression
b. open under extension

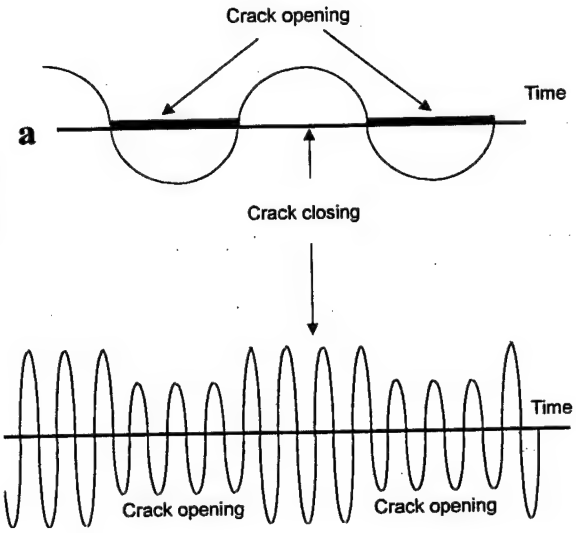

Figure 3.4. Amplitude modulation of probe signal: (a) vibration,
(b) ultrasonic signal

So the principle of the NWMS technique based on ultrasound modulation by vibration can be explained by using the following scheme:

Figure 3.5 shows the schematic presentation of the two frequency excitation applied to the undamaged part. One of these signal has frequency f_1 much less then another one with frequency f_2. These waves passed through the part without any changes in frequencies.

The other situation is observed in the specimen with a crack (Fig.3.6). The low frequency wave modulates the high frequency wave and the spectrum of modulated wave has additional spectral components. The spectrum consists of primary frequency components f_1 and f_2 and from two additional side components $f_+=f_1+f_2$ and $f_-=f_1-f_2$. These side components indicate the presence of crack.

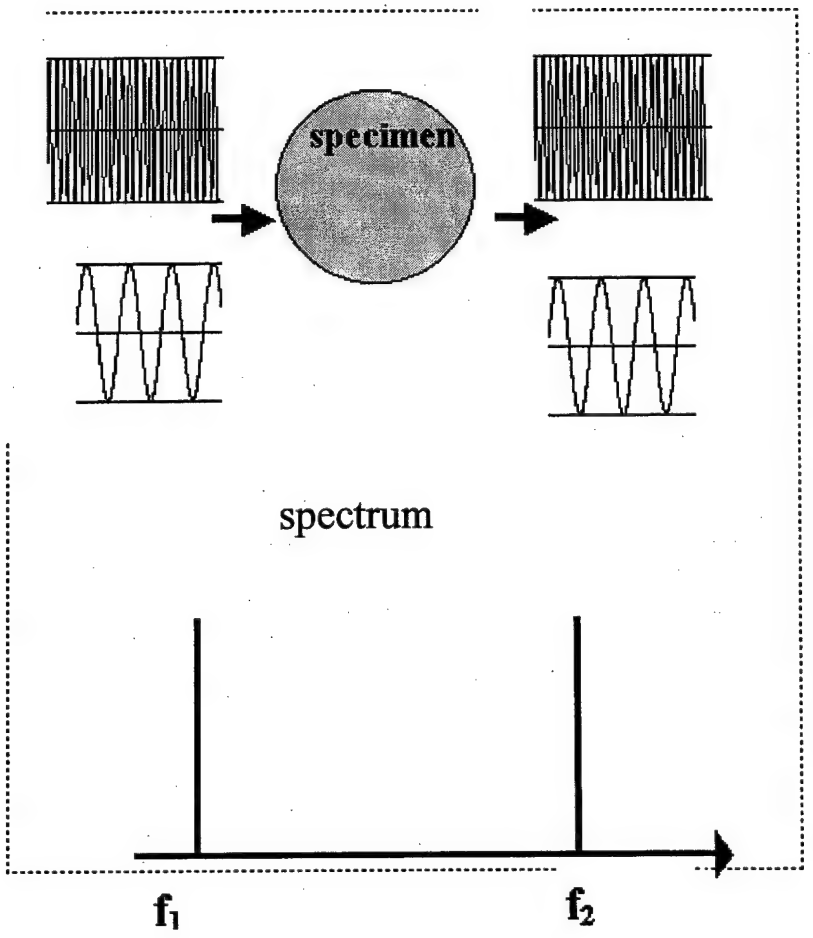

Figure3.5. The schematic presentation of waves passed through the intact specimen.

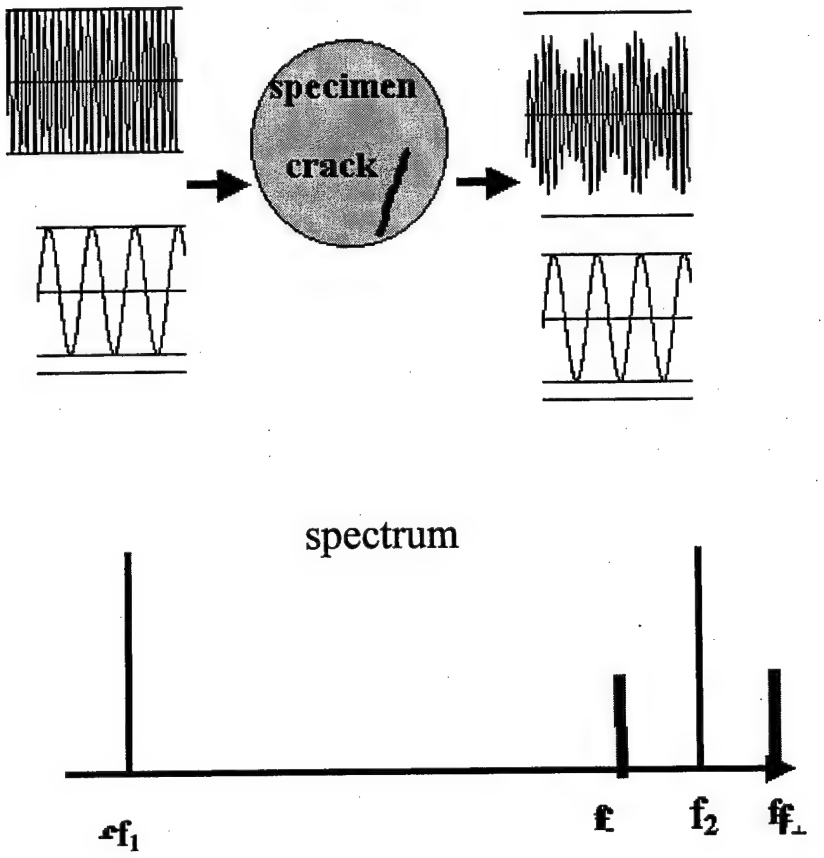

Figure 3.6. The schematic presentation of waves applied to the specimen with crack. The interaction of waves with frequencies f_1 and f_2 and leads to generation of side components $f_+=f_1+f_2$ and $f_-=f_1-f_2$. The presence of these side components indicates the crack presence.

4. Experimental Setup and Applied Processing. Polycarbonate Testing.

As it was described in previous part for NEWS we have to apply the two frequency wave to the investigated part and to observe the side components due to modulation.

There are several ways to apply two frequency waves; one is to use two separate high and low frequency transducers. Simpler way is to use one ultrasonic high frequency transducer and to produce low frequency vibration just by impact. Tide impact by hammer excites the free vibration of inverstigated part and these vibration gives modulation of probe ultrasonic wave.

The experimental setup to observe nonlinear acoustic interaction between ultrasound and vibration has to provide the high-frequency ultrasound excitation wave and the low-frequency vibration in the material under investigation, and measure the interaction product -- modulation of sound by vibration. This modulation manifests itself as a sideband component in the spectrum of the received ultrasound signal. The scheme of typical experimental setup is presented in fig. 4.1. The instrumentation consists of:

1. The low-frequency excitation part - instrumental hammer with attached piezoelectric sensor for triggering of recording signal.
2. The high-frequency ultrasound part includes high frequency generator, power amplifier. and piezoelectric sensors attached to the investigated part.
3. The registration part consist of piezoelectric sensor to transfer acoustical signal to electrical signal and LeCroy digital oscilloscope (Waverunner LT322), The primary processing was conducted by oscilloscope. The signal was also transferred to computer for secondary processing.

Fig.4.2. presents the photograph of the actual experimental setup.

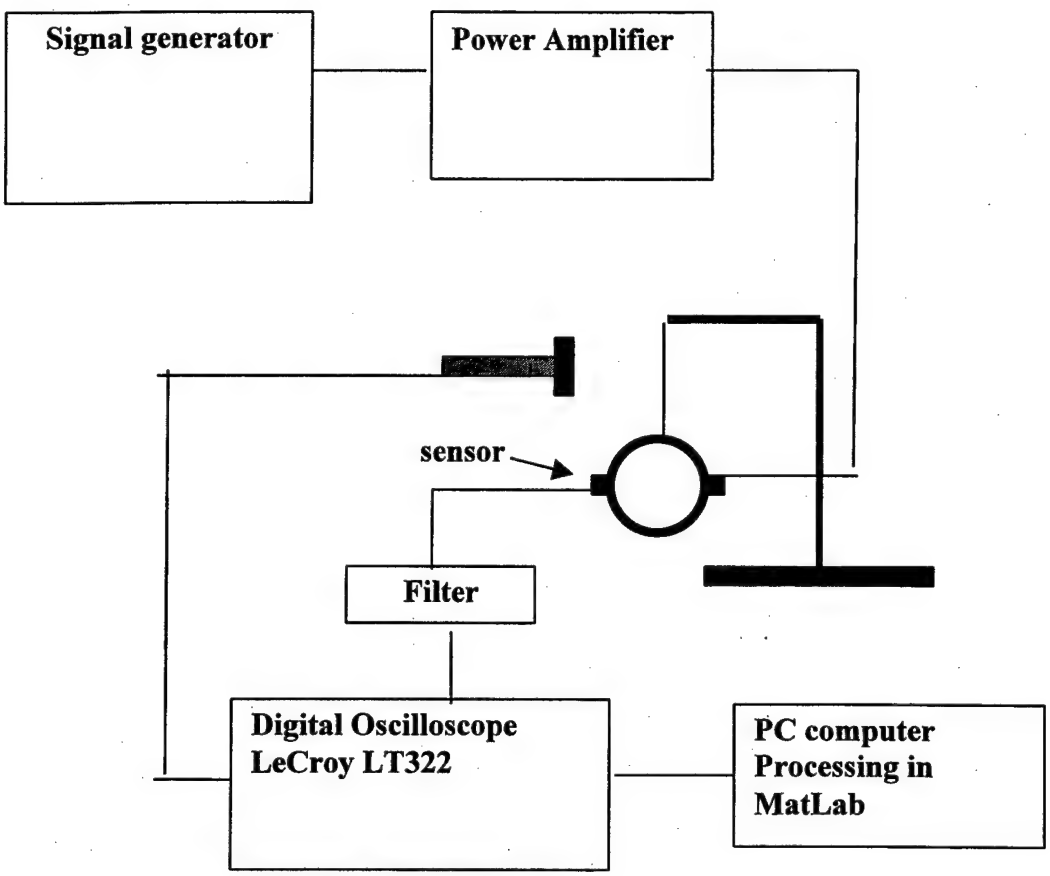

Figure 4.1. The experimental setup for NWMS measurements.

For a nonlinear acoustic test the samples were supported by soft foam or were hanged by thin threads. Two ultrasonic transducers were glued to the surface of each sample; one was used as a transmitter and another as a receiver of high frequency ultrasound wave. Low frequency vibration was generated with an instrumental hammer, which produced calibrated and repeatable impacts of controllable amplitudes. The hammer was equipped with an accelerometer used for synchronization with the data acquisition system.

The signal from accelerometer attached to the hammer is shown in Figure 4.3. The sensitivity of accelerometer with preamplifier was 0.01 mV/ m/sec^2, it means that maximum of acceleration during impact reaches 33000 m/sec^2. Taking into account that the hammer mass is 93 g the force produced by hammer is about 3000 N.

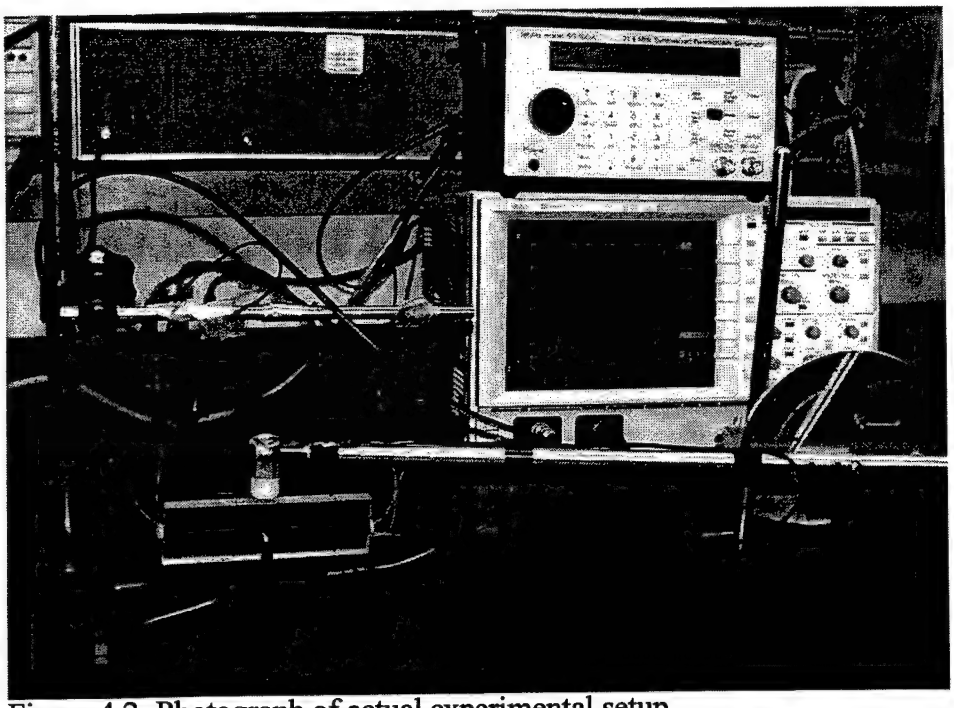

Figure 4.2. Photograph of actual experimental setup.

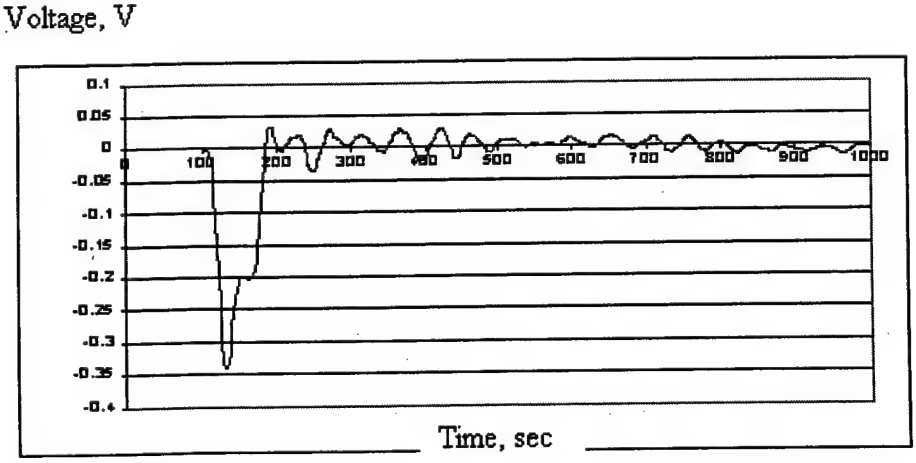

Figure 4.3. The snapshot of impulse produced by hammer.

The effect of ultrasound modulation by vibration can be clear observed in time domain for spaciman having relatively large size of defects. One of such parts is Automoble Bearing Cap presented in fig. 4.4. One of bearing caps has a crack with the highest level of nonlinearity among all samples. The time series of the received signal after impact for high frequency excitation 205 kHz is shown in Fig. 4.5. It can be seen that the modulation takes place just after the impact.

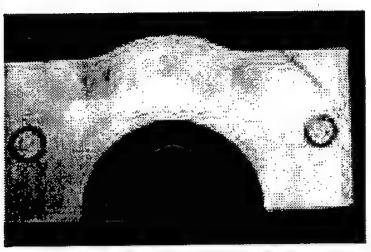

Figure 4.4. The picture of Automobile Bearing Cap

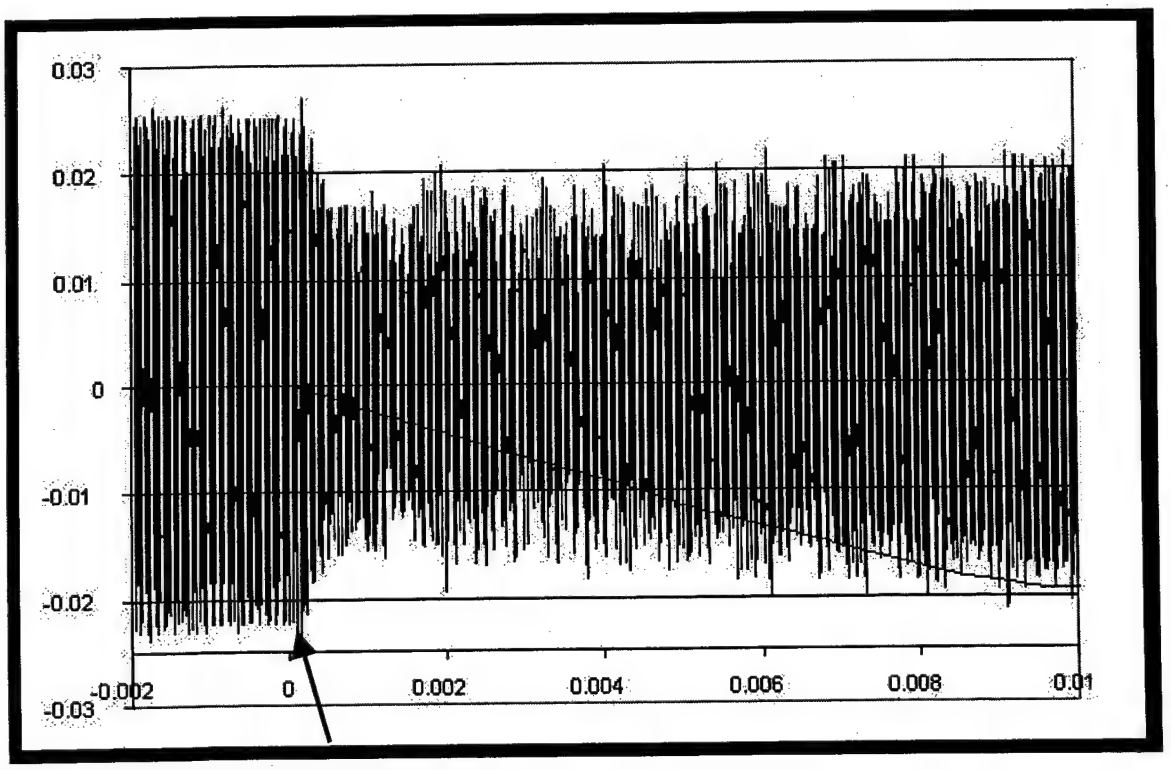

Figure 4.5. The time series of the detected signal signal from the brearing cap with crack (frequency 205 kHz). The moment of impact is shown by arrow and it is seen the amplitute modulation of the received sinal after impact.

The two spectra obtained by averaging of 10 impacts for the intact and cracked bearing cap and the bearing cap are presented on the fig.4.6 and fig.4.7. The frequency of excitation was 192 kHz. A similar difference in spectra is seen for any frequency studied.

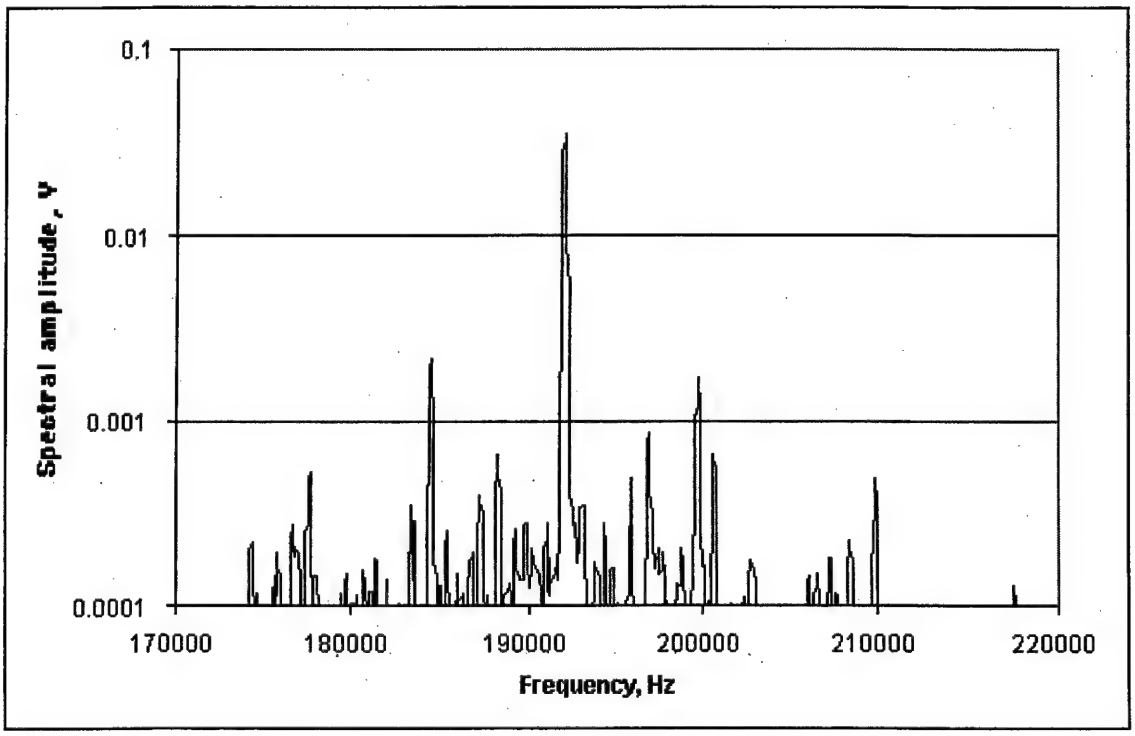

Fig.4.6. The spectrum of the received signal after impact for cracked bearing cap. There are many side components due to ultrasound modulation by vibration.

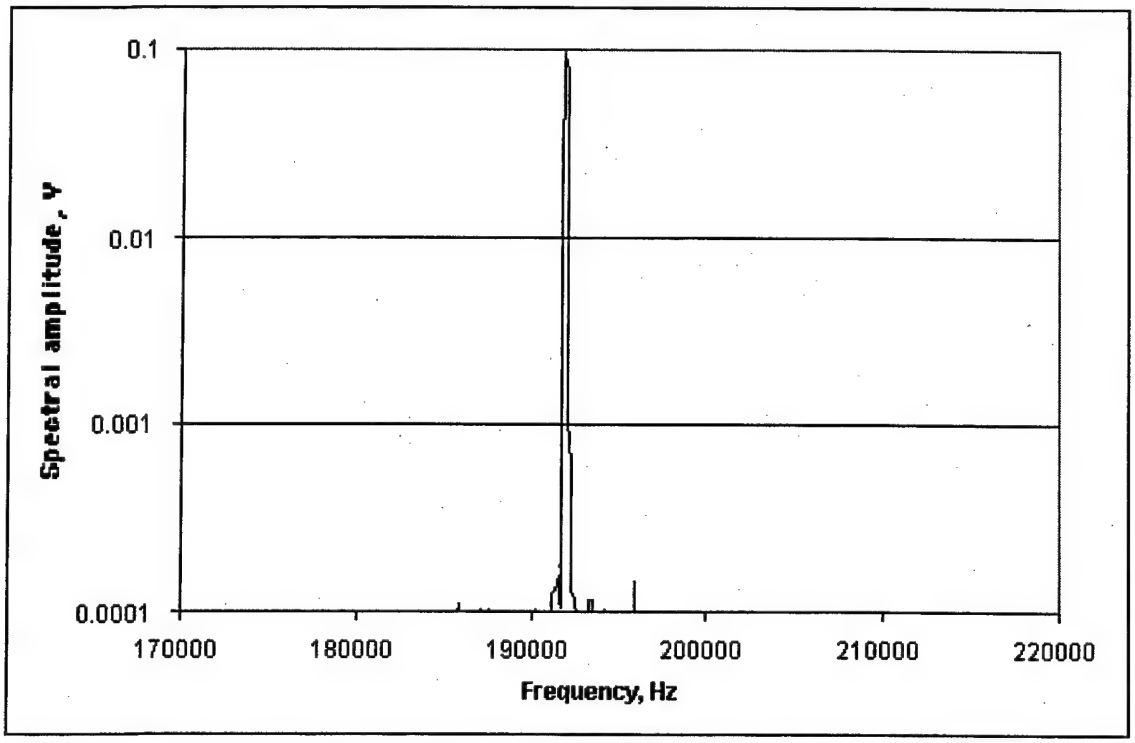

Fig.4.7. The spectrum of the received signal after impact for intact bearing cap. There is only main frequency component and no side components.

The results of modulation depends on the applied ultrasonic frequency, sensor position. The way to avoid such influence is summation average proceducer applied to the the signal with varied frequency.

We will illustrate the summation average procedure on the example of NWMS technique application for crack detection is polycarbonate sample.

The specimens were machined from the polycarbonate used for aircraft canopies. The specimen geometry is shown in Figure 4.8. The experimental setup presented in fig 4.1 and 4.2. was used. The fatigue cracks were developed during four-point bending cycling regime. The crack lengths are given in Table 4.1.

Table 4.1. Tests results. Polycarbonate specimens; 0.5 inches thickness; Four-point bending cycling regime.

Specimen Number	Crack length, mm	Number of cycles	Stress, psi
1	Reference specimen	0	0
2	2	85000	10000
3	6.3	128000	10000
4	Initiation	32000	10000

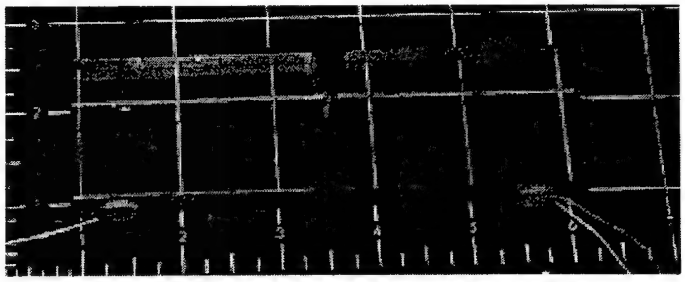

Figure 4.8. Polycarbonate specimen with attached sensors.

The spectra after impact for different samples and frequencies are presented in fig. 4.9.-4.15. The fig.4.9. shows the typical spectrum for undamaged specimen having low level of side components. Figures 4.10 – 4.13 present spectra for cracked specimen for different frequencies of ultrasonic wave. It is seen that the received spectra moved along frequency axis and these spectra can not be averaged directly. We have developed the summation averaged procedure that allows to average side components for different ultrasonic frequencies. This procedure is working by the following way:

Once the impact device strikes the object, a high-pass-filtered time signal is captured on the digitizing device. This signal contains the information required to discern whether or not damage exists in the test sample. In the simplest case, a Fourier transform is taken of the time signal, and modulation sidebands are looked for around the high frequency ultrasonic signal. This signal is stored on the computer for further analysis. A nonlinear effect from crack(s) in the test object creates modulation of ultrasound by vibration and side band component present in the sample. The levels of sidebands in undamaged objects are much less then in damaged object.

The next step in the experimental procedure is to change the pure tone frequency(ies), and repeat the experiment. This is called a step-frequency sweep. This procedure is repeated for some number of different pure tone frequencies, one at a time. For instance, one could use eleven pure tones successively at 185kHz, 186kHz, 187kHz....195kHz. (The spectra for frequencies 185, 190, 192 and 195 kHz are shown in fig. 4.10-4.13). At each pure tone frequency, the impact device is applied and the detected signal is collected. The spectra of any signal are transformed to low frequency band such matter that main frequency is transformed to zero. After such transformation a spectrum of any signal will consists of main component having frequency zero and side components with positive and negative frequencies around main frequency. These transformed spectra can be averaged and the result does not depend on ultrasonic high frequency signal.

The results of the such averaging are presented in Figures 4.14-4.17 for all four tested samples. The averaged level of the side components is the higher for the sample with biggest crack (fig.4.15) and becomes less to the sample with smaller crack (fig.4.16). The level of side components for polycarbonate without crack is much less (see fig. 4.14 and 4.17).

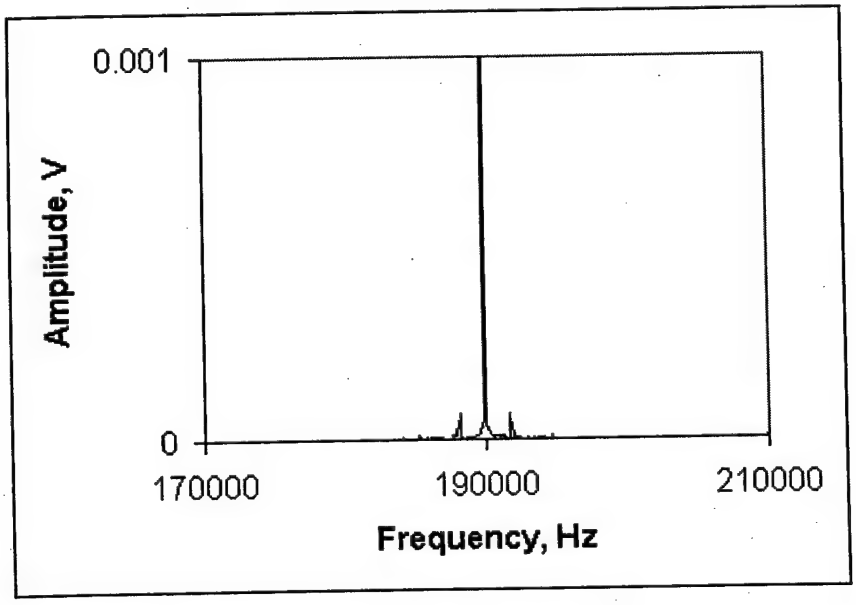

Figure 4.9. The spectrum of the ultrasonic signal with frequency 190 kHz for sample #0 (undamaged).

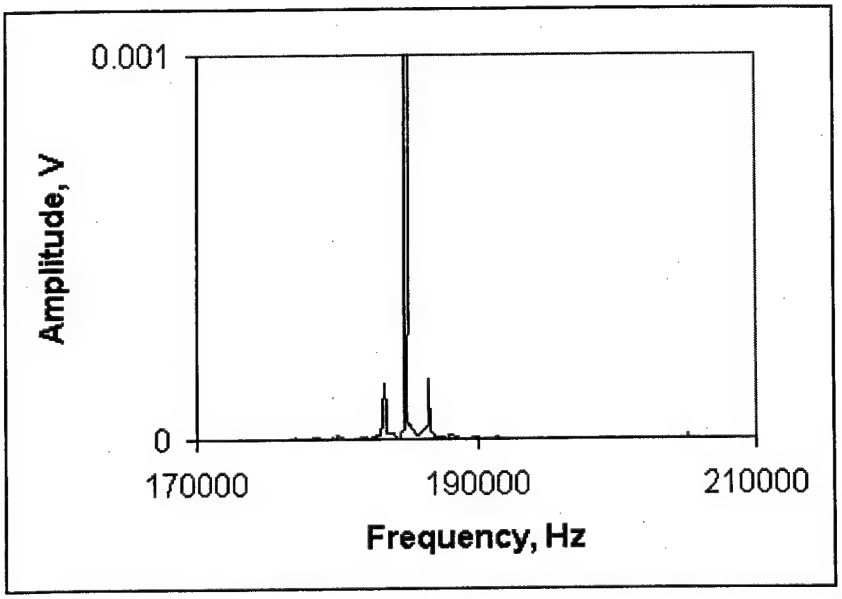

Figure 4.10 The spectrum of the ultrasonic signal with frequency 185 kHz for sample #1 (6.3 mm crack).

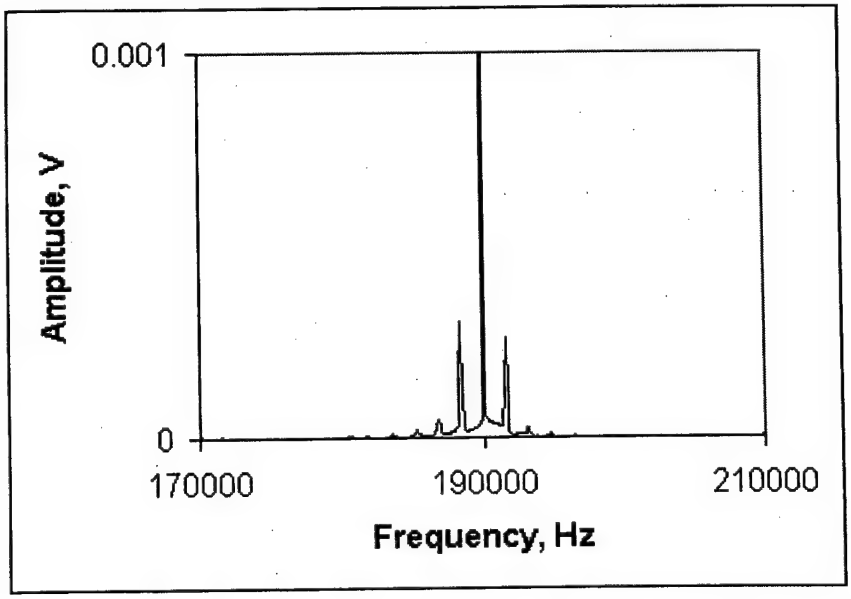

Figure 4.11. The spectrum of the ultrasonic signal with frequency 190 kHz for sample #1 (6.3 mm crack).

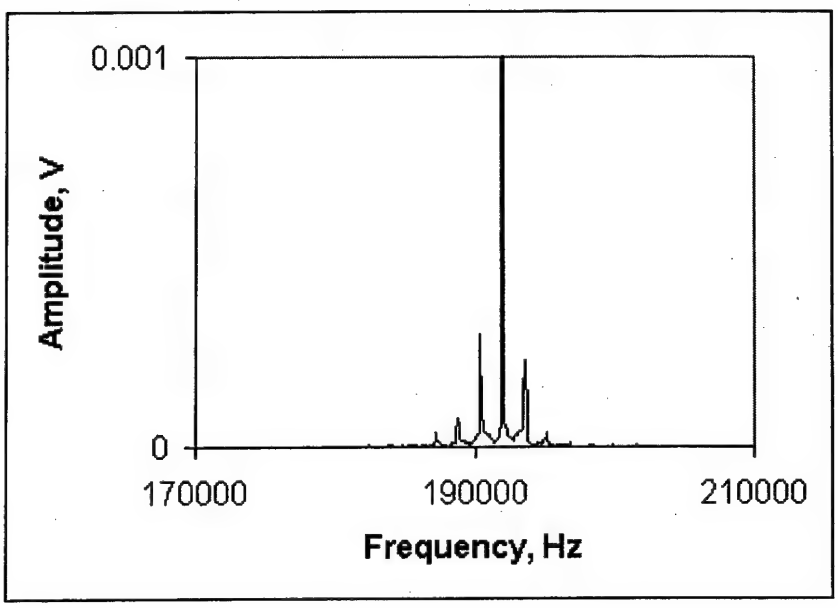

Figure 4.12. The spectrum of the ultrasonic signal with frequency 192 kHz for sample #1 (6.3 mm crack).

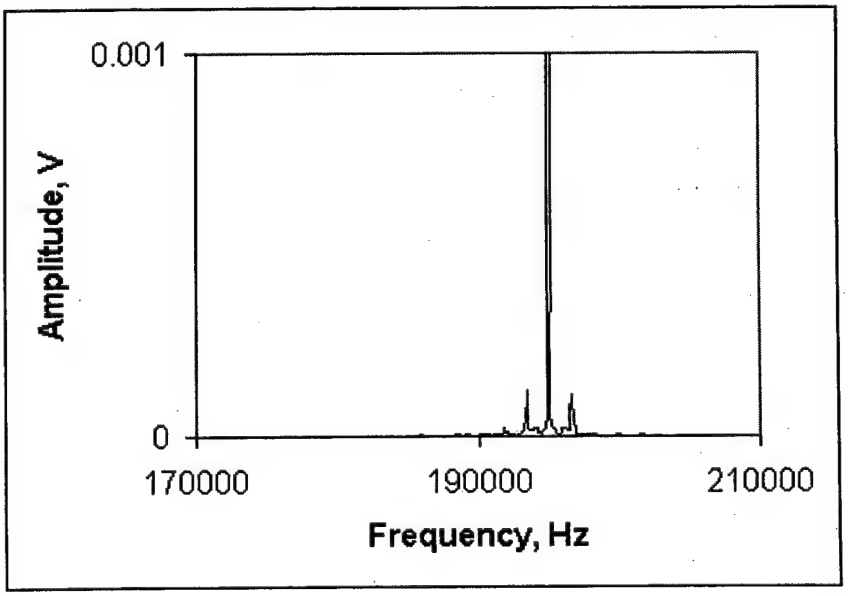

Figure4.13. The spectrum of the ultrasonic signal with frequency 195kHz for sample #1 (6.3 mm crack).

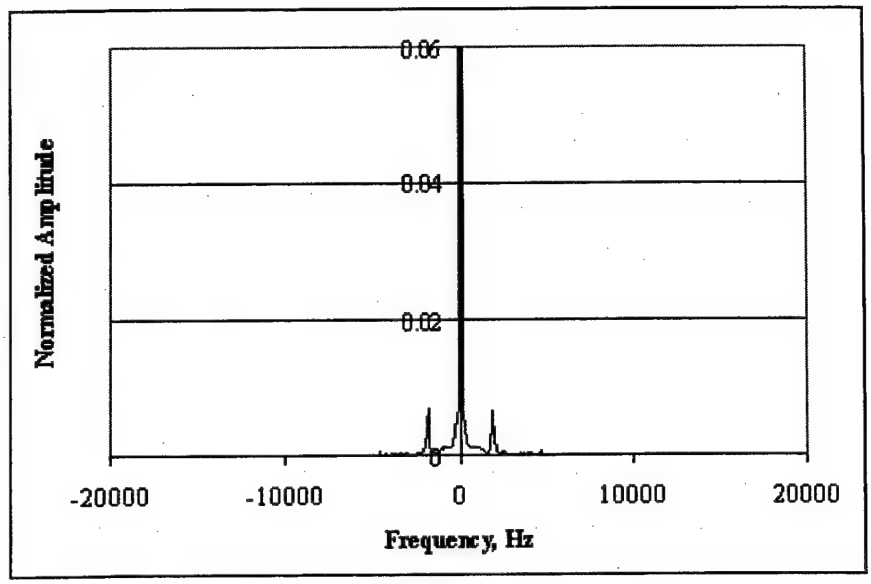

Figure 4.14. The spectrum of the normalized and averaged signal for sample #0 (undamaged).

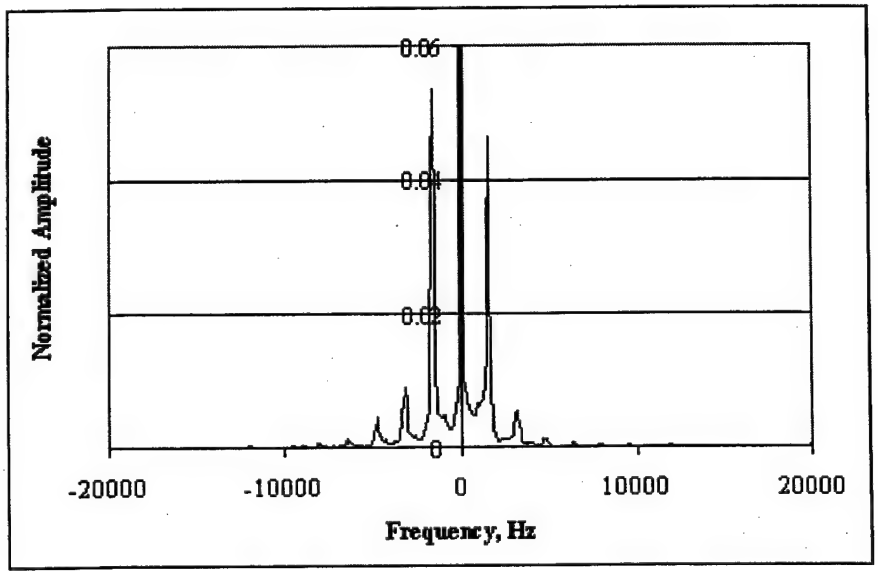

Figure4.15. The spectrum of the normalized and averaged signal for sample #1 (6.3 mm crack).

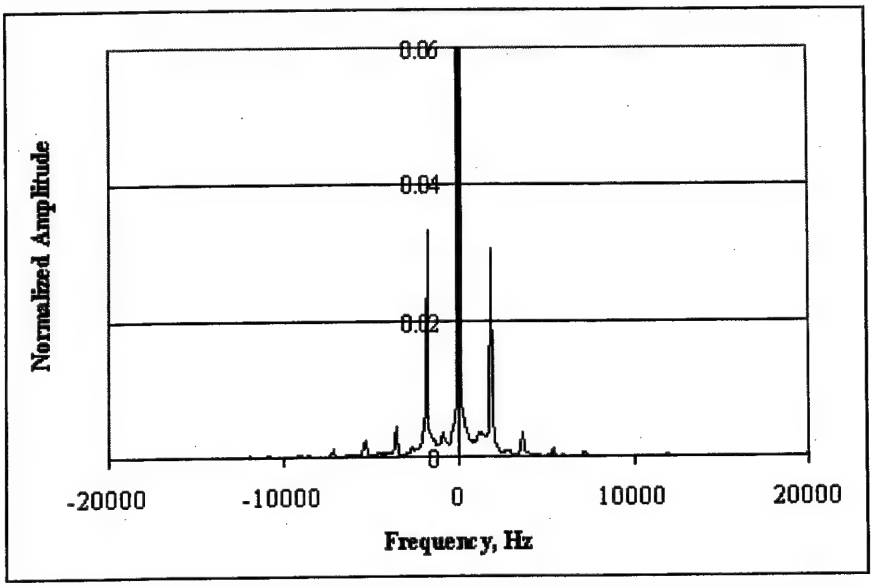

Figure 4.16 The spectrum of the normalized and averaged signal for sample #2 (2mm crack).

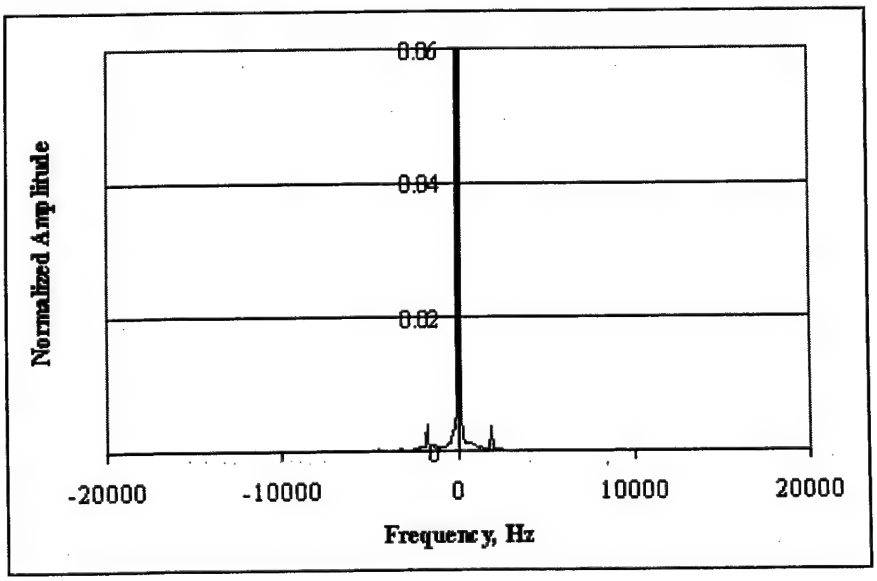

Figure 4.17. The spectrum of the normalized and averaged signal for sample #3 (undamaged).

This *summation average* procedure is used to improve the signal to noise ratio and to inspect the results of many experiments simultaneously. The result of the summation average provides a yes/no result. Is the object damaged or not? The number of frequencies and the number of steps in frequency are not critical. The more frequency steps the better the signal to noise ratio is in the average of the Fourier spectrum, and the more robust the measurement is because more and more sidebands are used in the decision. Because the averaging is done in the frequency domain, the phase of each successive time signal collected in unimportant.

5. Results of Experimental Investigations

This section of report presents applications of NEWS technique.

5.1. Observation of the modulation of ultrasonic waves by impact produced vibration in strain hardening components

This example demonstrates how the developed technique works for strain hardening aluminum components. These components have size 47x45 x5 mm^3 and the picture of component is shown in fig. 5.1.

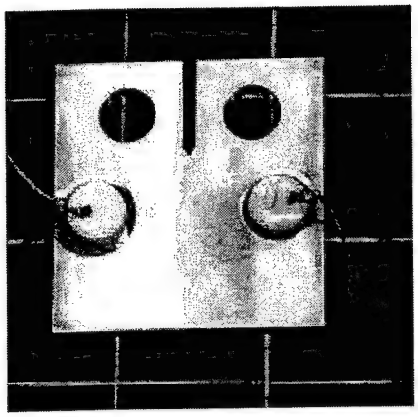

Figure5.1. Picture of the stress hardening component.

The crack was grown by cyclic loading. The crack had arisen in the tip of notch and this crack was hardly seen; we had to use microscope to observe the crack. The length of crack was from 1.5 to 3 mm.

Four damaged and four intact samples were tested. The cracked samples were marked as: # 55, # 47, # 65, # 43 and the intact sample were marked as A1, A2, A6, A7.

The experiment was carried out with small PZT piston sensors glued to the flat surface of samples(See fig.5.1 and 5.2.). The samples were hanged by a fine thread (wire).

The experimental setup is presented in fig.5.2.

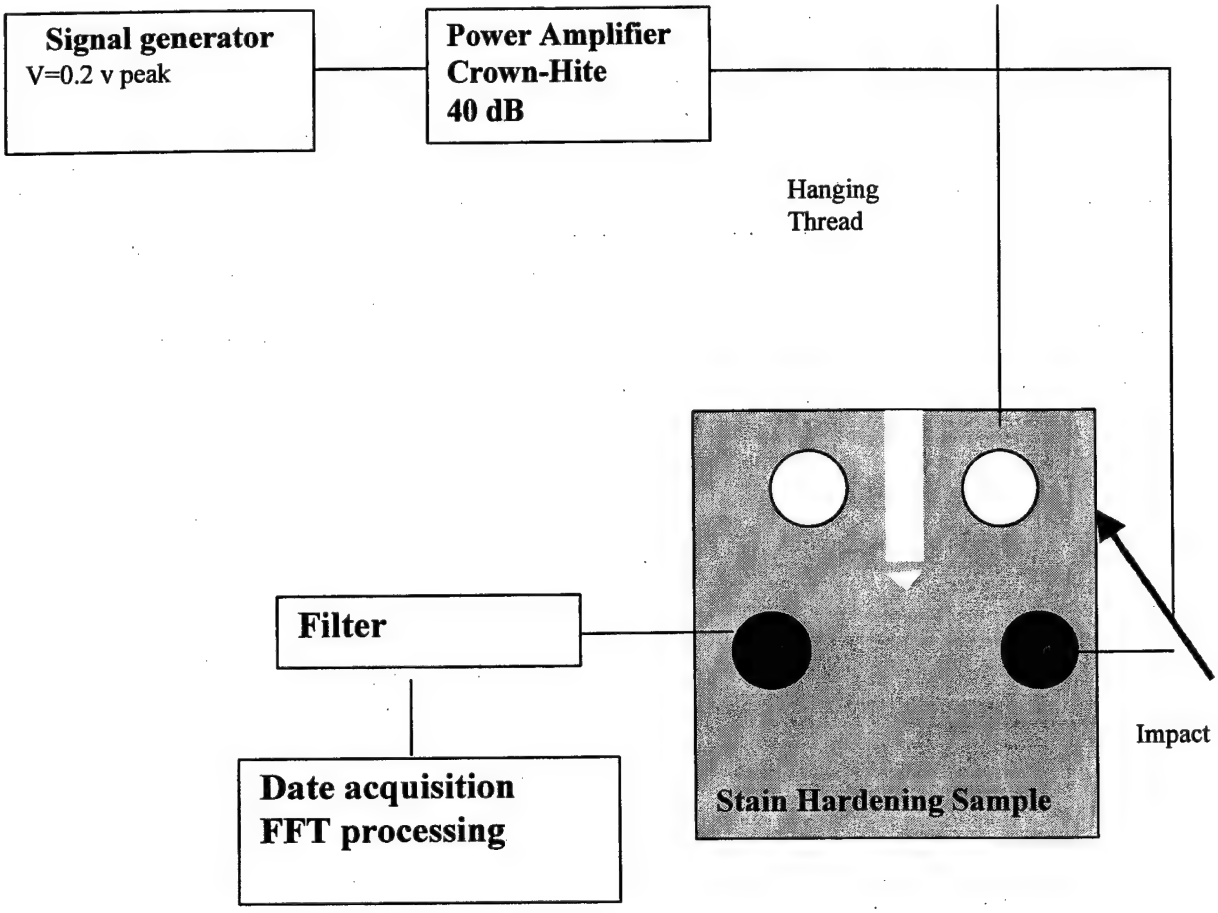

Figure5.2. The experimental setup to investigate stress hardening components.

As it was described above the presence of crack is indicated by interaction between high frequency ultrasonic wave and low frequency vibration produced by hammer impact.

The sample vibration produced by impact was picked up by the same piezoelectric sensor and were recorded by oscilloscope. The snapshot of low frequency vibration signal after impact is presented in fig. 5.3 and the spectrum of this signal is shown in fig. 5.4.

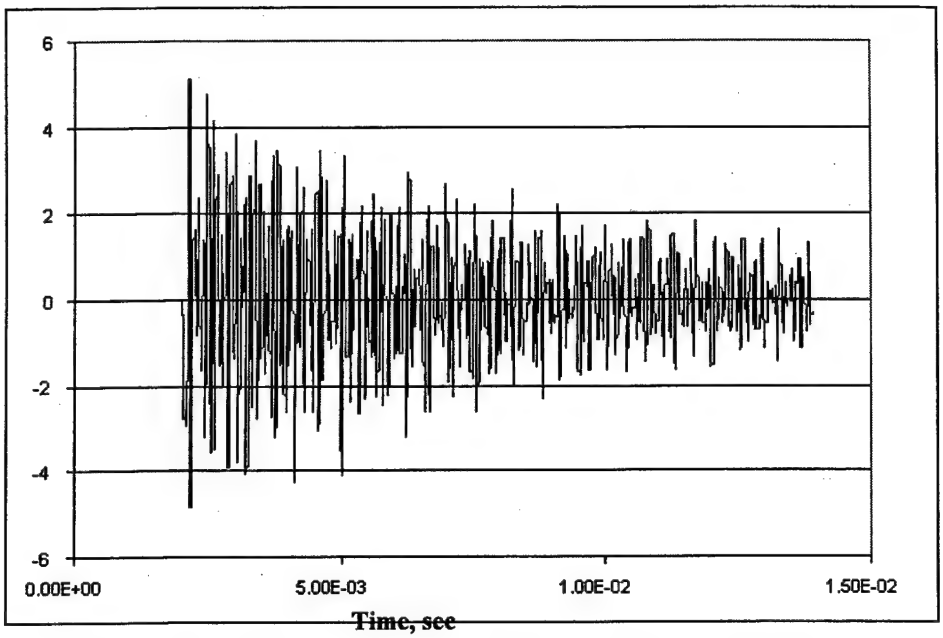

Figure5.3. The time sequence of vibration produced by impact

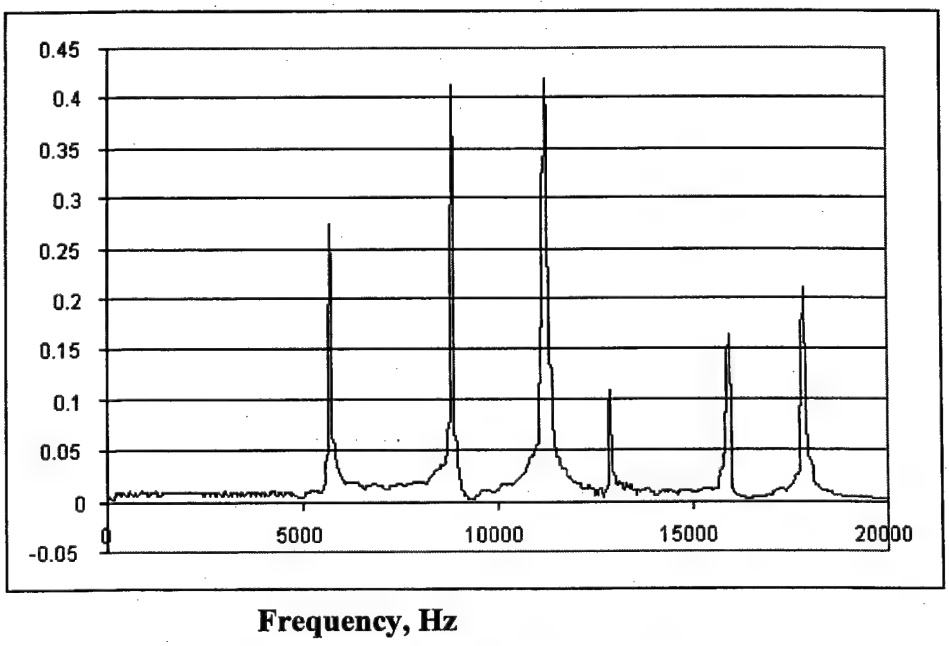

Figure5.4. The spectrum of impulse produced vibration

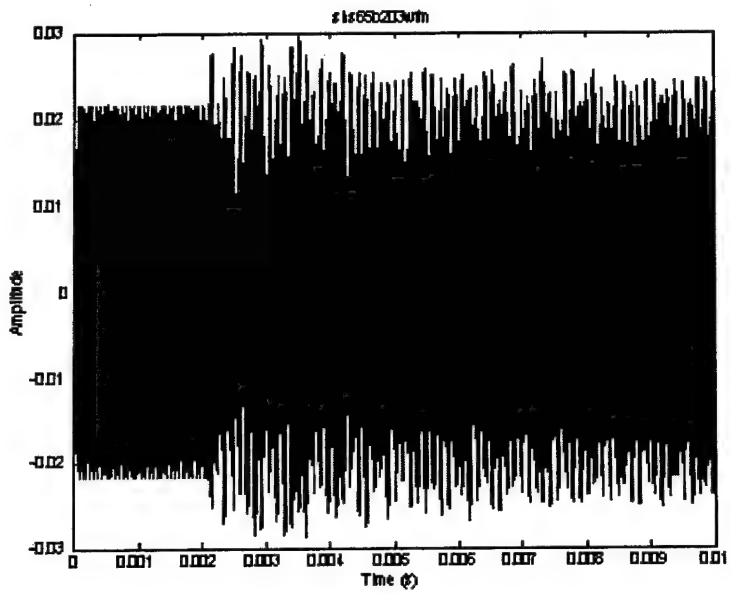

Figure 5.5. The snapshot of ultrasonic signal after impact for the cracked sample #75

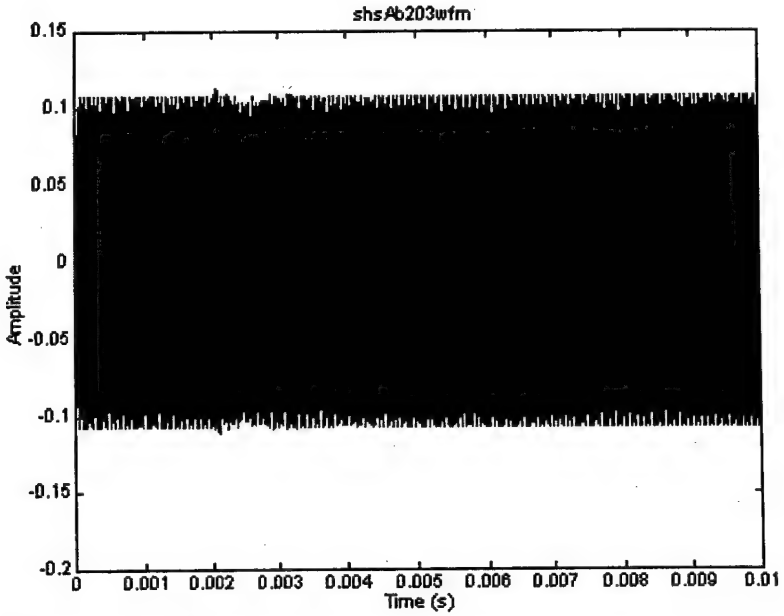

Figure 5.6. The snapshot of ultrasonic signal after impact for the intact sample.

Two waveforms of ultrasonic signals after impact for frequency 203 kHz for cracked and uncracked samples are given in fig.5.5 and 5.6. We can observe modulation of ultrasonic wave after impact in the cracked sample and there is no modulation for the sample without crack (see fig.5.6).

The more quantitative analysis have been conducted by using the summation averaged procedure described in previous part. This procedure was applied to the signal recorded in the frequency band 200-210 kHz for set from 8 samples and the results are presented in fig. 5.7-5.14.

The large difference of averaged spectra for damaged and undamaged samples can be clearly seen.

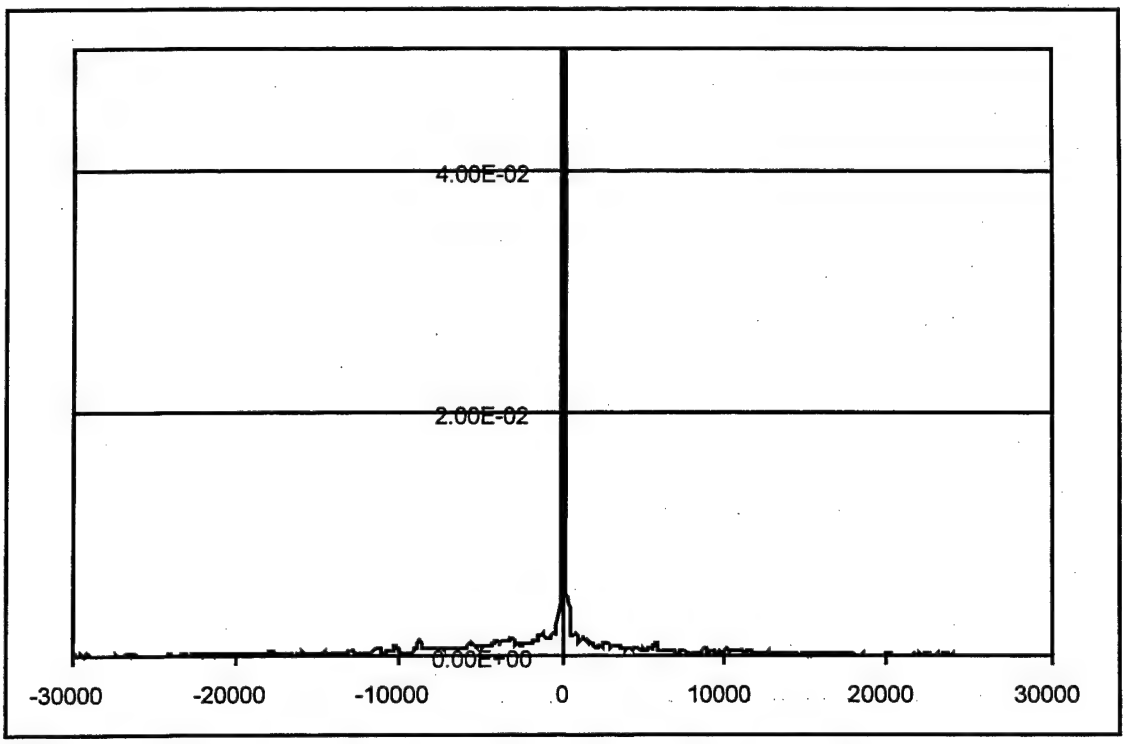

Figure 5.7. Avareged summation spectrum for sample #A1, uncracked

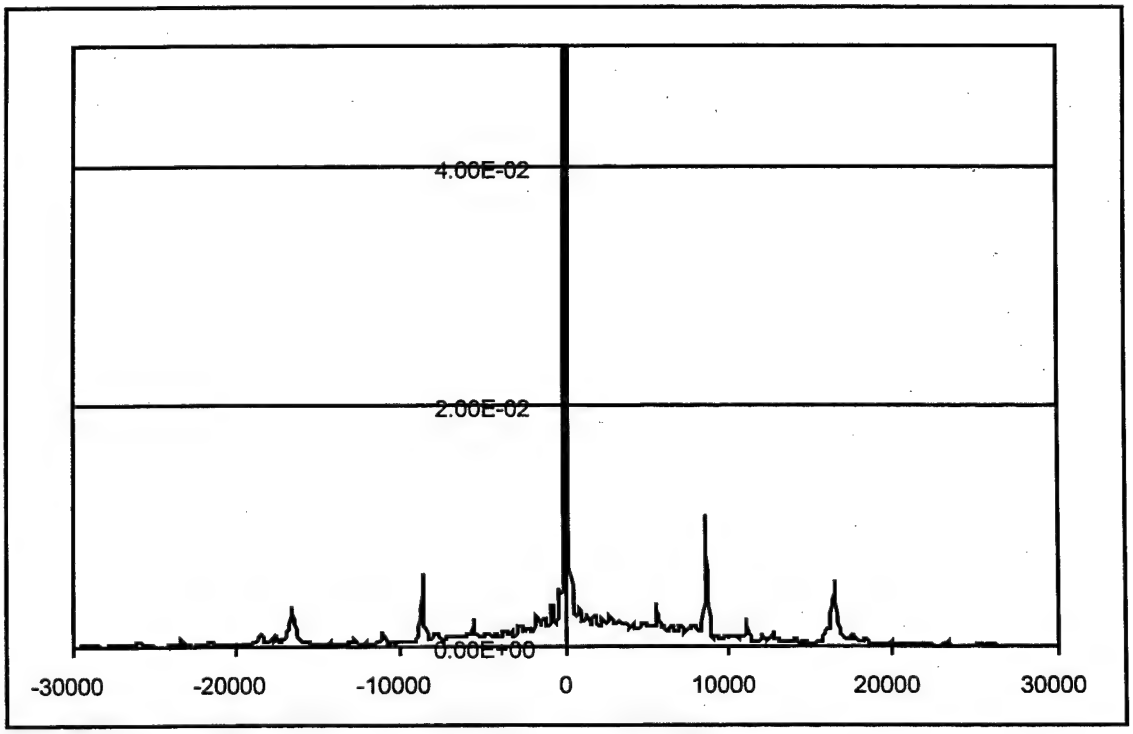

Fig 5.8. Averaged summation spectrum for sample #43, cracked

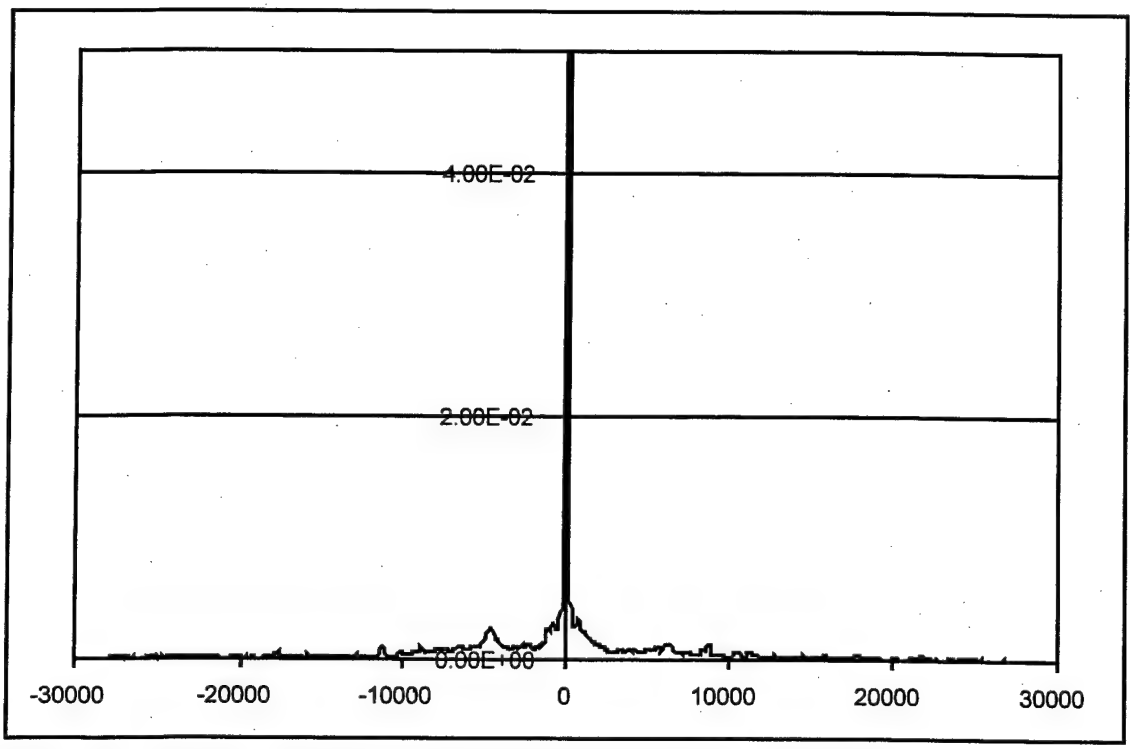

Figure 5.9. Averaged summation spectrum for sample #A2, uncracked

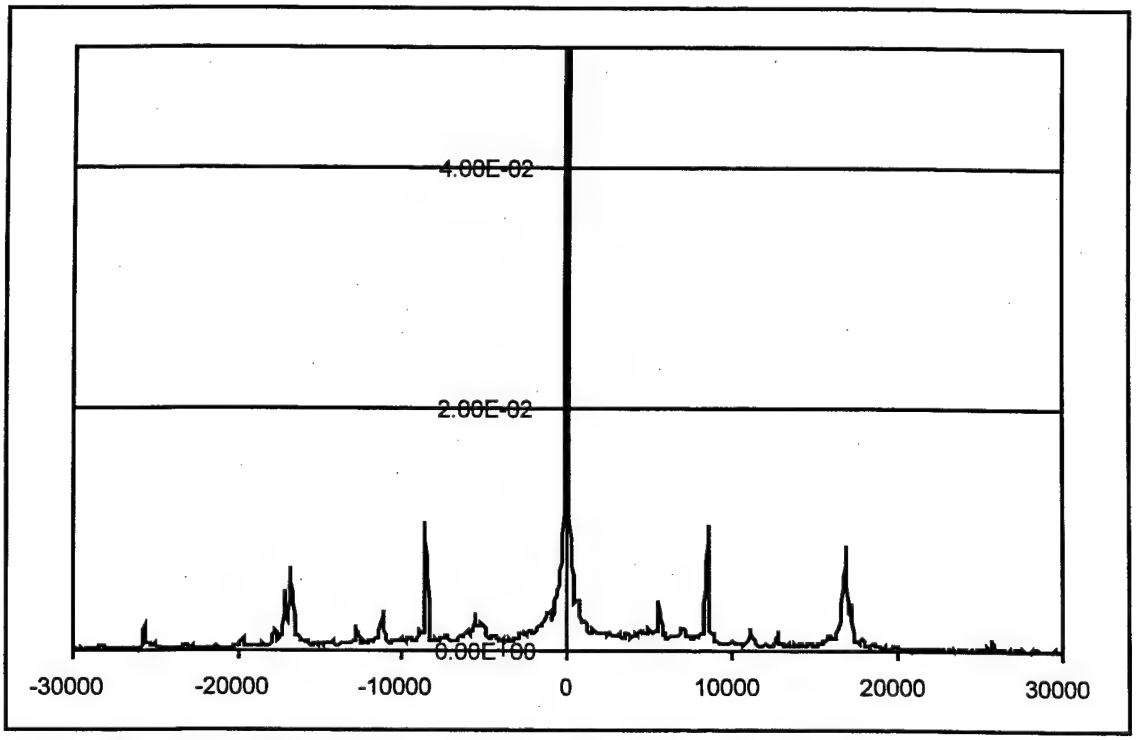

Figure 5.10. Avareged summation spectrum for sample #47, cracked

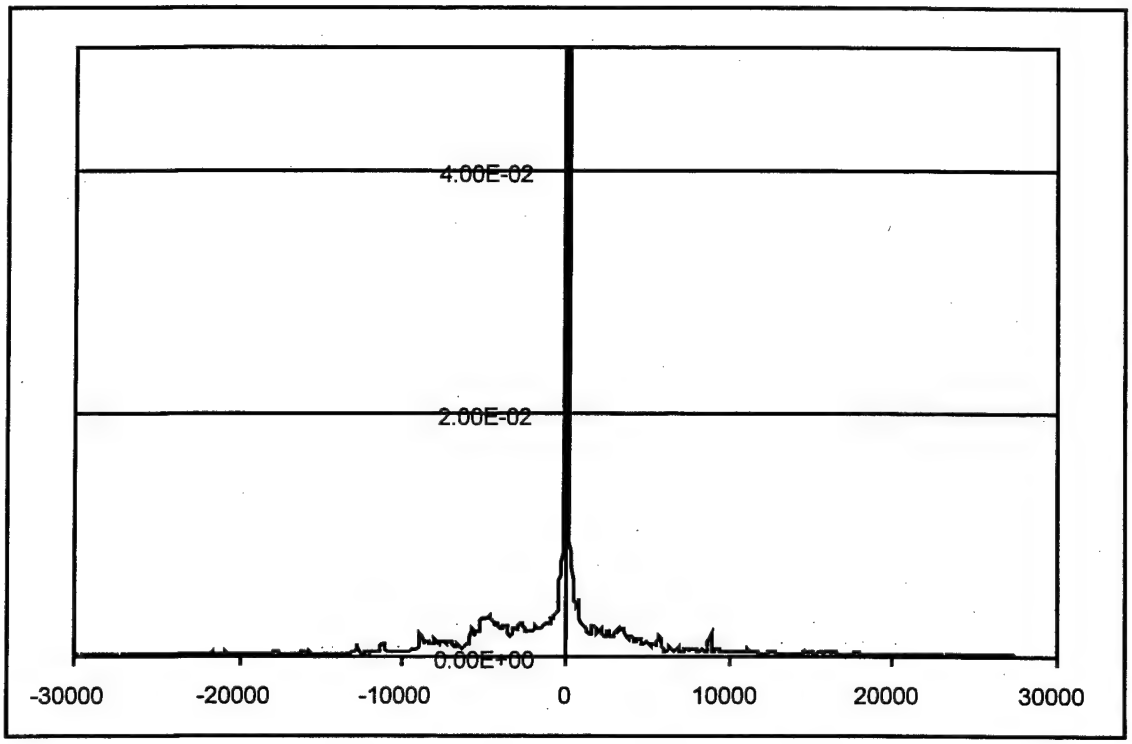

Figure 5.11. Avareged summation spectrum for sample #A5, uncracked

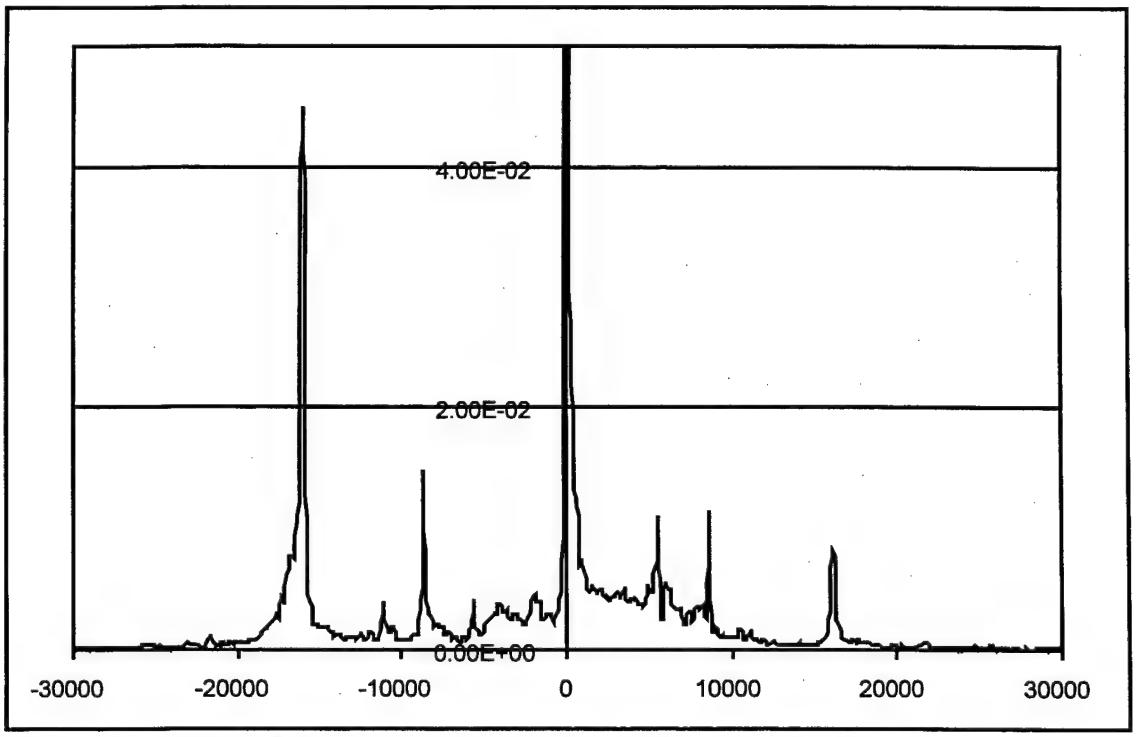

Figure 5.12. Averaged summation spectrum for sample #55, cracked

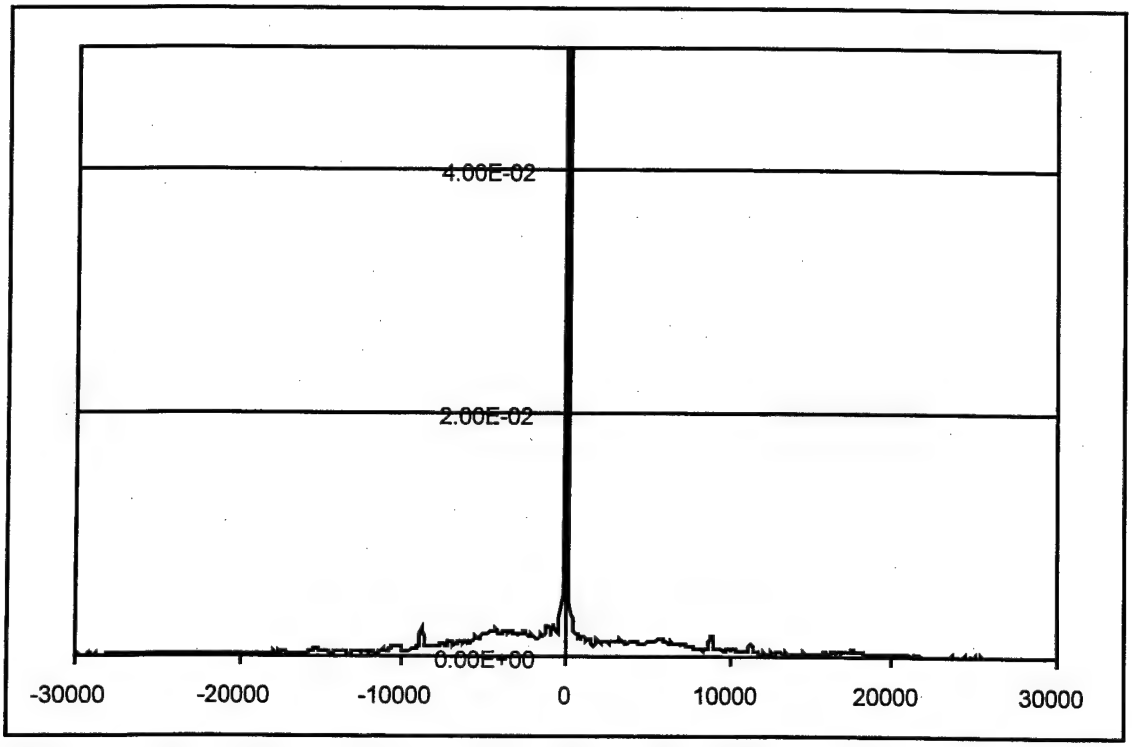

Figure 5.13. Averaged summation spectrum for sample #A7, uncracked

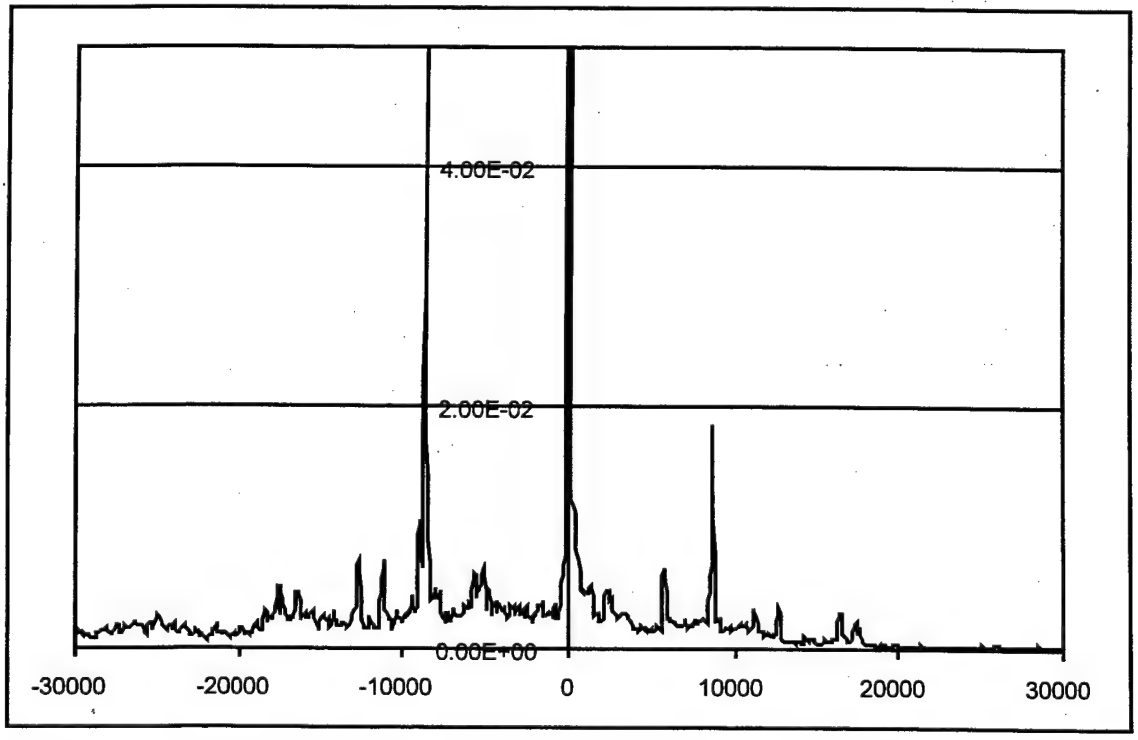

Figure 5.14. Averaged summation spectrum for sample #65, cracked

5.2. Test for bounded aluminum plates

The test had been conducted on adhesive bonded aluminum plates (fig. 5.15) supplied by Boeing. One plate was of them was intact and the other was affected by heating with temperature of 185 Degrees. This part is supposed to have lower strength properties.
The scheme of experimental setup is shown in fig.5.16.

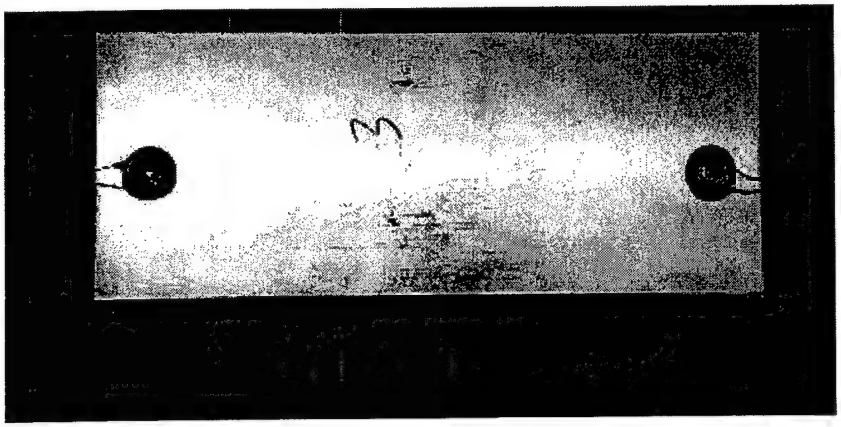

Figure 5.15. The picture of adhesive bonded aluminum plate.

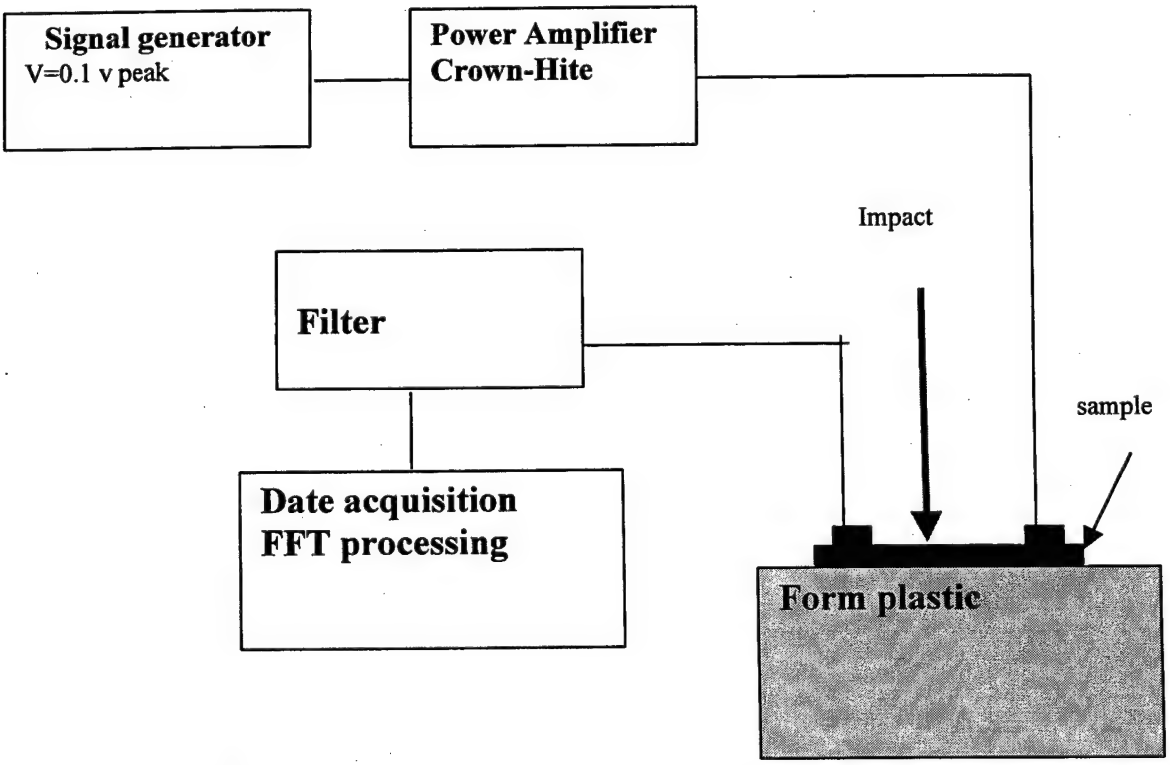

Figure 5.16. The experimental setup for aluminum plate measurements.

The summation averaged procedure was applied to the signal recorded in the frequency band 190-196 kHz and the results of are presented in fig. 5.17-5.18.

It is seen side components with frequency about 800 Hz in the damaged sample and there are not side components in the intact sample. The difference in the modulation is not so clear as in previous tests

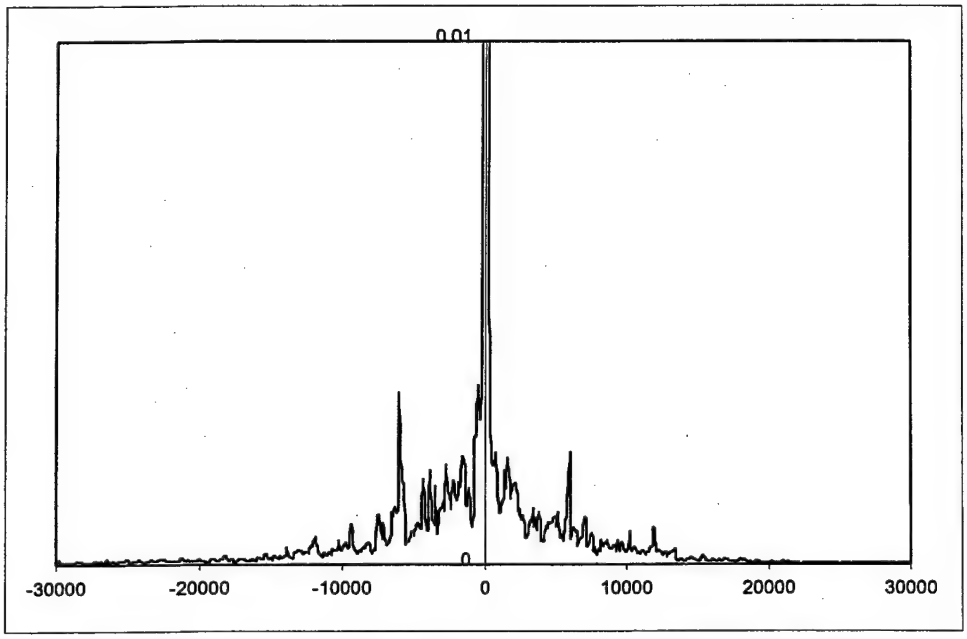

Figure 5.17. Summation averaged spectrum for the damaged sample #4

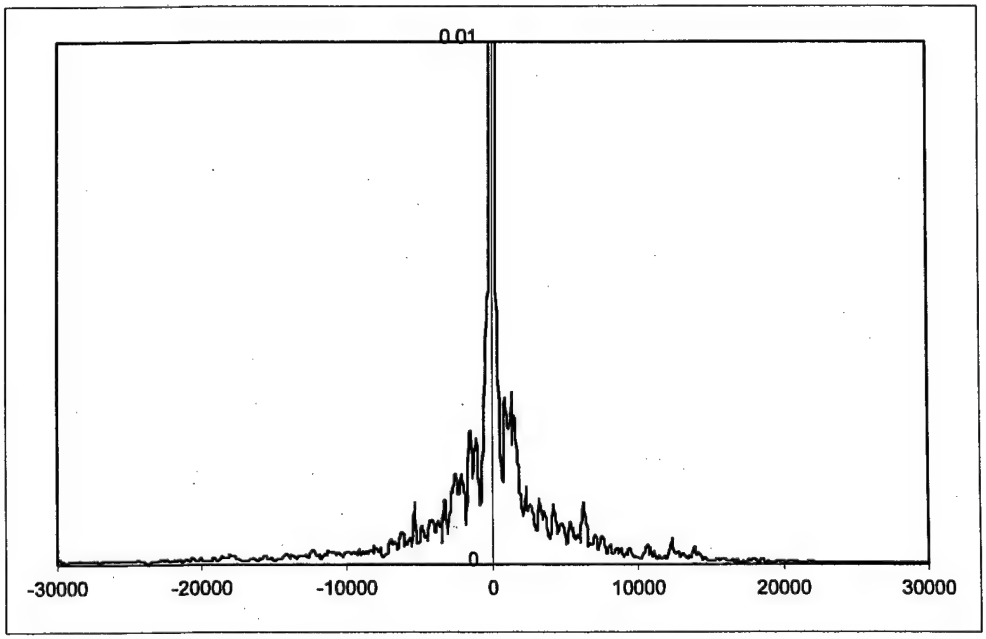

Figure 5.18. Summation averaged spectrum for the undamaged sample # 1

5.3. Application of NEWS for quality assessment of bending tubes

The test for bending tubes demonstrate that the developed technique can be applied not only for crack detection but also for quality assessment when crack did not exist.

The similar technique was applied for thin steel tubes used in aircraft industry. The picture of tube is presented in fig. 5.19.

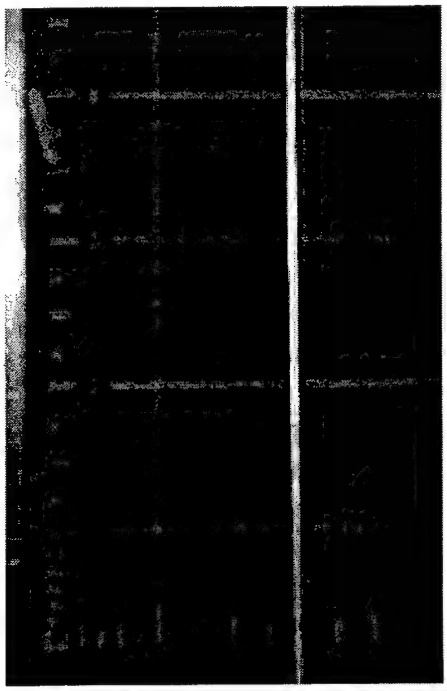

Figure 5.19. Picture of tube

To produce damage some of tubes were affected by bending up to 90 degrees and back. The numeration of tubes and parameters of bending are presented in table 5.1.

Table 5.1. Parameters of tested tubes.

Numeration	Length, mm	Number of Bending
A1	170	10
A2	165	1
A3	170	5
B1	210	3
B2	200	1
B3	200	25
B4	205	6
B5	215	20
B6	205	0
C1	138	0
C2	138	25

The results of summation averaging are shown in figures 5.20 -.

It is seen that the tubes bended 20 and more times (#B3, B5 and C2) have distinguish modulation (clear side band components(while other tubes have no modulation.

The observed results are the first experimental verification to for damage detection in small tubes and this method can be quickly improved be choosing the most sensitive frequency range and conditions for impact low frequency excitation

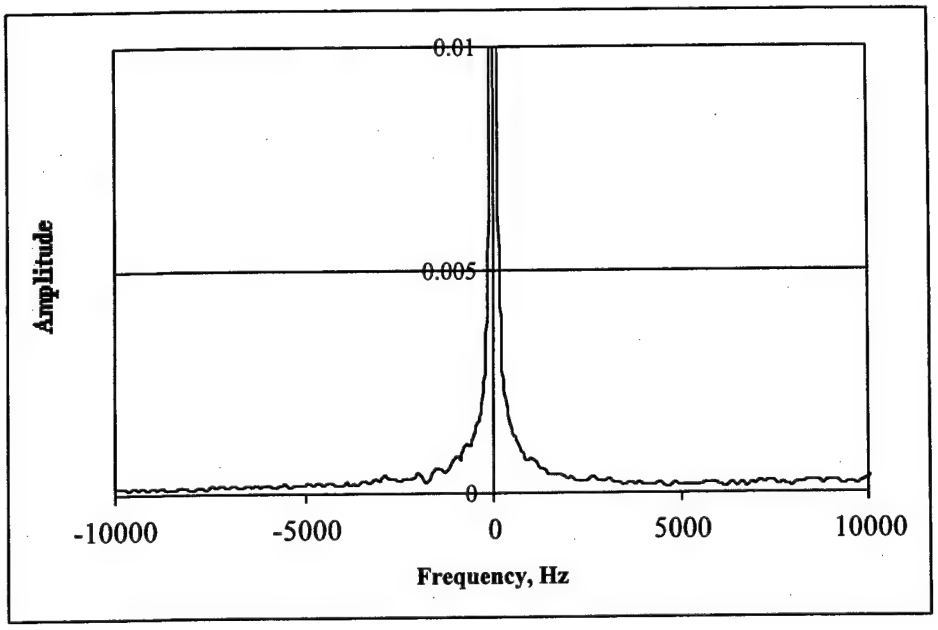

Figure 5.20 . Summation averaged spectrum for the tube A1 (10 bendings)

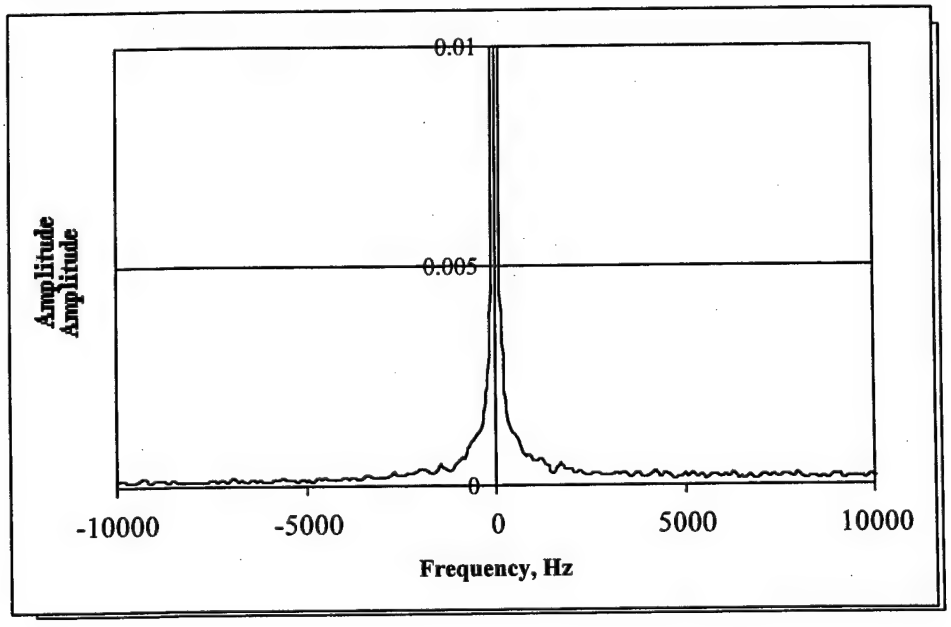

Figure 5.21. Summation averaged spectrum for tube # A2 (1 bending)

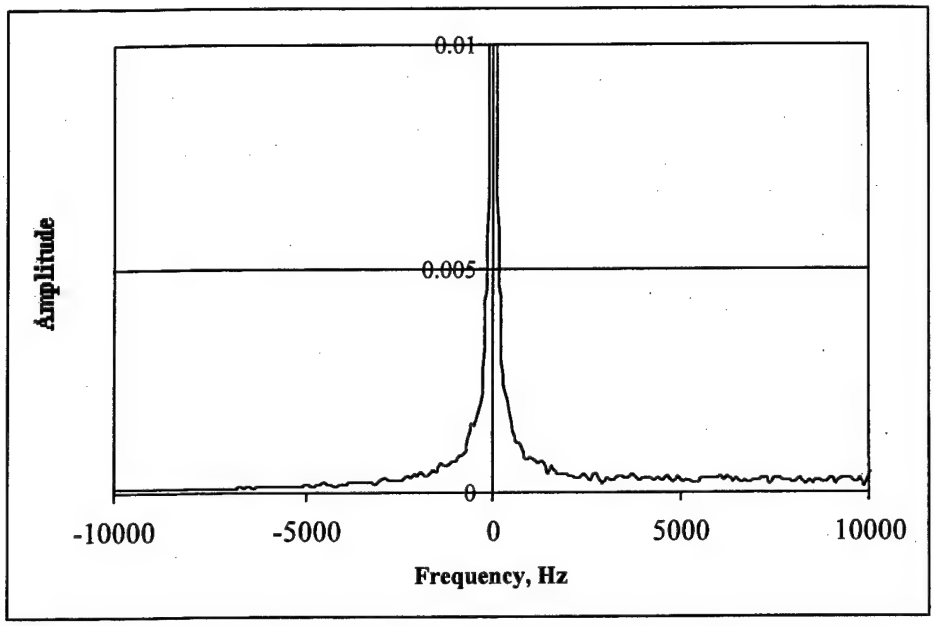

Figure 5.23. Summation averaged spectrum for tube # A3 (5 bendings)

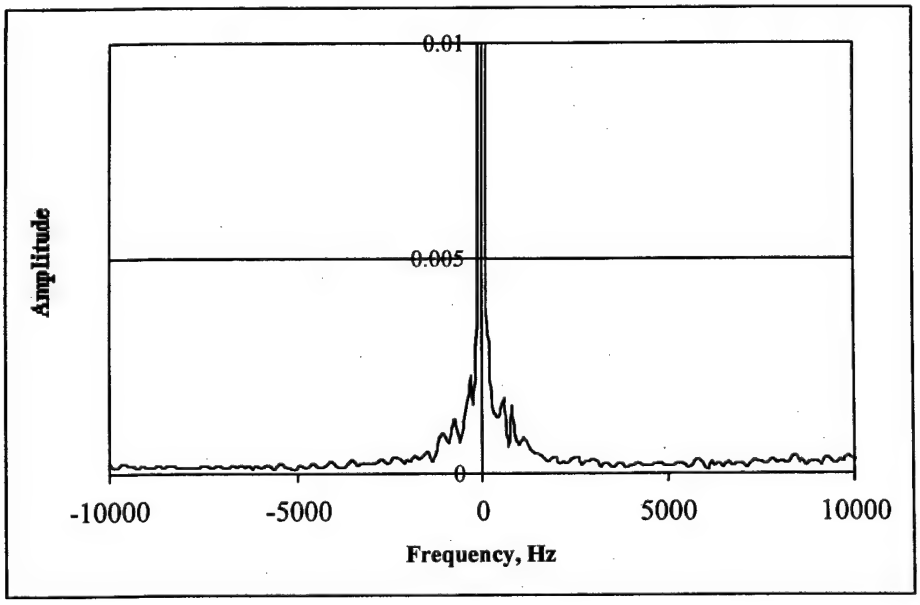

Figure 5.24. Summation averaged spectrum for tube # B3 (25 bending)

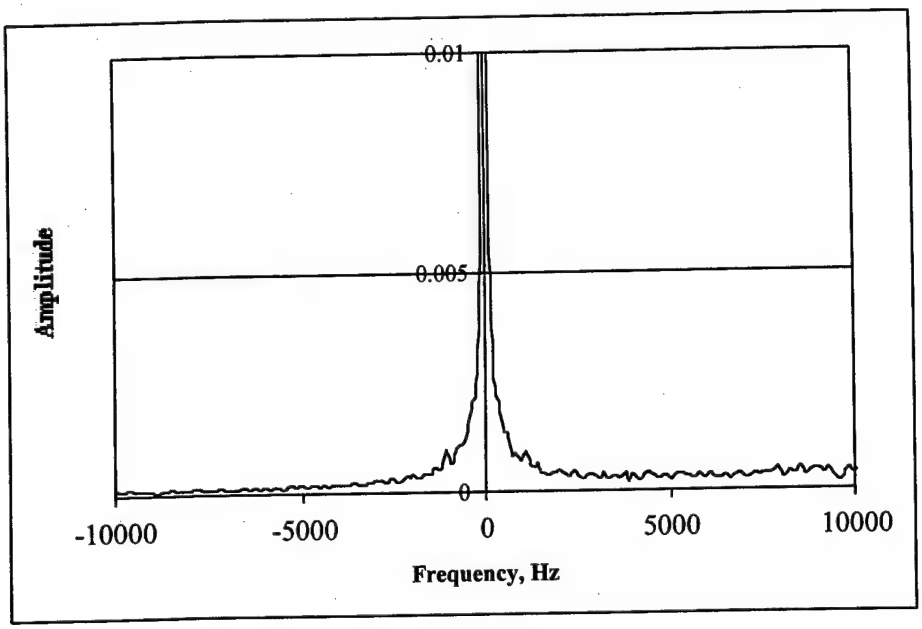

Figure 5.25. Summation averaged spectrum for tube # B4 (6 bendings)

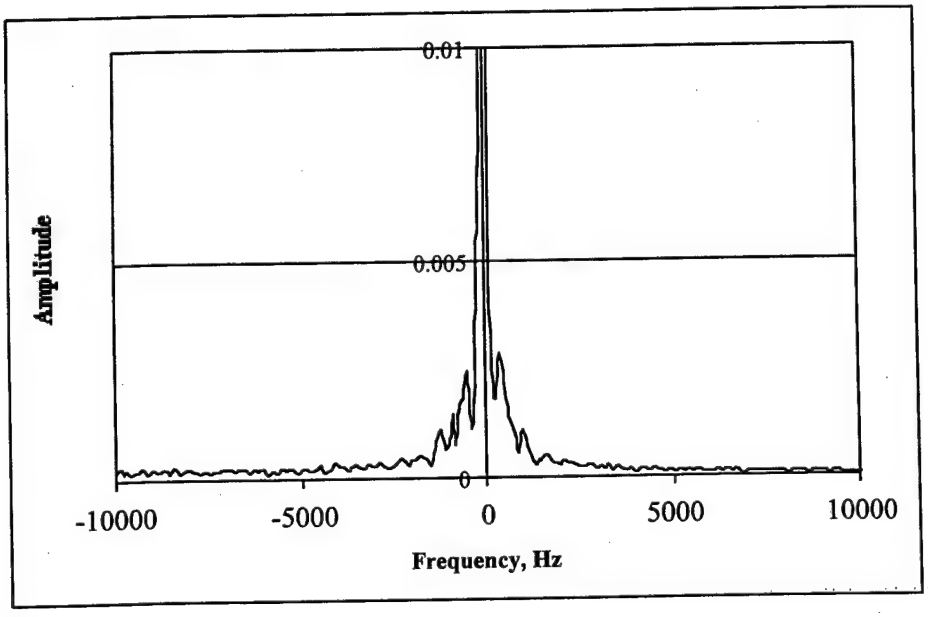

Figure 5.26. Summation averaged spectrum for tube # B5 (20 bendings)

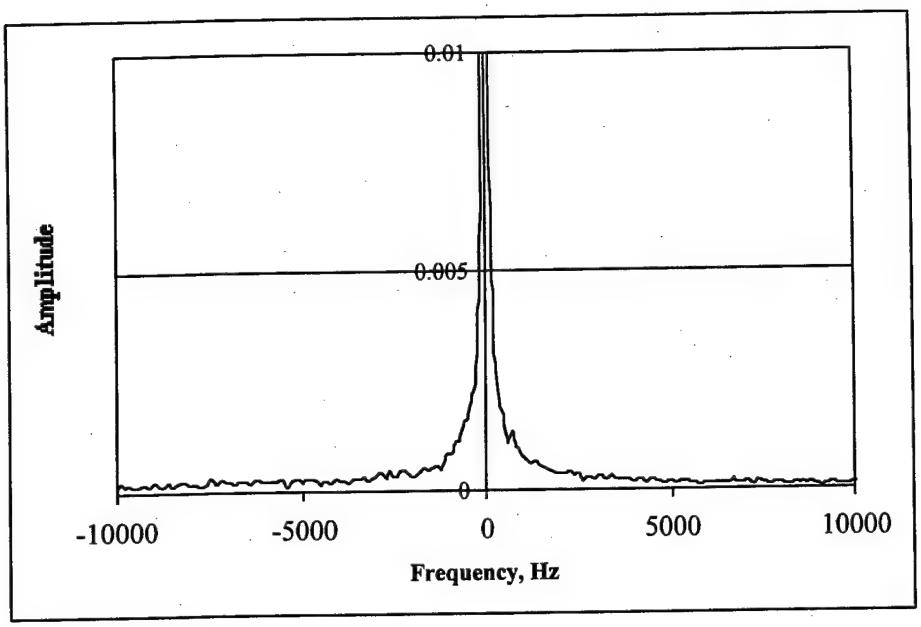

Figure 5.27. Summation averaged spectrum for tube # B6 (0 bending)

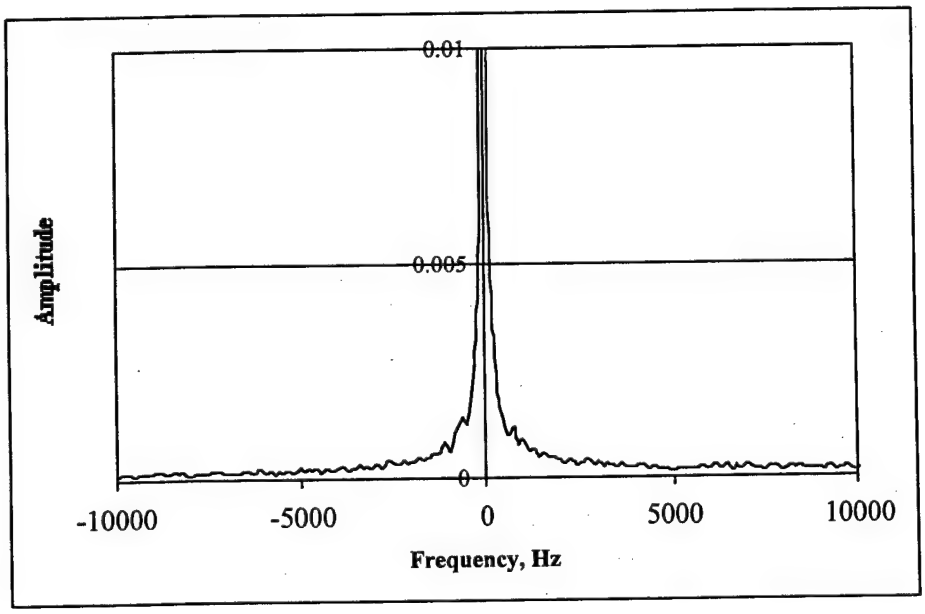

Figure 5.28. Summation averaged spectrum for tube # C1 (0 bending)

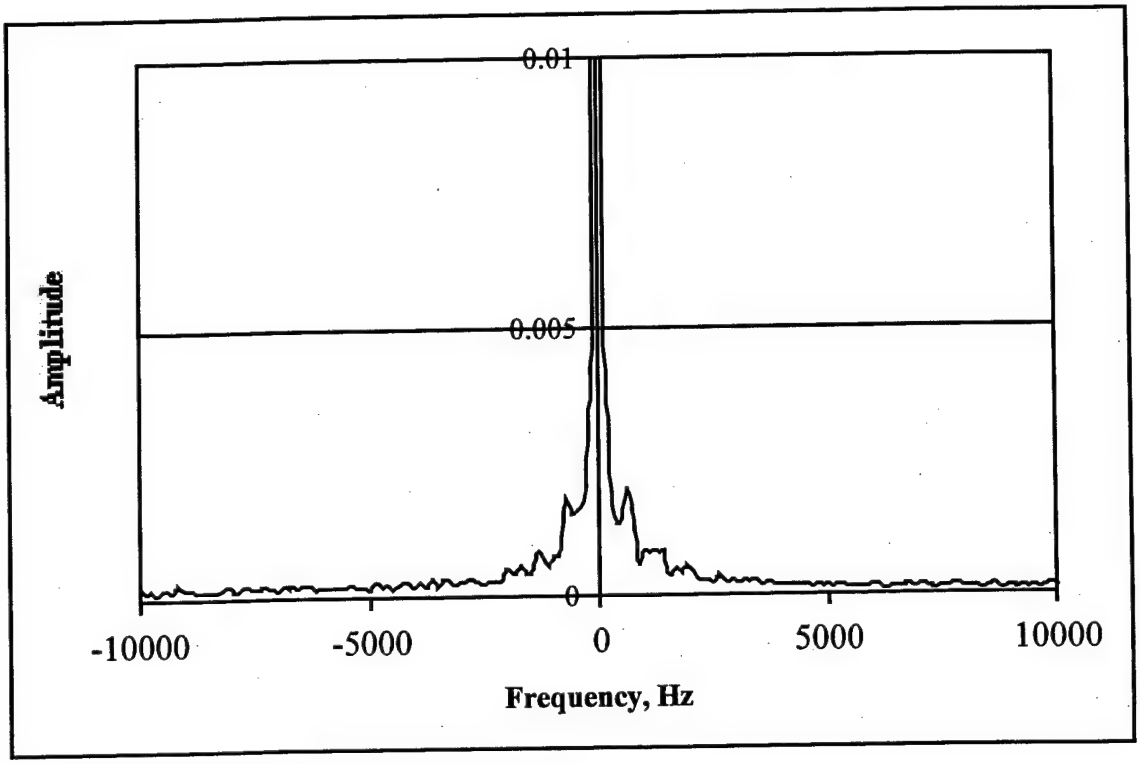

Figure 5.29. Summation averaged spectrum for tube # C2 (25 bendings)

6. Theoretical Models Describing the Modulation of Ultrasound by Vibration due to Defects

6. 1. The single crack model

The developed Vibro-Acoustic Modulation NDE technique deals with contact-type defects, such as cracks, unbonds, delaminations, etc. The physical nature of the defect-related nonlinearity can be most easily understood when we consider two simple models of contact-type defects. The first model was suggested by Richardson [3]. He considered a crack or contact defect as planar interface separating two semi-infinite elastic materials, with the surfaces in intimate contact but having no traction forces across the interface. As a longitudinally polarized elastic wave applied to the interface, the surfaces will stay together and move as one during the compression phase of the wave and then separate under the tensile phase. Such a periodic separation causes distortion of the passing wave (nonsymmetry of the compression and tensile phase) and leads leading to the high harmonics formation.

The second, more realistic model of a defect is a contact between two rough elastic surfaces [29, 30]. The applied stress will vary the contact area within the defect due to deformation of asperites in contact, leading to a nonlinear elasticity of the defect. Such a contact behaves as a nonlinear spring whose stiffness is proportional to the contact area within the defect interface. The linear model of the spring-type crack interface [31] connects displacements and stresses on both sides of an interface using spring stiffness constant K.

According to this model the internal stress $\Delta\sigma$ is normal to the crack interface is given as function of crack deformation by (6.1):

$$\Delta\sigma = K\xi, \qquad (6.1)$$

where ξ is the variation of the crack thickness, $\xi = U_+ - U_-$, $U_\pm$ are the deformations of the opposite sides of the crack. This simple model can be extended to include nonlinear behavior of the interface introducing dependence of the spring stiffness on the crack thickness, $K = K(\xi)$. It means that the applied vibration effectively changes the stiffness of the crack.

Using the Taylor's expansion of the spring stiffness dependence and leaving only the first-order term, since stresses in acoustical signals used in NDT are rather small, we obtain:

$$K = K_0 + \alpha\xi,$$

and

$$\Delta\sigma = (K_0 + \alpha\xi)\,\xi, \qquad (6.2)$$

where a is the nonlinear coefficient ($\alpha\xi << K_0$). This nonlinear model of a defect allows for description of various nonlinear effects, such as generation of second harmonic and modulation of ultrasound by vibration. The nonlinear coefficient, a, can be used for the quantitative description of these effects.

Some aspects of the sound modulation by vibration can be understood using theoretical model of a plane crack in a thin bar, as shown in Fig.6.1. As a nonlinear element, the defect can transform part of the incident acoustic energy into acoustic waves with different frequencies (harmonics and combination frequencies), effectively becoming a source of the nonlinear acoustic waves. In the case of modulation of ultrasound by vibration, we consider a flaw as a simple plane source of the acoustic waves with combination frequencies $\omega_3 = \omega_1 \pm \omega_2$, where is the frequency of applied vibration and ω_2 is the frequency of the incident ultrasonic wave.

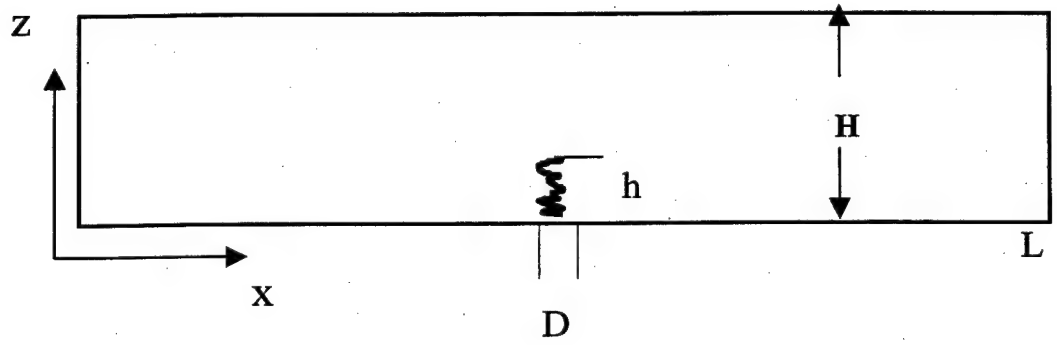

Figure 6.1 . The considered model of the crack in solid bar

For simplicity, we analyze interaction of waves propagating only in x-direction having wavelength of vibration greater than bar thickness $H << L$, where L is the bar length, so the thin bar approximation can be used. The crack interface is normal to the direction of wave propagation.

Let us consider the interaction at the crack interface of low frequency flexural vibration (modulating vibration) having longitudinal deformation

$$u_1(x,z,t) = U_1(x,z) \cos \omega_1 t \qquad (6.3)$$

with high frequency longitudinal ultrasonic which having deformation

$$u_2(x,z,t) = U_2(x,z) \cos \omega_2 t \qquad (6.4)$$

We assume that the crack has an effective thickness D and length h which are smaller than the wavelengths of the incident waves, so the crack does not have significant effect on the distribution of strain and stress fields in both low and high frequency waves.

The applied stresses change the thickness of the crack, so the crack thickness variation under the applied stresses can be determined as

$$\xi = D\frac{\partial(u_1+u_2)}{dx} = D\frac{\partial U_1}{\partial x}\cos\omega_1 t + D\frac{\partial U_2}{\partial x}\cos\omega_2 t \quad . \qquad (6.5)$$

The nonlinearity of the crack is characterized by the coefficient α defined by (6.2). This nonlinearity leads to interaction (modulation) of the higher frequency ultrasonic wave by the lower frequency vibration. As a result of such modulation the sidebands or wave with combination frequencies will be formed ($\omega_3 = \omega_1 \pm \omega_2$).

Substitution of.(6.5) into 6.2) gives an expression for the stress $\Delta\sigma_3$ at the combination frequencies:

$$\Delta\sigma_3 = \alpha D^2 \frac{\partial U_1(x_0,z_0)}{dx}\frac{\partial U_2(x_0,z_0)}{dx}\cos\omega_3 t, \qquad (6.6)$$

where x_0, z_0 are the coordinates of the crack. This stress, applied to the surrounding crack material produces the acoustical wave with sum and difference (combination) frequencies.

Let us consider standing wave flexural vibrations (resonance vibration), which are common for many practical applications. This situation also takes place in the experiment described below.

The standing low frequency flexural waves in thin elastic bar are determined by the formula :

$$w = A\cos k_1 x \cos\omega_1 t . \qquad (6.7)$$

Here w is the deformation of the bar in z direction, A is the amplitude of the deformation.

Boundary conditions for the bar free ends define the wave number as

$$k_1 L = \pi n \qquad (6.8)$$

Where n =1,2, ... is the number of mode.

The dispersion relationship for the flexural waves in thin elastic bar has the following form [32]:

$$k_1 = \left(\frac{12(1-\nu^2)\rho\omega_1^2}{EH^2}\right)^{1/4}, \qquad (6.9)$$

where E and ν are the Young's and Poisson's moduli of the bar material respectively; ρ is its the density.

The Equations (6.8) and (6.9) allow to find eigenfrequencies for flexural waves

$$f_n = \frac{n^2 \pi H \sqrt{E}}{4L^2 \sqrt{3\rho(1-\nu^2)}}$$

The longitudinal strain du_1/dx produced by the flexural wave is determined as [32]:

$$du_1/dx = z\frac{\partial^2 w}{\partial x^2} = -zk_1^2 A \cos k_1 x \cos\omega_1 t \ . \qquad (6.10)$$

Here z=0 corresponds to the neutral plane of the bar.

We consider the interaction between standing longitudinal ultrasonic and vibration flexible waves. In case of standing longitudinal ultrasonic wave its displacement is:

$$U_2 = B \cos k_2 x \,, \qquad (6.11)$$

where $k_2 = \omega_2/c_1$ *and* c_1 is the speed of the probing longitudinal wave:

$$c_1 = \sqrt{E/\rho} \,, \qquad (6.12)$$

Substitution (6.10) and (6.11) into (6) yields the equation for the crack generated force, F, at the combination frequencies $\omega_3 = \omega_1 \pm \omega_2$:

$$\mathrm{F} = lh\,\Delta\sigma_3 = alhz_0 k_1^2 k_2 D^2 AB \cos k_1 x_0 \sin k_2 x_0 \cos\omega_3 t \,, \qquad (6.13)$$

We consider the rectangular crack passing the whole bar.

Force F applied to the bar generates ultrasonic waves $U_3 \cos\omega_3 t$ at the respective combination frequencies ω_3. Since the wavelengths of these waves are greater than the bar thickness, we assume that the force F is uniformly distributed across the bar cross-section at the crack location $x = x_0$ and generates plane (zero-mode) longitudinal waves.

The resulting displacement distribution along the bar at the frequencies ω_3 can be presented in the form

$$U_3 = \begin{cases} C_1 \cos k_3 x & \text{if } x < x_0 \\ C_2 \cos k_3 (L-x) & \text{if } x \geq x_0 \end{cases} \qquad (6.14)$$

This form is chosen to satisfy the free boundary conditions at the end of the bar

$dU_3/dx\,|_{x=0,L} = 0$

and at the cross-section of the applied force F at $x = x_0$. Coefficients C_1 and C_2 are defined by the conditions of displacement continuity at the cross-section $x = x_0$:

$$U_{3+} = U_{3-} \qquad (6.15)$$

and the stress "jump" due to the applied force F:

$$\sigma_{3+} - \sigma_{3-} = 2\,F/S \quad , \qquad (6.16)$$

where S is the cross-section area of the tested plate.

The stress-strain relationship for the longitudinal deformations in the bar has the form:

$$\sigma_3 = E\frac{\partial U_3}{\partial x} \qquad (6.17)$$

The coefficients C_1 and C_2 can be found. Substituting (6.14, 6.17) into (6.15, 6.16)

Finally, the amplitude, U_3, of the longitudinal plane wave with the combination frequencies ω_3 is defined as:

$$U_3 = z_0 \alpha k_1^2 k_2 lhD^2 \frac{AB}{Sk_3 \sin(k_3 L)} \cos[k_3(L - x_0)]\cos(k_1 x_0)\sin(k_2 x_0) \qquad (6.18)$$

The term $1/\sin(k_3 L)$ in (6.18) indicates resonance nature of the waves with the combination frequencies. The dissipation of these waves can be accounted by introducing complex wave number

$$k_3 = k_3\,(1 + i/2Q)\,, \qquad (6.19)$$

here Q is the quality factor of the resonance oscillations of the bar at the frequencies ω_3.

Besides this resonance term, the solution (6.18) contains a few more frequency dependent terms, which could complicate the interpretation of the measurements. This problem can

be avoided by averaging of the measured nonlinear response across the frequency range. There could be two types of averaging yielding two criteria T_E and T_A:

The energy averaging

$$T_E = \frac{\sum_{n=1}^{N} U_3^2(f_n)/U_o^2(f_n)}{N} , \qquad (6.20)$$

and the amplitude averaging

$$T_A = \frac{\sum_{n=1}^{N} | U_3(f_n)/U_o(f_n) |}{N} . \qquad (6.21)$$

In the experiments we used the amplitude averaging of the received signals for the following reason. Near the resonance the amplitude is proportional to the quality factor Q, while the width of the resonance curve is proportional to $1/Q$. Therefore the amplitude averaging (integration) of the frequency response yields criteria independent (or weakly dependent) on the dissipation in the system.

As could be seen from Eqs. (6.18, 6.21) the amplitude of the modulation components and their frequency averaged values are linearly proportional to the amplitude of vibration A, amplitude of ultrasonic wave B, and the crack depth l.

$$T_A \sim U_3 \sim z_0 \alpha h l D^2 AB \qquad (6.22)$$

These dependencies were verified $U_3(f_n)$ experimentally.

The side component calculation had been conducted for several cases.

The polycarbonate plate

The first example is polycarbonate plate with 150 mm length and 10 mm thickness. The results of side component calculation for different crack positions are presented in fig.6.2 – 6.4 (modulation frequency 1 kHz, Q=500, frequency band 150 –250 kHz) are presented.

The variation of the side components for the frequency band 300-350 kHz is shown in figures 6.5 and 6.6. It can be noted when the frequency is increased a side component amplitude is decreased and the resonance peaks became smoother

The influence of tested object length is illustrated by fig.6.7. This figure presents the calculation results for plate with 250 mm length. The spectra show more resonance peaks in the same frequency band then for shorter plate.

It is observed that the level of side component depends on frequency. To eliminate effect of frequency on results of measurements we used the averaging of the side components according formula (6.21). The averaged values of the side components were calculated for the examples presented above and the results are given in figure 6.8. It also can be noted that the averaged level is slightly depends on the crack position and this variation decreases with the increasing of the frequency band.

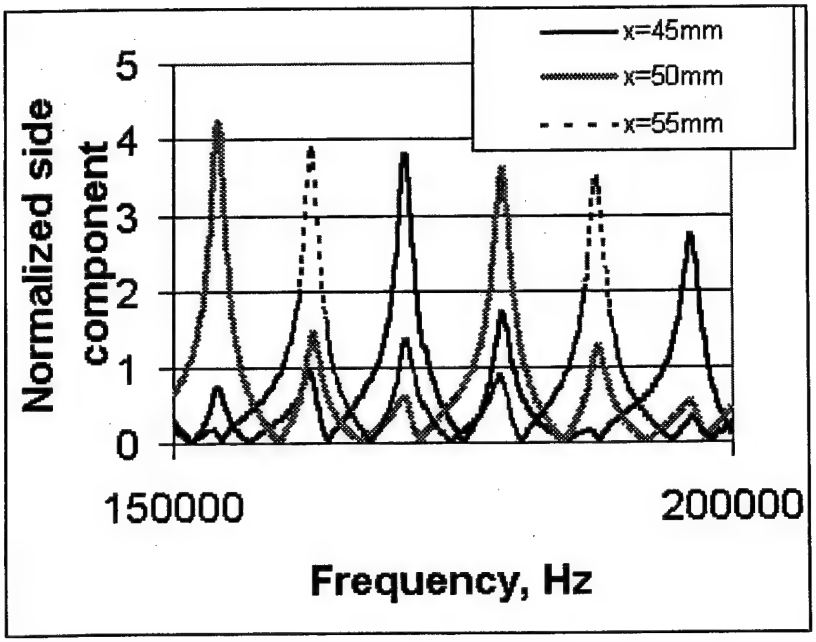

Figure 6.2. Effect of frequency on side spectral component for different crack positions. Specimen length =150 mm, frequency band from 150 to 200 kHz, Q factor Q=500.

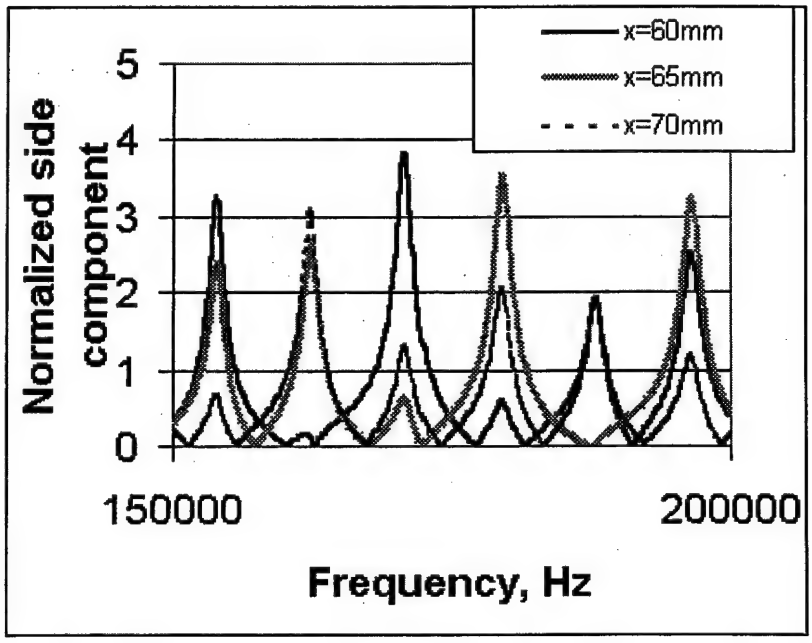

Figure 6.3. Effect of frequency on side spectral component for different crack positions. Specimen length =150 mm, frequency band from 150 to 200 kHz, Q factor Q=500.

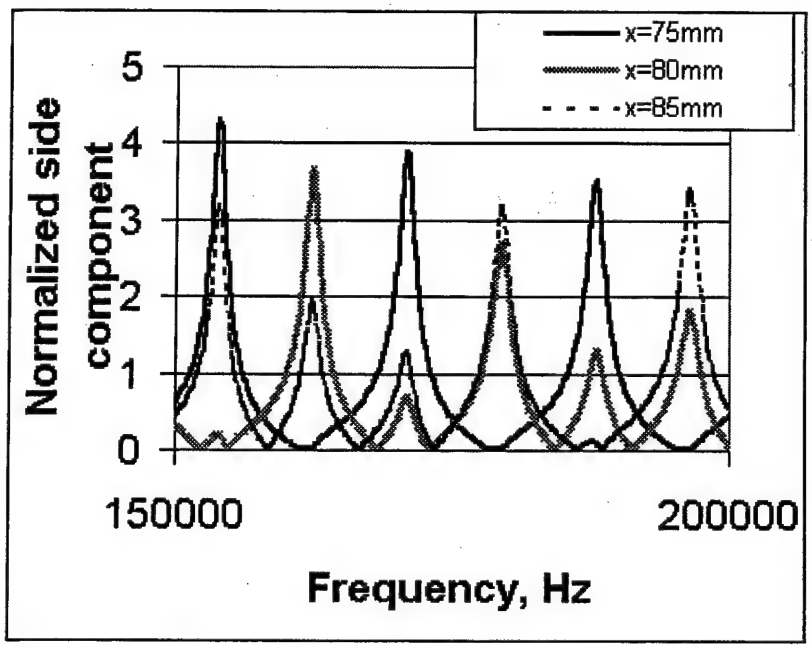

Figure 6.4. Effect of frequency on side spectral component for different crack positions. Specimen length =150 mm, frequency band from 150 to 200 kHz, Q factor Q=500.

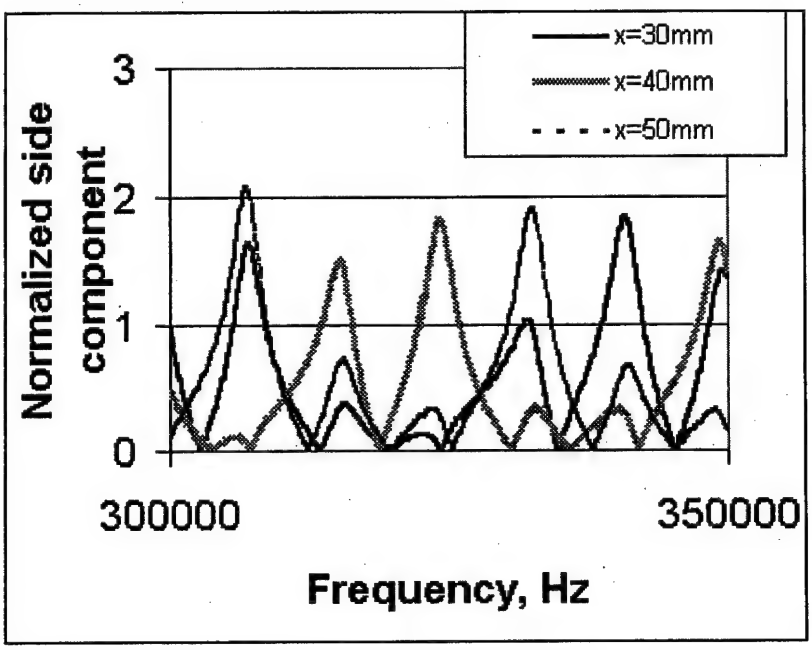

Figure 6.5. Effect of frequency on side spectral component for different crack positions. Specimen length =150 mm, frequency band from 300 to 350 kHz, Q factor Q=500.

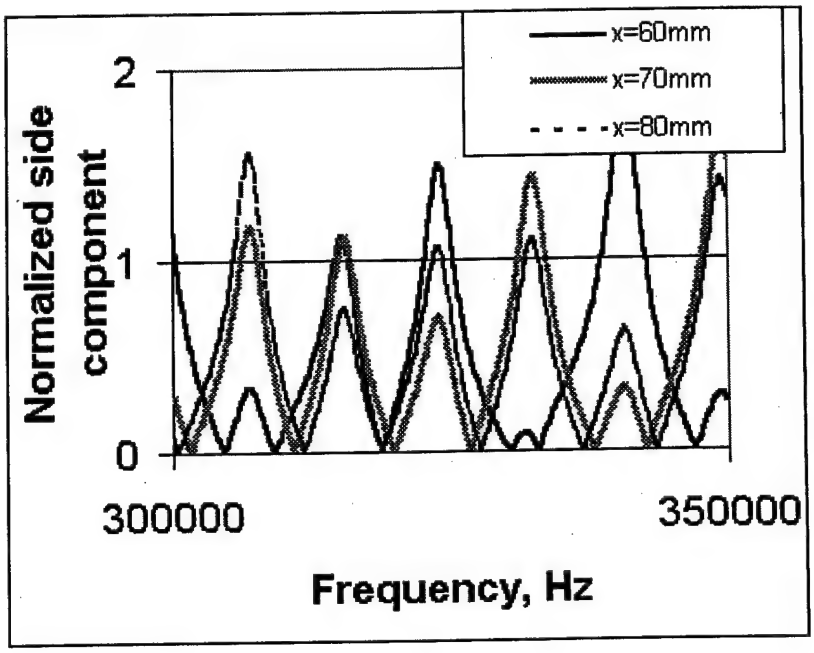

Figure 6.6. Effect of frequency on side spectral component for different crack positions. Specimen length =150 mm, frequency band from 300 to 350 kHz, Q factor Q=500.

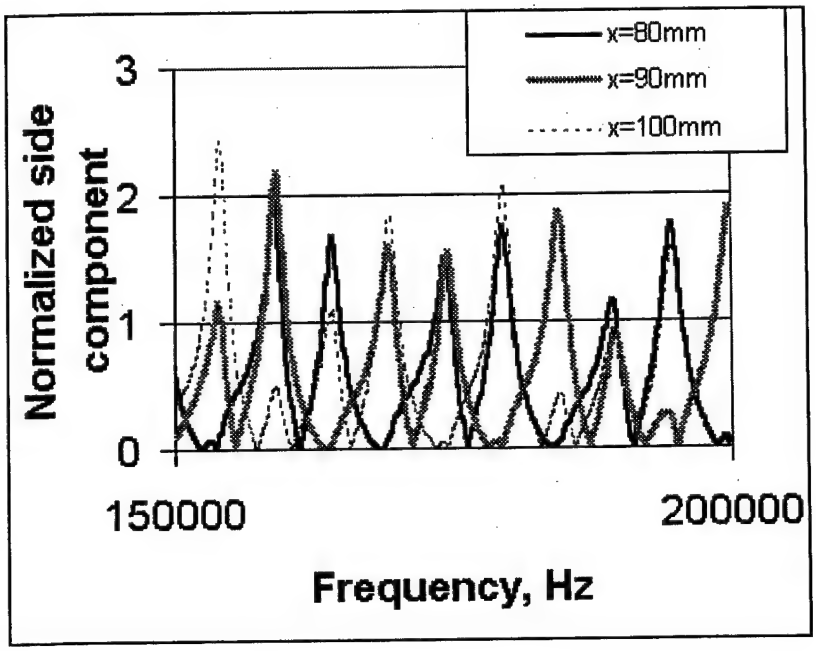

Figure 6.7. Effect of frequency on side spectral component for different crack positions. Specimen length =250 mm, frequency band from 150 to 200 kHz, Q factor Q=500.

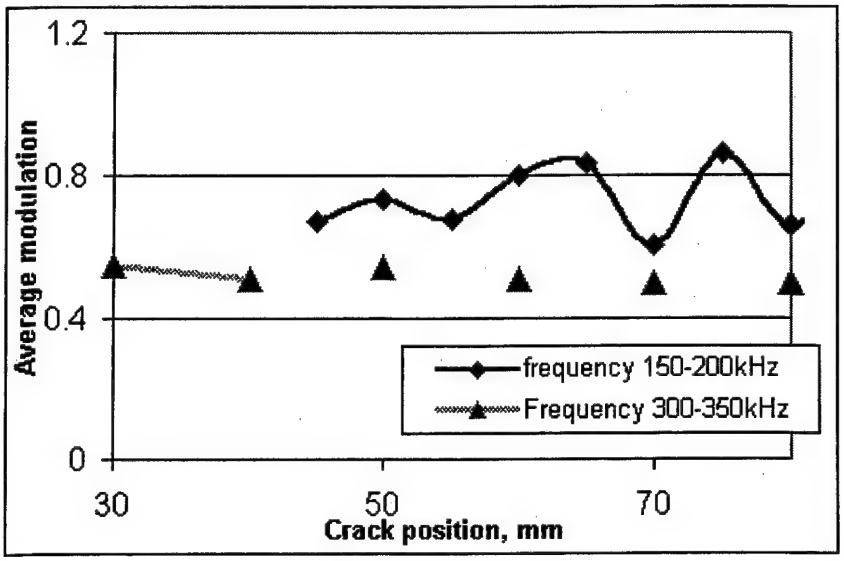

Figure 6.8. The dependence of average modulation level on crack position for two frequency ranges. The sample length is 150 mm.

6.2. Acoustic Crack Model for Scattered Damage

The acoustical model of a single crack was discussed in the previous part of report. The experimental results presented in sections 4 proved that the developed technique is also applicable for detection of material degradation when no cracks have been observed. The model for acoustical properties of material with a system of microcracks proposed below.

We assume that tested specimens have uniform distribution of microcracks (scattered damage) oriented isotropically and orientation of microcracks has the same probability.

Let's first consider a linear elastic isotropic media (matrix) with Young's modulus E_o, Poisson's ratio ν_o and the shear modulus $G_o = E_o / 2(1+\nu_o)$. The matrix contains cracks, which, for simplicity, are assumed to be identical, circular of radius r and distributed randomly (in the homogeneous manner) relative to both their locations and orientations. The crack density is defined as

$$\rho = \frac{nr^3}{V} \tag{6.23}$$

where n is the number of cracks in characteristic volume V.

Based on [34] Young's modulus E and Poisson's ratio ν of the media with system of randomly oriented microcracks with crack density ρ is :

$$E = E_o\left[1+\frac{16(1-\nu_o^2)(1-\nu_0/4)}{9(1+\nu_o/2)}\rho\right]^{-1}, \quad \nu = \nu_o\frac{E}{E_o} \tag{6.24}$$

The shear modulus G of the cracked media is:

$$G = \frac{E}{2(1+\nu)} \tag{6.25}$$

From (6.24) and (6.25), it is seen that the cracks transform the isotropic matrix into a new, also isotropic matrix with new elastic moduli.

Our goal is to find the parameter that characterizes interaction of ultrasonic wave modulation with vibration. This nonlinear acoustic parameter γ describes the derivation "stress-strain" dependence of the material from Hook's law. For longitudinal deformations this parameter is:

$$\sigma(\varepsilon) = E_o\,(\varepsilon+\gamma\varepsilon^2/2) \tag{6.26}$$

Therefore, the nonlinear parameter γ can be given as:

$$\gamma = \frac{1\partial^2\sigma}{E_o\partial\varepsilon^2}, \tag{6.27}$$

or in terms of E and σ *as:*

$$\gamma = \frac{\partial E}{\partial \sigma} \qquad (6.28)$$

Under assumption that crack concentration and variation is small the Eq.(6.24) can be written in form

$$E = E_0 + \Delta E$$

$$\Delta E = K\rho, \qquad (6.29)$$

Where

$$K = \left[\frac{16(1-\nu_o^2)(1-\nu_0/4)}{9(1+\nu_o/2)}\right]$$

The nonlinear parameter can be also expressed in term of applied stress and crack density on applied stress:

$$\gamma = K\frac{\partial \rho}{\partial \sigma} \qquad (6.30)$$

Hence, if we can find dependence of the density of open crack density on applied stress σ we will be able to determine nonlinear parameter γ.

Let's consider bilinear model approach. According this model all cracks are opened under the tension stress ($\sigma > 0$) and are closed under the compression stress ($\sigma < 0$). This model cannot adequately describe observed phenomena and we will consider more realistic model that includes the presence of residual stresses. Suppose that there are residual stresses in material and crack can be opened if the applied stress exceeds residual stress. Let describe residual stress by function of stress distribution $W(\sigma_*)$.
It means that $W(\sigma_*)\,d\sigma_*$ is a probability that residual stress in any crack is in the interval from σ_* to $\sigma_* + d\sigma_*$.

Let consider the Normal distribution of residual stresses:

$$W(\sigma_*) = \frac{1}{\sqrt{2\pi}\Delta}\exp\left(-\frac{1\sigma_*^2}{2\Delta^2}\right) \qquad (6.31)$$

Where Δ is variance of residual stress distribution. Suppose that the average value of the residual stress is close to zero.

First let's consider the case when the longitudinal stress σ is applied to the thick bar having uniform crack distribution. Let consider the cracks having the normal **n** oriented

at an angle φ to the z axis (Fig.6.9). The normal stress applied to these cracks is defined by equation:

$$\sigma_{nn} = \sigma \cos^2 \varphi$$

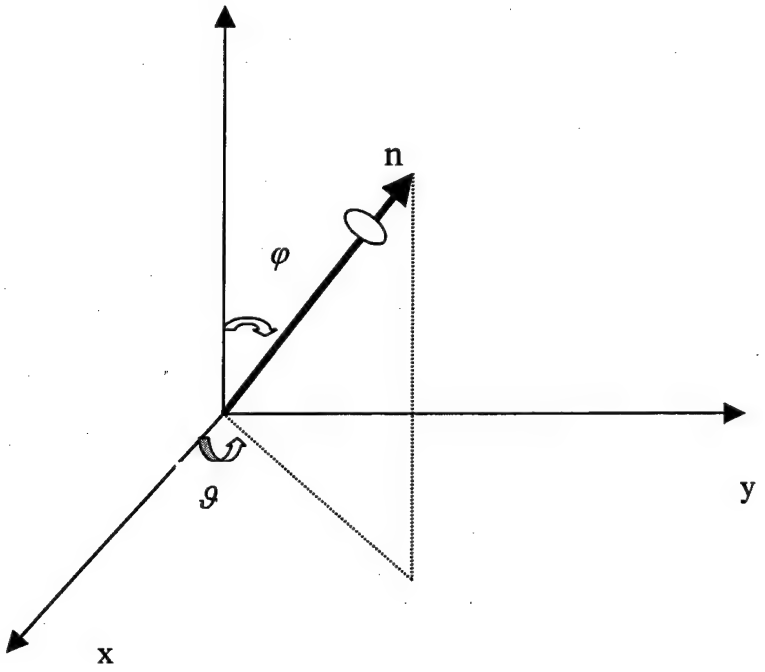

Figure 6.9. The coordinate system described crack orientation

The crack density having orientation of the normal between (φ,θ) and (φ+dφ, θ+dθ) is defined by equation:

$$N(\varphi,\theta) = \frac{\sin\varphi}{4\pi} \qquad (6.32)$$

(0<φ<π, 0<θ<2π).

The crack is opened if the normal stress applied to the crack exceeds residual stress acted on the crack. The density of the opened cracks can calculated as

$$\rho(\sigma) = \rho_o \int_{-\infty}^{\sigma\cos^2\varphi} W(\sigma_*)d\sigma_* \int_0^{\pi}\int_0^{2\pi} N(\varphi,\theta)\,d\theta\,d\varphi \qquad (6.33)$$

Where ρ_o is the crack density when all cracks are opened.

The nonlinear parameter γ can be found by derivative of this equation according (6.30)

$$\gamma = K\frac{\partial \rho}{\partial \sigma} = \rho_o \frac{K\partial}{2\partial\sigma}\int_{-\infty}^{\sigma\cos^2\varphi} W(\sigma_*)d\sigma_* \int_0^{\pi}\sin\varphi d\varphi \tag{6.32}$$

This differentiation with respect to a parameter can be conducted by Leibnitz's rule

$$\frac{\partial}{\partial\lambda}\int_a^{v(\lambda)} f(x,\lambda)dx = \int_a^{v(\lambda)} \frac{\partial f(x,\lambda)}{\partial\lambda}dx + f(v,\lambda)\frac{\partial v}{\partial\lambda} \tag{6.33}$$

Rearranging (6.33) :

$$\gamma = \frac{\rho_o}{2}KW(0)\int_0^{\pi}\cos^2\varphi\sin\varphi d\varphi = \frac{\rho_o}{3}KW(0) \tag{6.34}$$

Substitution of residual stress distribution from (6.31) gives the final answer for nonlinear parameter of the cracked media:

$$\gamma = \frac{\rho_o K}{3\sqrt{2\pi\Delta}} \tag{6.35}$$

It can be noted that the nonlinear parameter is proportional to the crack density and inverse proportional to the variance of residual stress distribution.

7. Impulse Nonlinear Method of Crack Location

The NEWS technique used CW ultrasonic signal and described above proved high sensitivity for "pass –fail" test but cannot be used to locate a crack position. We propose that the crack location can be defined by a pulse modulation method. This technique provides precise defect location and the concept is shown in fig.7.1.

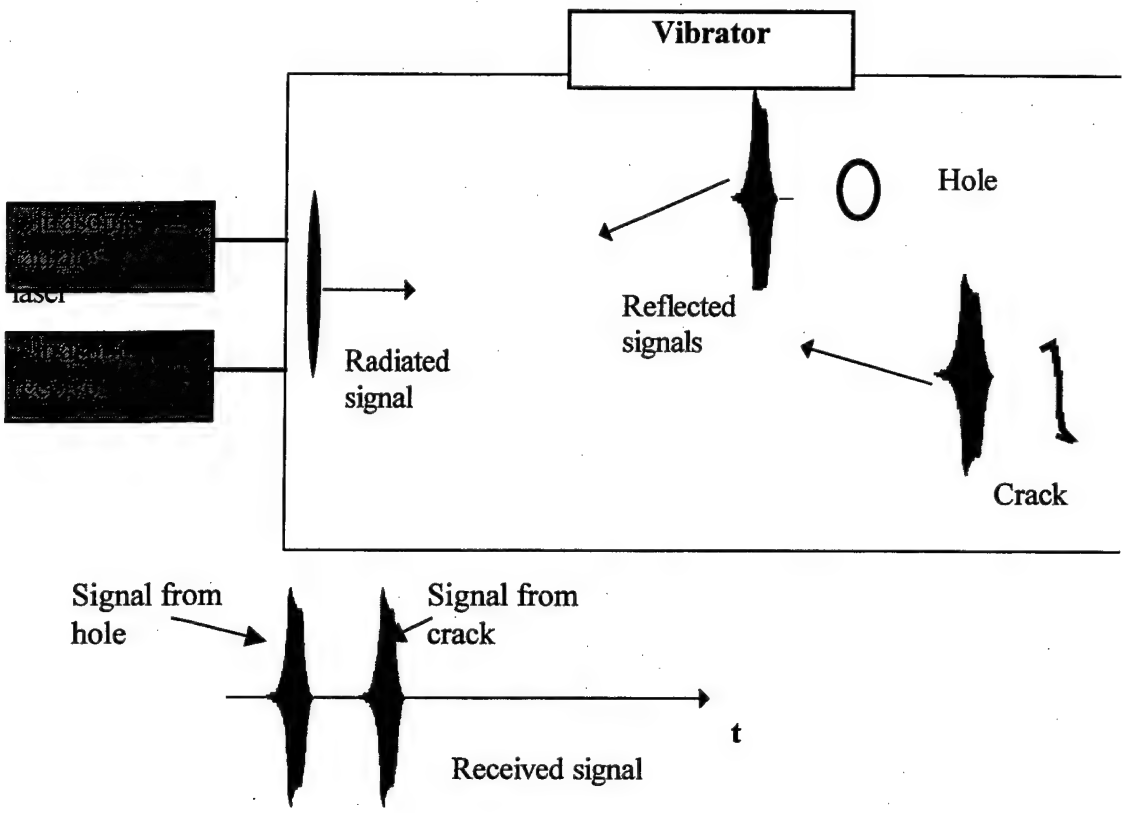

Figure 7.1. Schematic of nonlinear acoustic technique for flow location.

The acoustical transducer in conventional technique produces an ultrasound impulse propagating in the specimen. This impulse is reflected from different kinds of inhomogeneities. For example, and the reflected signals from a hole and a crack are presented in fig.7.1. Reflected signals came at different time but there is no way to distinguish what signal is reflected from the crack and what signal from the hole. These signals can be easily distinguished if mechanical vibration can be applied to the specimen. Due to vibration the amplitude and phase of the ultrasound signal reflected from crack will be modulated, while the signal reflected from linear defect (the hole) has no modulation. This situation is illustrated in fig.7.2.

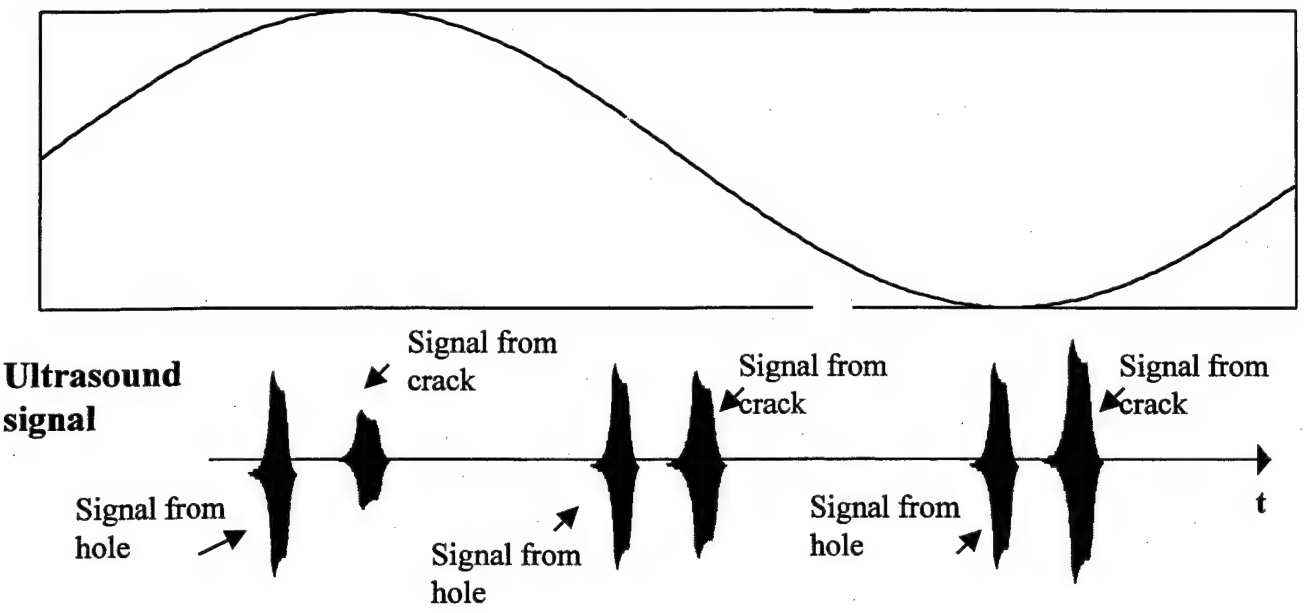

Figure 7.2.. The time tracks of the ultrasound signal reflected at different phases of the vibration.

The upper part of this figure presents the harmonic vibration with low frequency. The lower part of the fig. 7.2 shows signals reflected from the defects at different times. The first pair is reflected at the moment when the applied vibration stress reaches the maximum. At this time the crack is compressed and the signal reflected from the crack has minimal amplitude. The second pair of impulses is shown at time when the vibration stress is small and there is no change in the reflected impulse. The third pair is extension phase of the vibration, at that moment the crack is maximally opened and the reflection signal is higher than in previous phases. The modulation of this signal manifests the crack presence allows us to distinguish the crack-like defects from other inhomogeneities.

The test demonstrated this approach was carried out by using a piezoceramic transmitter of ultrasound wave.

First experiments were conducted on cylindrical aluminum rods of (length = 91cm; diameter 1 cm). The rods with a crack and with a notch were investigated.

The experimental setup is shown in fig. 7.3. The high frequency piezoceramic transducer and receiver were used for radiation and reception of the ultrasound wave with frequency of 1.2 MHz. Low-frequency vibrations of the rod were excited by a vibrator (mass 557 g). The vibrator can provide different excitation frequencies and for our experiment the

frequency around 10.5 Hz was chosen, which is the main flexural resonance frequency of the rod loaded with the mass of vibrator (557 g).

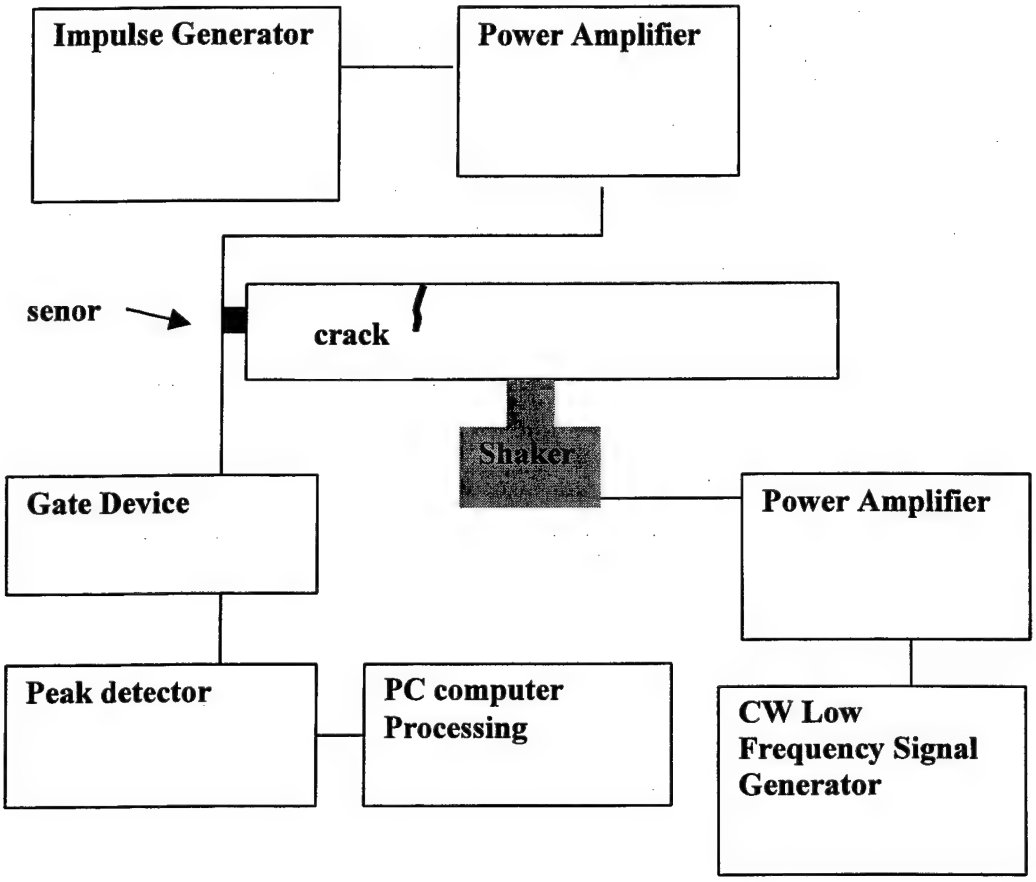

Figure 7.3. The experimental setup to impulse nonlinear method of crack location.

The time tracks of the received signals reflected from the notch and the crack are presented in fig.7.4. It is seen that there is no clear difference between the signals reflected from the defects.

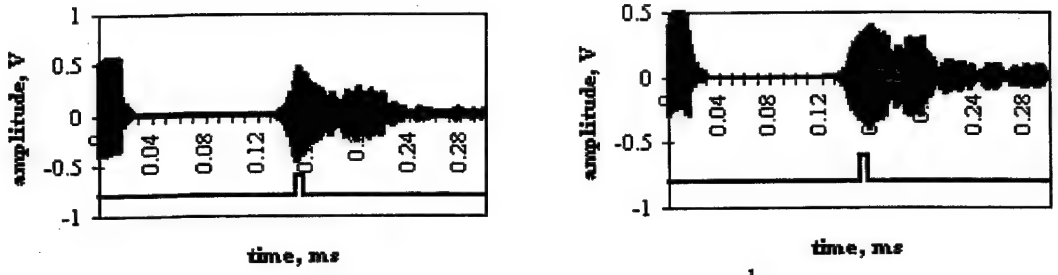

Figure 7.4. The time tracks of the signals reflected from the notch (a), and the crack (b)

The received ultrasound signals passed trough the gating device, which allows the receipt of signals during a definite time interval. In the experiment this time interval was chosen as 6 ms. The starting time can vary to allow us to pick up the signal from different distances. From the gating device the signal was sent to a peak detector and the sequence of the impulses was observed after detection. This sequence is modulated by low frequency vibration if a signal is coming from the crack. The manifestation of such modulation can be easily seen in the spectrum of the detected signal. The presence of modulation gives a harmonic component with the vibration frequency while there are no such components in the spectrum of the signal reflected from the hole (see Figure 7.5.).

It is clear that this effect can be used to distinguish cracks from other kinds of inhomogeneities.

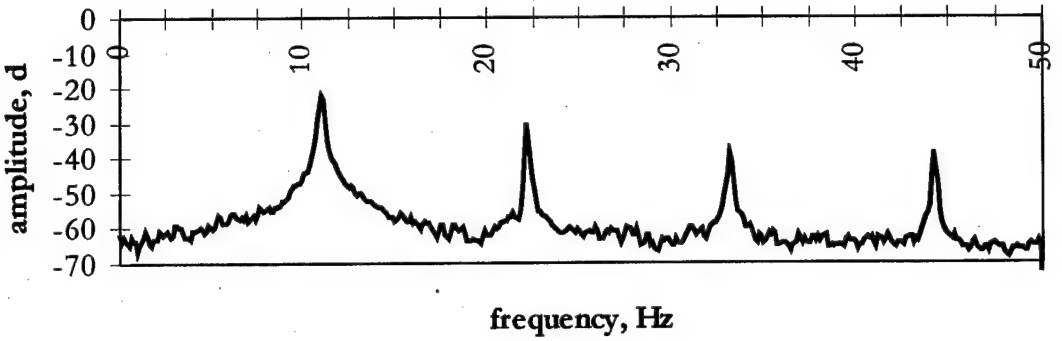

Figure 7.5a. The spectrum of the signal reflected from the crack.

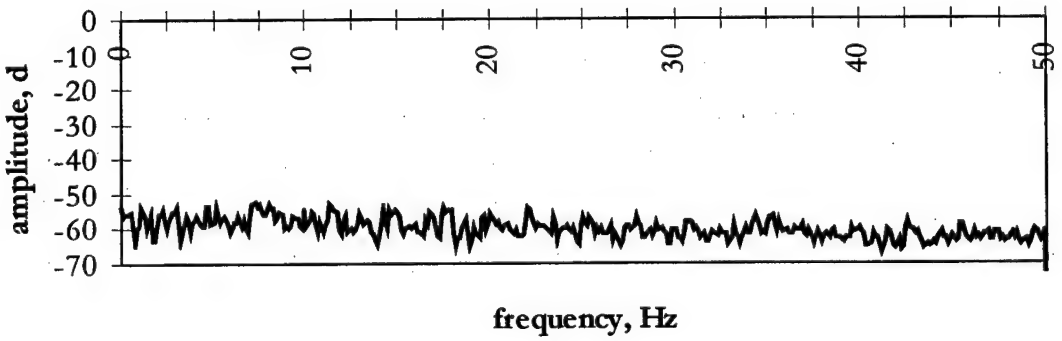

Figure 7.5.b. The spectrum of the signal reflected from the hole.

The another experiments have been conducted by using higher probe ultrasonic frequency (3 MHz) that allowed to increase the spatial impulse resolution. The steel plate having length about 145 mm and width 60 mm was used for demonstration. The crack in the plate was grown in UIC under cyclic loading. The sensor was placed on the side of plate and the technique described above was applied to get received impulse.

Figures 7.6 and 7.7. demonstrates the result of measurements. The linear reflection signals and side level in nonlinear processing are presented in 3D form. Axis Z is transverse coordinate of plate where sensor was placed. The distance between sensor and point of reflection is measured along X axis. This coordinate is connected with time of the reflected signal by using formula:

x=2ct

Where c is the sound speed of the tested signal..

It is clear seen that the linear technique gives very similar signal s from the crack and the hole whereas the nonlinear processing provides very distinguish difference between cracks and defect without nonlinear properties (like holes).

The amplitude dependence for nonlinear signal was also checked. The fig.7.8. presents the result nonlinear imaging for two different level of low frequency vibration. It is seen that the side component value increases with vibration amplitude.

The fig.7.9. gives the dependence of the side component signal versus vibration displacement. It is seen that this dependence is close to the linear one. It confirms the theoretical model presented in section 6 of the report .

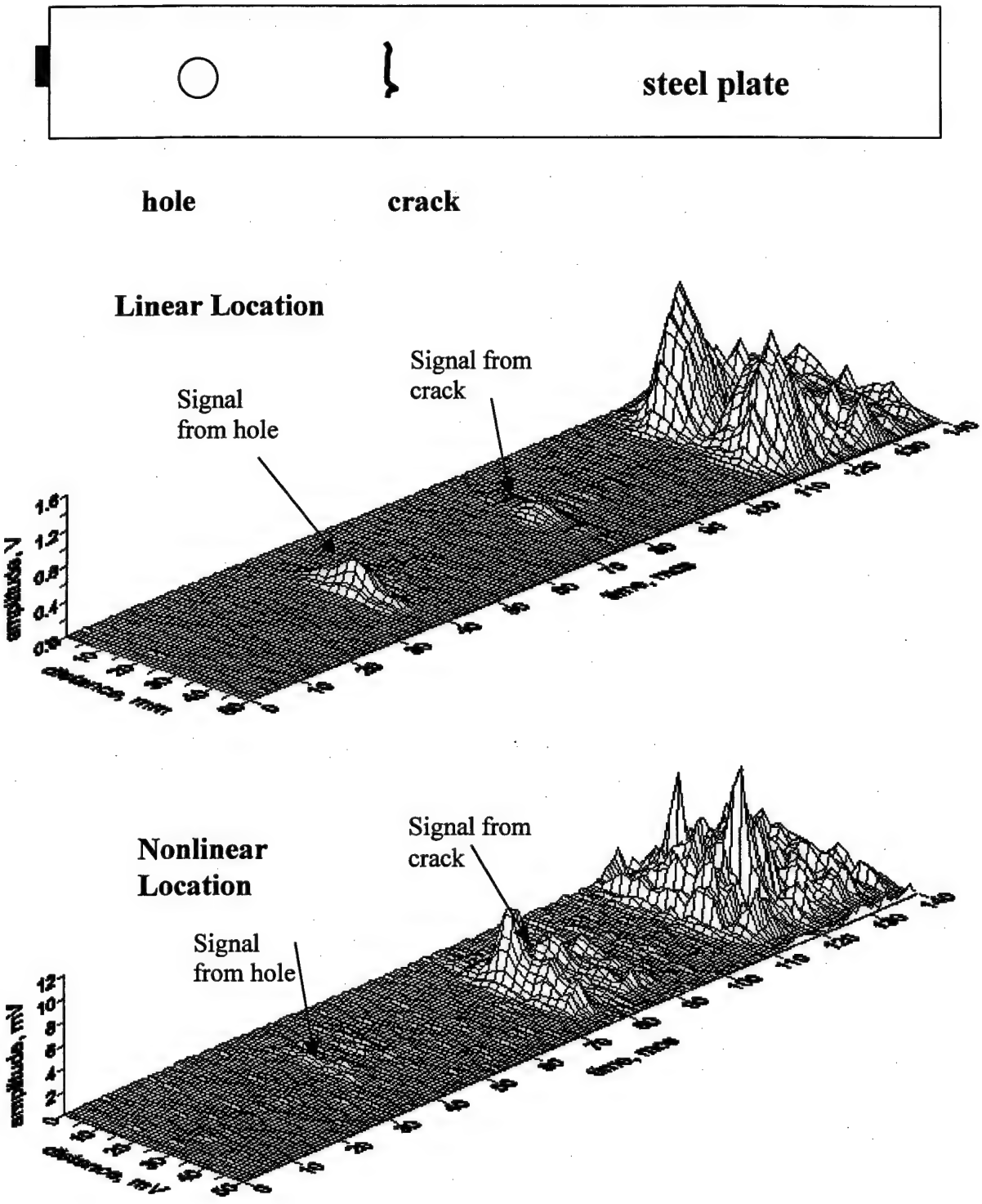

Figure 7.6. Comparison of linear and nonlinear location. Hole is situated closer to the sensor then the crack. The nonlinear signal from the crack significantly exceeds the nonlinear signal from the hole. The signals near the plate end are due to the reflection from the end.

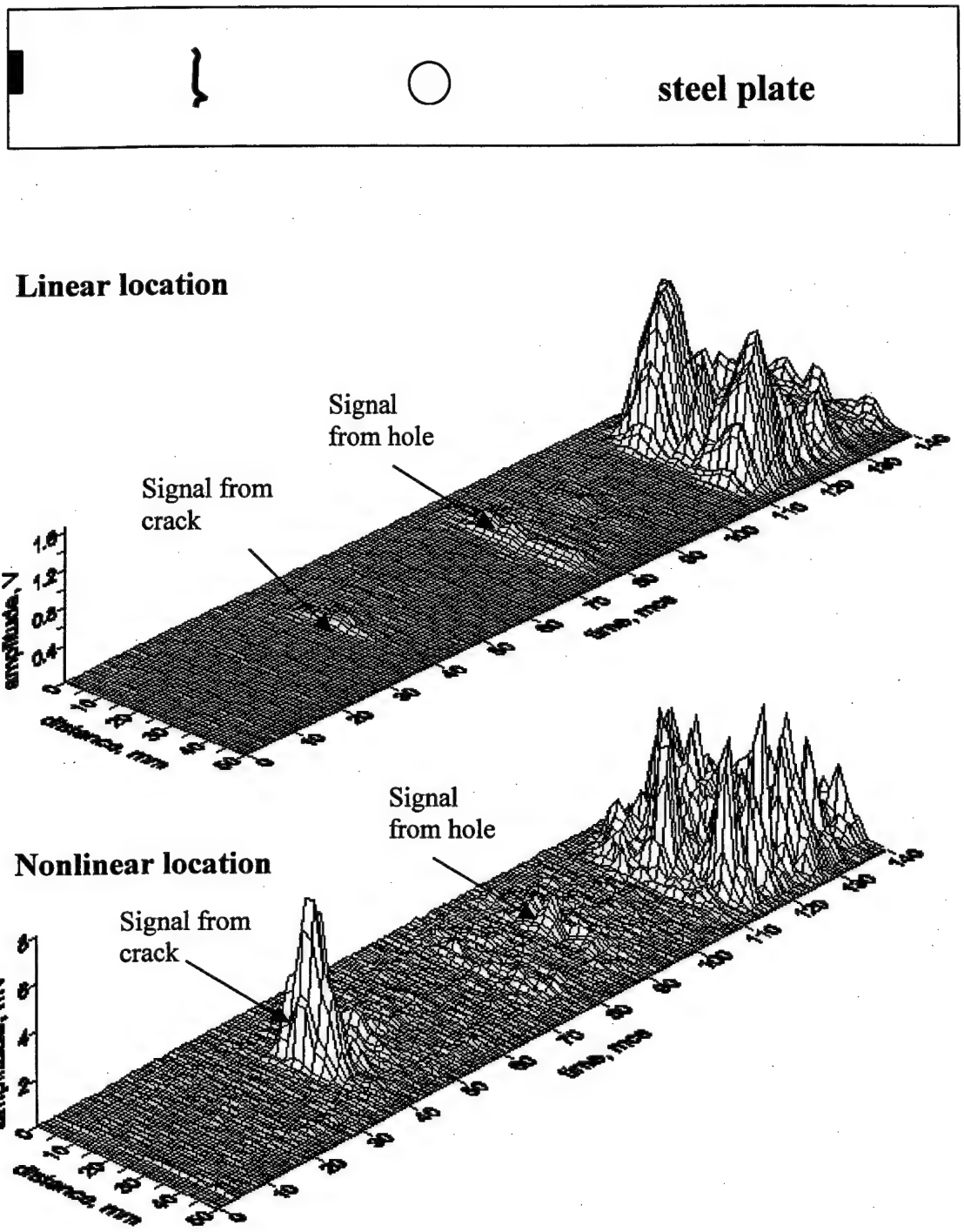

Figure 7.7. Comparison of linear and nonlinear location. The crack is situated closer to the sensor then the hole. The nonlinear signal from the crack significantly exceeds the nonlinear signal from the hole. The signals near the plate end are due to the reflection from the end.

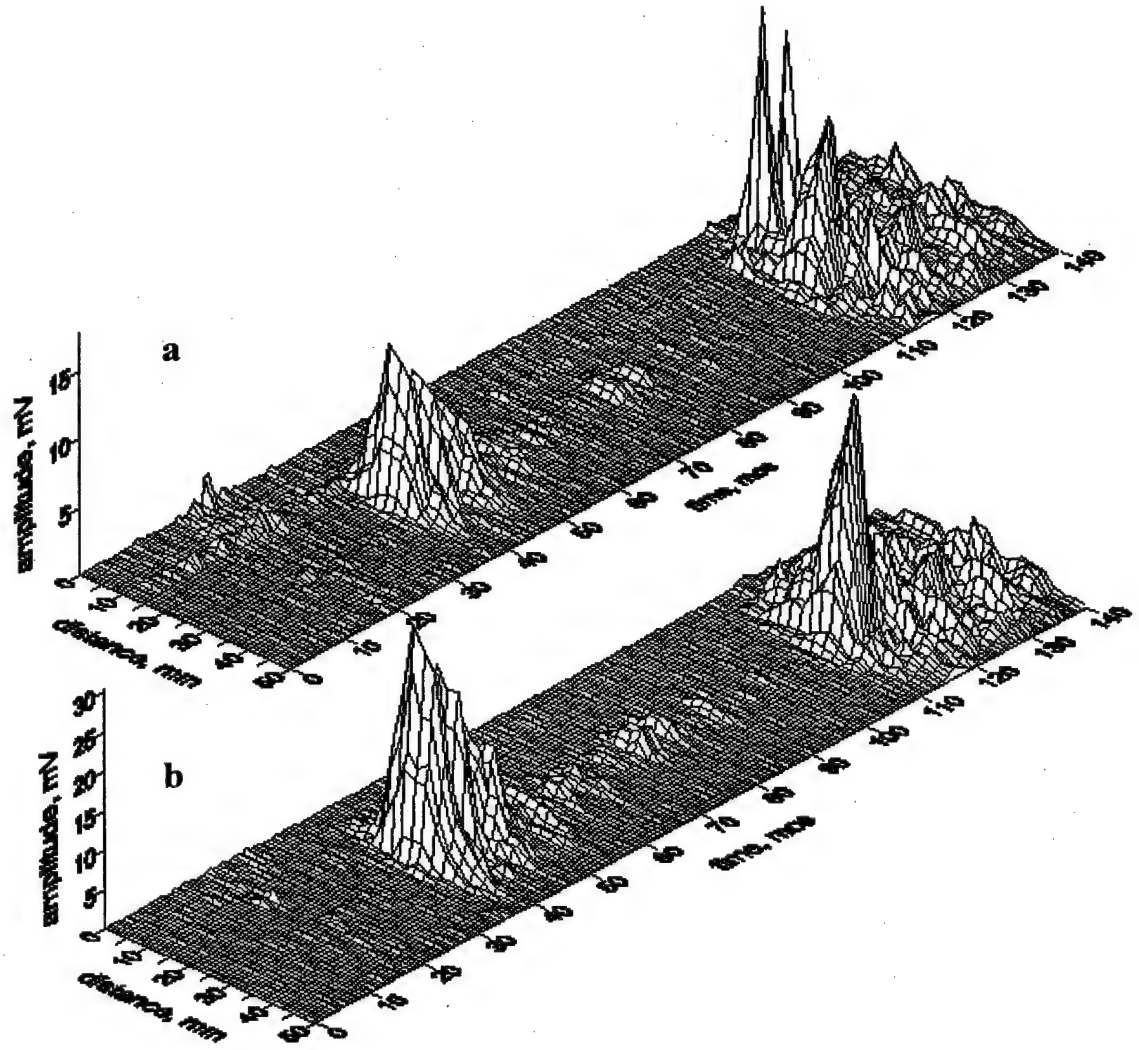

Figure 7.8. The results of nonlinear location for different level of low frequency vibration, a – the vibration displacement is 0.1 mm, b – the vibration displacement is 0.5 mm

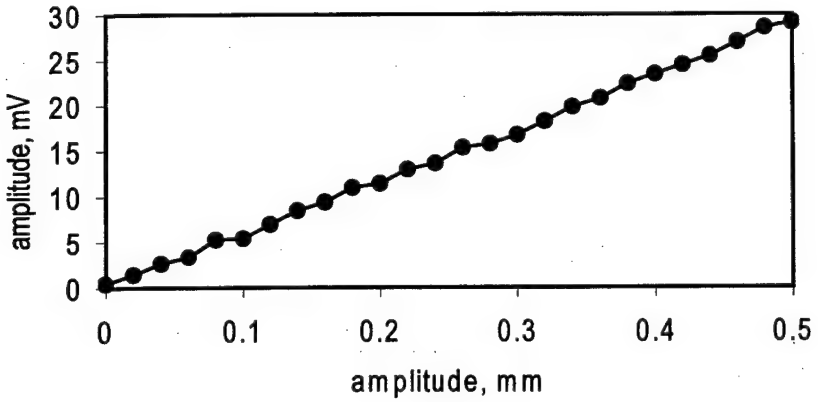

Figure 7.9. The dependence of the side band signal from the vibration amplitude.

8. Kinematics and Mechanical Design of the Instrumental Hammer

This part of report gives the calculation of the instrumental hammer parameter that can provide necessary impact excitation

The hammer has to provide the following parameters:

Impact Impulse: from 200 to 2000 N msec

Distance to sample: from 5 to 20mm

Source of energy: spring.

8.2. Process of impact

The main parameter that the hammer has to provide is the impact impulse

$$S = F\,t,$$

Where

F is force, t is the impulse duration.

Because the hummer head is bounced after the impact

$S = m\,(u+v)$,
where

m - mass of the hammer head
u – speed after impact
v - speed before impact

Coefficient of restitution :

$$k = u/v$$

When the speed is v =3 m/s , k = 0.6-0.8 for steel – steel impact

$$u = kv$$

$$S = m\,(k+1)\,v$$

Speed of the hammer head to provide required impulse is

$$v = S/m\,(k+1) \qquad (8.1)$$

8.3. Calculation of spring parameters.

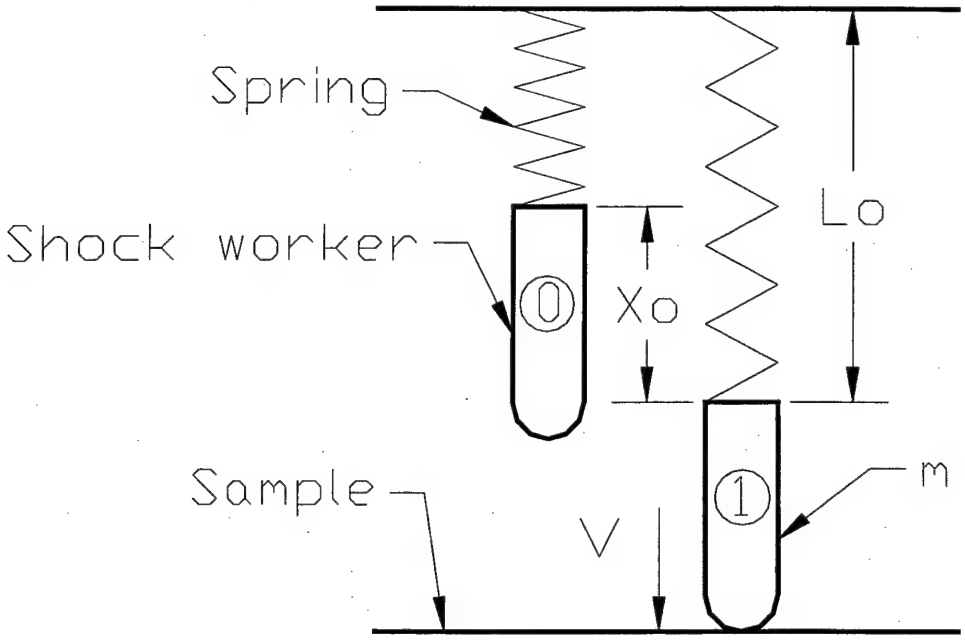

Figure 8.1. Process of shock.

Lo = free length of spring
Xo = deformation of spring before impulse

Change of kinetic energy of system

$mv''/2 - mv''o/2 = \Sigma A$, where

vo = initial speed
v = final speed
A = total work

Work of spring force F:

$F = C X$,

where

C = stiffness
X = deformation

$A = C (X''o - X''1) / 2$

At the end of release deformation of spring is zero and the work is:

$A = C X''o / 2$

Therefore,

$mv'' / 2 = C X''o / 2$

Speed at the end of flight:

$v = Xo \sqrt{C/m}$ (8.2)

From (8.1) and (8.2)

$S / m (K+1) = Xo \sqrt{C/m}$, where

Stiffness:

$C = [S / Xo (K+1)]'' / m$ (8.3)

If:
S = 0.5N Sec
Xo = 0.04 m (1.6")
K=0.7
m = 0.1 kg
C = 550 N/m

From (8.2):

v = 2.83 m/sec

Work is made by spring force and weight of the worker (shock from up to down)

$\Sigma A = C X''o / 2 + m g Xo = mv'' / 2,$

where

$v = \sqrt{(CX''o/m+2gXo)}$

If:
m = 0.1 kg
C = 500 N/m
Xo = 0.04 m
V = 2.96 m/sec
Difference is (2.96 - 2.83) / 2.83 = 0.047 or 4.7%

Conclusion: weight doesn't significantly affect the speed

8.4. Shock worker without free flight

Range of regulation by one spring.

Schematic is shown in Figure 8.2.

Lo = free length of spring
ΔX = motion of shock worker
X = deformation of spring for regulation

Xo = deformation of spring before impact
X1 = deformation of spring after impact
S1 = min. impulse from the spring
S2 = max. impulse from the spring

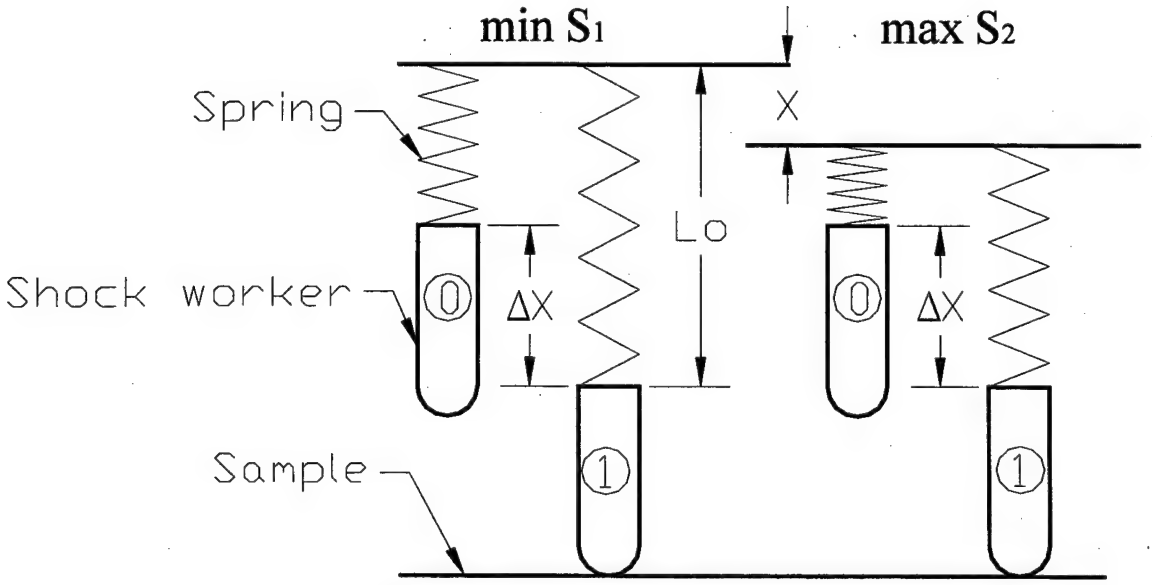

Figure 8.2. Regulation by one spring

For S1: Xo = ΔX
X1 = 0

For S2: Xo = X + ΔX
X1 = X

Change of kinematical energy of system

$mv''/2 = C (X''o-X''1) / 2$, where

$v = \sqrt{C(X''o - X''1)}/m$ (8.4)

$V2 / V1 = S2 / S1 = Ks$, where

V1 and V2-min. and max. speed

$V 2 = Ks V1$ (8.5)

For min S1:

$V1 = \sqrt{C(\Delta X''-0)}/m$

For max S2

:

$V2 = \sqrt{C(X+\Delta X)''-X'')}/m = \sqrt{C(\Delta X''+2\Delta X X)/m}$

$V2 = Ks V1$

$\sqrt{C(\Delta X''+2\Delta X X)/m} = Ks \Delta X$, where

X = deformation of spring for regulation

$X = (Ks''-1) \Delta X/2$

For ratio:
Ks = S2 /S1 = 2000/200 = 10
And $\Delta X = 25mm$

X = 1112mm. That is too much

For ratio:
Ks = 1.5
And $\Delta X = 25mm$

X = 15mm

For ratio:
Ks =2 X=37.5mm

Therefore one spring can regulate for Ks in the range from 1.5 to 2

Variation of speed by change of the distance between worker and sample (internal range of spring deformation)

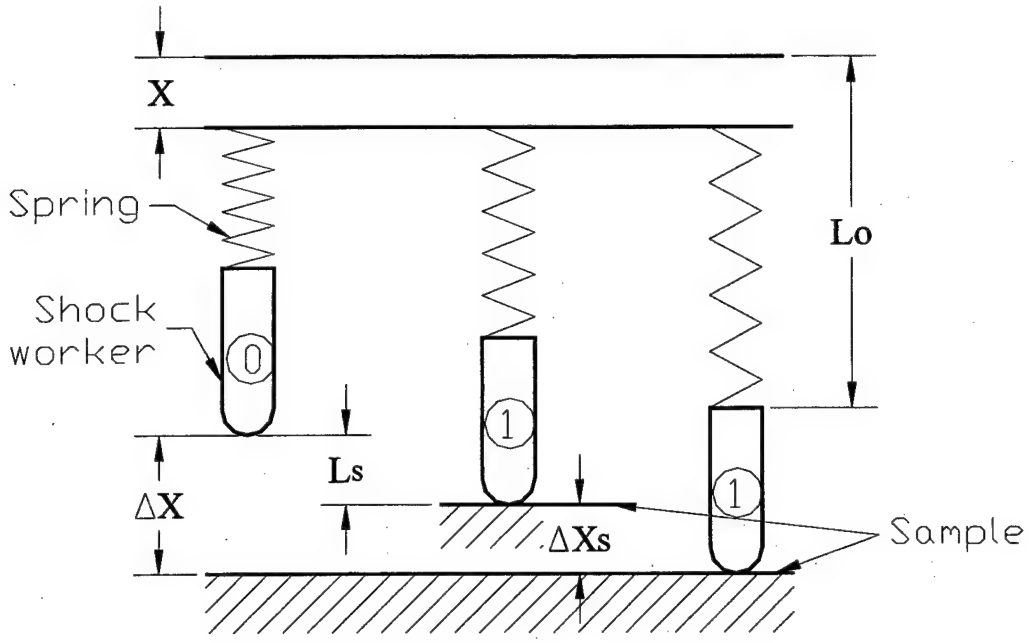

Figure 8.3. Change of the distance between shock worker and sample (internal range of spring deformation)

Lo - free length of spring
ΔX -motion of shock worker
X - deformation of spring for regulation
Ls -distance to sample
ΔXs -unused deformation of spring

Mark in:
$i = Ls / \Delta X$

$Ls = \Delta X\, i$
$\Delta Xs = \Delta X - \Delta X\, i$

From 4:

$V = \sqrt{C(Xo''-X1'')/m}$

Xo = deformation of spring before impact, $Xo = \Delta X + X$
X1 = deformation of spring after impact, $X1 = \Delta Xs+X = \Delta X-\Delta X\, i +X$

Mark in $A = \Delta X + X$, then

$$V=\sqrt{C[A''-(A-\Delta X\, i)'']}/m=\sqrt{C\,[2\,A\,\Delta X\, I-(\Delta X\, i)'']/m} \qquad (7)$$

Below is the speed of worker at the instant of impact when distance between worker and sample is changed.
C = 500 N/m, m = 0.1 kg, ΔX = 0.03 m, X = 0.01 m, A =0.04m

i	0	0.17	0.4	0.67	0.8	1
Ls	0	5	12	20	24	30
V	0	1.37	2.02	2.45	2.59	2.74

Note that speed varies significantly when the distance between worker and sample is changed (for the distance from 5 to 20 mm the difference in speed is 44%).

8.5. Modification with free flight of worker (monoblock).

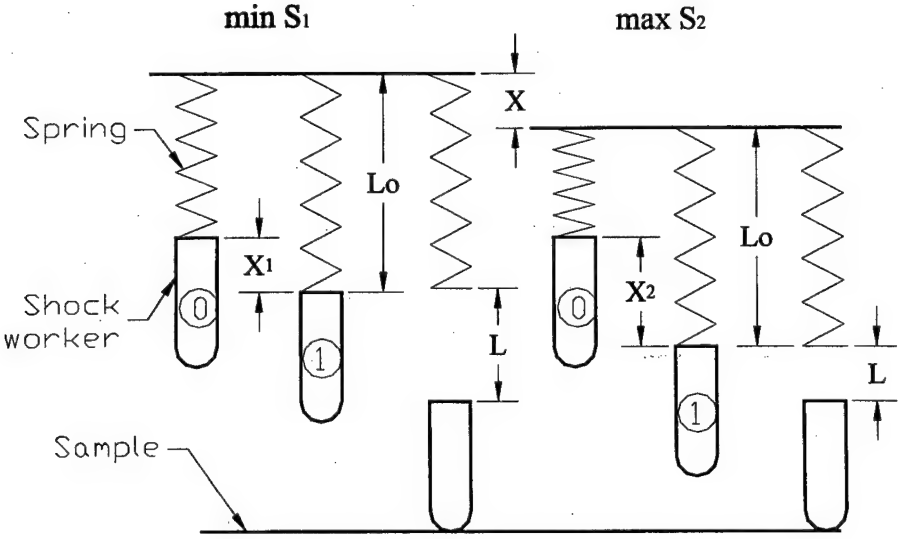

Figure 8.4. Free flight of worker

Lo = free length of spring
X = deformation of spring to regulate
X1 = deformation of spring to minimize S1
X2 = deformation of spring to maximize S2
L = distance of free flight

In free flight the speed of the worker varies insignificantly when the distance between the worker and sample is changed.

Friction force:

$F = m\ g\ f$, where:

m = mass of shock worker
g = acceleration of gravity
f = coefficient of friction

$F=m\ a$, where a = acceleration and $a = g\ f$

Speed of flight is defined by :
$V'' = 2a\ L$, where L = distance

$V'' = 2g\ f\ L$

After differentiation we have:

$2V\ \Delta V=2gf\ \Delta L$

and speed change is

$\Delta V = g\ f\ \Delta L / V$

If: $g = 9.8$ m/sec", $f = 0.1$, $V = 2.8$ m/sec, $\Delta L = 0.04$ m

$\Delta V = 0.014$ m/sec and
$\Delta V / V = 0.005 = 0.5\ \%$

In free flight speed and impulse are changed insignificantly

Shock worker time of flight is:

$t =2\ L / V$

If: $L = 0.04$m, $V = 2.8$m/sec, $t = 0.028$sec

Definitions of common parameters:

Min. impulse: min S1

Deformation of spring before shock

Xo=X1

Max. impulse : max S2

Deformation of spring before shock

$Xo = X\,2 = X + X1$

Formula (8.2) gives:

$V1 = X1\sqrt{C}/m$

$V2 = (X + X1)\sqrt{C}/m$

It is followed from formula (8.5):

$V2 = Ks\ V1$

$V2 = (X + X1)\sqrt{C} / m = Ks\ X1\sqrt{C}/m$, where

$X + X1 = Ks\ X1$

Deformation of spring to regulate impulse from min S1 to max S2 :

$X = X1\ (Ks-1)$ (8.8)

If: X1 = 15 mm
Ks = 1.8,
X = 12mm
X2 = 27mm

Ranges of regulations (Ks = 1.8)

4 springs are used for regulation

# spring	min S1	max S2
1	0.2	0.36
2	0.36	0.65
3	0.65	1.17
4	1.11	2

Stiffness is defined by formula (3):

$C = [S / Xo\ (K+1)]\ ''/m$

Mass of worker: m = 0.1kg

Force of spring:

$P1 = C\,X1;\ P2 = C\,X2$

Values of common parameters :

# Spring	S1,2 N sec	X1,2 mm	C N/m	P1,2 kg
1	0.2	15	615	0.5
	0.36	27	615	1.7
2	0.36	15	2000	3
	0.65	27	2000	5.4
3	0.65	15	6500	9.8
	1.17	27	6500	17.5
4	1.11	15	19000	28.4
	2	27	19000	51.1

From the drawing of monoblock in figure 8.5:

Spring directly reacts on the worker. Lift of worker can be done manually or by electromagnet. Worker is fixed in top by lock. When electromagnet goes down it releases lock and shock worker moves down to sample fast. The lock can be released manually. Electromagnet is turning on at once right after impact and lifts shock worker up.

8.6. Modification with free flight of worker with cock.

Device has 2 elements on one axis: worker and cock. Compressing spring directly reacts on the cock. Lift of cock is done manually or by electromagnet. The cock is fixed by lock on top.

When electromagnet goes down it releases lock and cock moves down fast to shock worker . The lock can be released manually.

Electromagnet is turning on at once after shock and lifts cock up. Shock worker goes up after impact and is held up by light spring. To avoid going down, shock worker has soft pad. This device has less axial dimension.

Design is given in Figure 8.6.

8.7. Modification with free flight of worker with rotating arm.

Device has 2 elements: worker and rotating arm . Extension spring directly reacts on the arm. Lift of arm is done manually or by electromagnet. The arm is fixed by lock on top. When electromagnet goes down it releases lock and arm moves down fast to shock worker . The lock can be released manually.

Electromagnet is turning on at once after shock and lifts arm up.

Shock worker goes up after impact and is held up by light spring. To avoid going down, shock worker has soft pad. This device has less axial dimension.

Design is given in Figure 8.7.

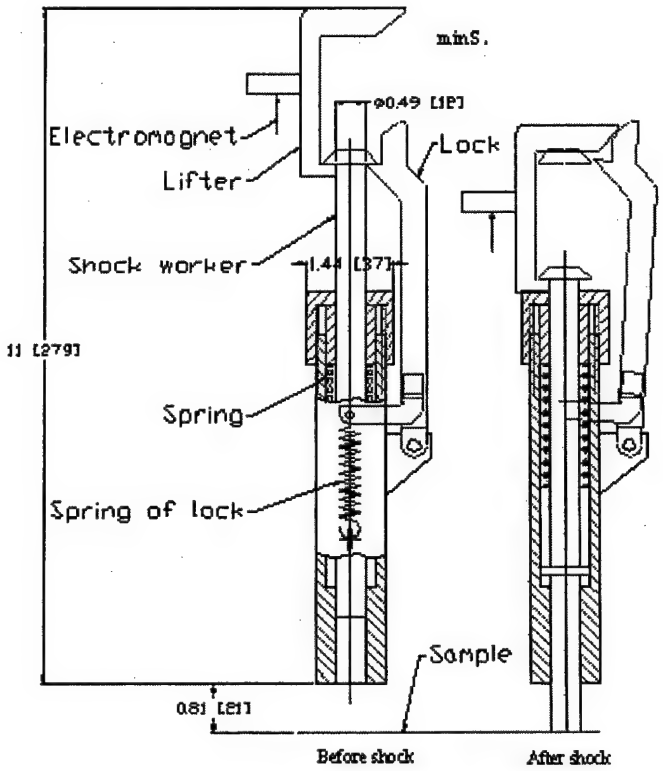

Figure 8.5. Monoblock

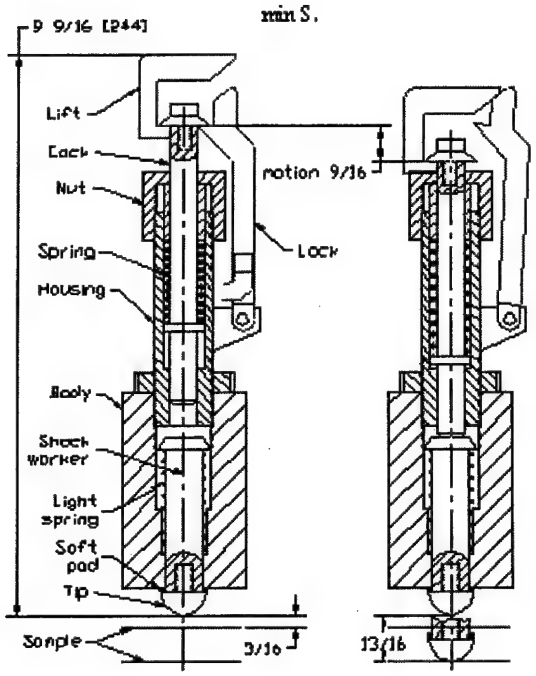

Figure 8.6. Modification : free flight of shock worker with cock

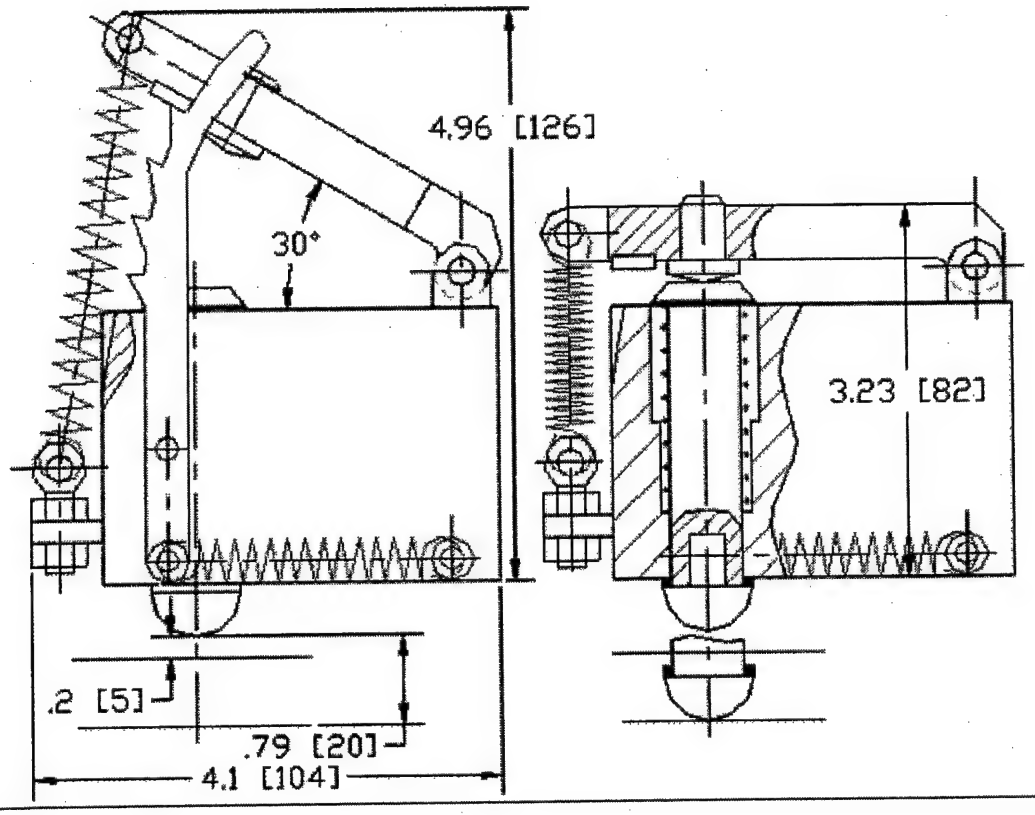

Figure 8.7. Modification: free flight of shock worker with rotating arm.

9. Conclusion.

The successful fulfillment of Phase I project allows to propose Phase II that will provide an advanced development of new technology and instrumentation for reliability assessment. As demonstrated in Phase I the concepts are feasible but need significant refinement and optimization to bring them to a commercially usable state. When brought to this state at the end of Phase II the suggested technique will find wide use for life time prediction and reliability assessment. It is our belief that nonlinear methods may be routinely used in applications as diverse as monitoring reactor containment wall damage; inspecting aircraft and spacecraft; observing fatigue damage in buildings, bridges, tunnels, gas and oil pipe lines; et cetera.

The information formulated during Phase II will allow transfer of technology to other Air Force and military entities and to the commercial market. In Phase III, Smart Material Design plans to market different kinds of NEWS devices started from small and lower power devices for single part testing up to large and powerful equipment infrastructural testing (including large parts of aircrafts, bridges, buildings, etc). Phase II proposal will establish a solid foundation for successful commercialization.

There are potentially a large number of applications of enormous economic and safety impact that will evolve from non-linear acoustic research proposed in this project. It is not understatement to suggest that within 10 years non-linear methods for the reliability assessment of aging structures may be routinely used in applications as diverse as inspecting aircraft and spacecraft, monitoring reactor containment wall damage, observing fatigue damage in buildings, bridges, tunnels, gas and oil pipe lines, etc.

The proposed nonlinear acoustic approach is much more sensitive to fatigue damage than the commonly used ultrasonic non-destructive techniques. The sensitivity of non-linear wave methods to the appearance and progression of material damage is orders of magnitude higher than that of conventional methods of non-destructive testing. Thus, measurement of this non-linear behavior may well be the most sensitive method for the study of fatigue damage initiation and cracking. That is why we are confident that national research laboratories and universities will be also interested in implementation of proposed non-linear acoustic technique for the fundamental research projects.

Preliminary investigations with non-linear acoustic approach for the damage assessment were conducted on request and with cooperation of: Boeing; Shell; British Airspace; Dynamic Response Systems, Incorporated; Ford; Los Alamos National Laboratory; Gas Research Institute; Purdue University Calumet; Electric Power Research Institute; University of Illinois at Chicago; and the National Institute of Standards and Technology. Contacts have been initiated with Wright-Patterson Air Force Base; American Petroleum Institute; LaserSonix Technologies, Incorporated; Iowa State University, and Texaco. The positive results of preliminary investigations are well above expectations and all above cited companies support the project and expressed commitments to the use of non-linear acoustic instrumentation when it will be available on the market. Dynamic

Response Systems, Inc. and LaserSonix Technologies, Incorporated, expressed their commitments to participate in manufacturing and marketing of the instrumentation.

10. References

1. Chudnovsky A., Kunin B., Gorelik M. Modeling of brittle fracture based on the concept of crack trajectory ensemble. Engineering Fracture Mechanics, 1997, 58 (5-6), 437-457.
2. Buck, O.,W.L. Morris, W.L. and Richardson, J.N. "Acoustic Harmonic Generation at Unbonded Interfaces and Fatigue Cracks", *Appl.Phys.Letters* , 1978, 33(5), 371-373
3. Richardson, M, "Harmonic Generation at an Unbonded Interface. I. Planar Interface Between Semi-infinite Elastic Media"' *Int. J. Eng. Sci.*, 1979, 17, 73-75.
4. Sutin, A.M., et.all (1985) ,USSR patent No.219786 - Method and Equipment for Quality Control of the Attachment of Thermal Protecting Tiles for the Soviet Orbital Shuttle "Buran".
5. Sutin A.M., Delclos C., and Lenclud M. Investigations of the second harmonic generation due to cracks in large carbon electrodes. Proc. 2-nd Symp. Acoustical and vibratory surveillance methods and diagnostic techniques Senlis (France), 10-12 October 1995, p.725-735.
6. Sutin A.M. and Donskoy D.M. Vibro-acoustic modulation nondestructive evaluation technique. Nondestructive Evaluation of Aging Aircraft, Airports and Aerospace Hardware II. Proc. of International Society for Optical Engineering, 1998, 3397, 226-237.
7. Mull M.A., Chudnovsky A., Moet A. A probabilistic approach to fracture toughness of composites. Philosophical Magazine A, 1987, 56 (3), 419-443.
8. Kunin B.A. A probabilistic model for predicting scatter in brittle fracture. Ph.D.Thesis, University of Illinois at Chicago, Chicago, IL, 1992.
9. Gorelik M., Novel application of the Monte-Carlo method in statistical fracture mechanics. Ph.D.Thesis, University of Illinois at Chicago, Chicago, IL, 1993.
10. Chudnovsky A., Gorelik M. Statistical fracture mechanics - basic concepts and numerical realization. In. Probabilities and Materials: Tasks, Model and Applications, ed. D.Breysse. Kluwer, Boston MA, 1994
11. Gorelik M., Calomino A.M., Chudnovsky A. Experimental and analytical studies of crack initiation and arrest in hot pressed silicon nitrides. In Fracture Mechanics, 25 th Volume, ASTM STP 1220, eds. F.Erdogan and R.F.Hartranft. ASTM, 1994
12. Issa M., Gorelik M., Hammad A. A new probabilistic model for the fracture toughness in concrete. Proceedings of the 6-th Specialty Conference on Probabilistic, Structural and Geotechnical Reliability, ed. K.Y.Lin, Denver, CO, 1992, p.467.
13. Chudnovsky A., Kunin B. Statistical fracture mechanics. In. Microscopic Simulation of Complex Hydrodynamic Phenomena, Vol.292, ed.M.Marschal and B.L.Holian. Plenum Press, NY, 1992.
14. Chudnovsky A., Kunin B. A probabilistic model of brittle crack formation. Journal of Applied Physics, 1987, 62, 4124-4129.

15. Johnson, P.A. The new wave in acoustic testing. Materials World, the Journal of the Institute of Materials, 1999, 7, 544-546.
16. Guyer R.A., Johnson P. Nonlinear mesoscopic elasticity: evidence for a new class of materials . Physics Today. 1999, **52.** 4. P.30-36.
17. Donskoy DM, Sutin AM. Vibro-acoustic modulation nondestructive evaluation technique. Journal of Intelligent Material System and Structures, 1998, **9**: (9), p.765-771
18. Zaitsev V.Yu., Sutin A.M., Belyaeva I.Yu., and Nazarov V.E., Nonliner interaction of acoustical wave due to cracks and its possible usage for cracks detection. Journal of Vibration and Control, 1995, v.1, no.3, p.335-344.
19. Sutin A.M., and Nazarov V.E. Nonlinear acoustic methods of crack diagnostics. Radiophysics & Quantum Electronics , 1995, v.38, n.3/4, 109-120.
20. Korotkov A.S., Slavinskii M.M., Sutin A.M. Variation of acoustic nonlinear parameters with the concentration of defects in steel. Acoustical Physics, 1994, v.40, no.1, p.84-87.
21. Korotkov A.S., and Sutin A.M. Modulation of ultrasound by vibrations in metal constructions with cracks. Acoustics Letters, 1994, v.18, No.4, p. 59-62.of Sciences, Physics of the Solid Earth, 1995, v.30, n.12, 1064-1071
22. P.A. Johnson, A. Sutin and K. E-A. Van Den Abeele, "Application of Nonlinear Wave Modulation Spectroscopy to Discern Material Damage.", Emerging Technologies in NDT, Van Hemelrijck, Anastassopoulos & Philippidis (eds), (Balkema, Rotterdam), p.159-166 (2000).
23. D.M. Donskoy, A.E. Ekimov and A.M. Sutin. "Detection and characterization of defects with vibro-acoustic modulation technique", Emerging Technologies in NDT, Van Hemelrijck, Anastassopoulos & Philippidis (eds), (Balkema, Rotterdam), p.153-157 (2000).
24. Sutin A.M. and Donskoy D.M. Nonlinear vibro-acoustic nondestructive testing technique. Nondestructive Characterization of Materials VIII , Ed.R.E.Green, 1998, Plenum Publishing Corporation, NY, p.133-138.
25. Sutin A.M. and Donskoy D.M. Principles and applications of nonlinear acoustic nondestructive testing. Proc. 16-th Intern. Congress on Acoustics and 135 Meeting Acoustical Society of America, 1998, p 1553-1554.
26. Sutin A.M. Nonlinear acoustic non-destructive testing of cracks. Nonlinear Acoustics in Perspective, 14th-Intern. Symp. on Nonlinear Acoustics Ed. R.J. Wei, Najing University Press, China, 1996, p. 328-333.
27. Baron D.T. Simulation of Crack Layer Growth and Reliability for Plastics. Ph.D. Thesis, The University of Illinois at Chicago, 1996.
28. Kazakov V.V., Sutin A.M., Didenkulov I.N., Ekimov A.E. Nonlinear Vibro-acoustic imaging. Ninth International Symposium on Nondescructive Characterization of Materials. Abstracts. Sydney, Australia, June 28- July 2., 1999.
29. Rudenko O and Chin An Vu, "Nonlinear Acoustic Properties of a Rough Surface Contact and Acousto-Diagnostics of a Roughness Height Distribution", *Acoustical Physics,* **40**(4), pp.593-596, 1994.
30. Nazarov V.E. and Sutin A.M., "Nonlinear elastic constants of solids with cracks", *J. Acoust. Soc. Am.*, **102** (6), pp. 3349-3354, 1997.

31. Rokhlin S.I. and Matikas T.E., "Ultrasonic Characterization of Surfaces and Interfaces", *Materials Research Society Bulletin*, **21**(10), pp.18-29, 1996.
32. Landau L.M.and Lifshits E.M., *Theory of Elasticity*, Pergamon, NY, 1986
33. Chudnovsky A., Crack Layer Theory, NASA CR-174634 (1984)
34. Kachanov M., Elastic Solids with Many Cracks And Related Problems, Advances in Appl. Mech., vol. 30 (1993); 259-445

Appendix

Support Letters

Wayne E. Woodmansee
Technical Fellow
Operations Technology

Boeing Commercial Airplane Group
P.O. Box 3707 MS 73-30
Seattle, WA 98124-2207

8 February 1999

Dr. Yulian Kin
Professor of Mechanical engineering
Purdue Calumet University
Hammond, IN 46323

Dear Professor Kin,

Professor Alexander Sutin has informed me that he will be working with your on a proposal to the NSF dealing with nonlinear Acoustic NDE. I have supplied adhesively bonded test articles to Prof. Sutin for evaluation with his non-linear acoustic techniques, and I am very interested in the results he has obtained. I believe the proposed work will use nonlinear acoustic techniques for the detection and investigation of fatigue damage. This is an area in which Boeing is very interested, particularly for the in-service detection of fatigue damage to aircraft components. Measurements of cumulative fatigue damage or predictions of the remaining lifetime of a component or structure would be very valuable to the aircraft industry.

I was impressed with the results Professor Sutin has obtained with his nonlinear techniques, and I look forward to the outcome of your application of nonlinear techniques to investigations of fatigue damage.

Sincerely yours,

Wayne Woodmansee
Sr. Technical Fellow
425-965-3188
wayne.e.woodmansee@boeing.com

Honeywell

Engines & Systems
Honeywell
111 S. 34th St, P.O. Box 52181
Phoenix, AZ 85072-2181

Dr. Yulian B.Kin
President
Smart Material Design, Inc.
3114 Belwood Lane,
Glenview, Illinois 60025
fax: 847 729 1813
e-mail: kin@calumet.purdue.edu

April 18, 2000

RE: **Quantitative Non-Destructive Evaluation and Reliability Assessment of the Aging Aircraft Structure Components**
Principal Investigator: Dr. Alexander Sutin

Dear Dr. Kin,

I am writing this letter in support of the further development of above citied project. The suggested technique appears to have significant potential for nondestructive inspection of aircraft engine parts. If proven successful, we expect that this technique may open a new opportunity in fatigue crack detection applicable to Honeywell components.

Where appropriate, Honeywell will provide aircraft engine parts and crack samples (on loan) for testing/demonstration, and where possible, we will also provide engineering support of the Nonlinear Acoustic technique in comparison assessments with existing techniques and demonstration on applicable engine hardware.

Sincerely yours

Tim Duffy
Manager, Advanced Materials Technologies
Materials &Process Engineering
Honeywell Engines and Systems

LosAlamos
Nonlinear Elasticity Project
Group EES-4
Earth and Environmental
Sciences Division
Los Alamos National Laboratory
Los Alamos, New Mexico 87545

los alamos national laboratory

Doctor Yulian B. Kin
Purdue University Calumet
Engineering Department
Hammond, IN 46323
Phone: 219 989 2684
e-mail: kin@calumet.purdue.edu

RE: DEVELOPMENT OF NONLINEAR ACOUSTIC INSTRUMENTATION

Dear Dr. Kin,

I am writing in support of the further development of the above-cited project. I understand that Smart Material Design, Inc., Purdue University, and University of Illinois are intending to extend their research in nondestructive characterization of materials and aging structures. Los Alamos National Laboratory is one of the few laboratories in the world working in this direction as well. We see countless applications to aging structures, quality control in assembly lines, damage inspection from earthquakes, etc., and see collaboration as a benefit to all.

We have had a long-term collaboration with Dr.Sutin. He has conducted experimental research on new methods for nonlinear acoustic Nondestructive Testing in Los Alamos and elsewhere, and has been the primary person in the world responsible for development of wave modulation methods. As you know, we have also been working with Dynamic

Resonance Systems, Inc., with the intention of ultimately marketing a device. May I suggest that Los Alamos, DRS, U. Illinois Chicago, Purdue and your group cooperate on this venture?

I would be happy to discuss details with you in person or by telephone.

Sincerely,

Paul Johnson
Leader
Nonlinear Elasticity Project
paj@lanl.gov

Equipment available at LANL

2 DRS Resonance Ultrasound Spectroscopy units
4 ENI high power, high frequency amplifiers
2 Crown audio amplifiers
Hafler audio amplifier
Krohn-Hite audio and ultrasonic power amp
5-10 wave source generators (HP, Analogic, Krohn-Hite)
Analogic 16 bit digital oscilloscopes
2 LeCroy 8 bit digital oscilloscopes
several Tektronix analog scopes
Tectronix waveform analyzer
HP Impedence Analyzer
Analogic arbitrary function generator
3 lock-in amplifiers
HP pulse generator
Bruel and Kjaer Accelerometers, pre-amps and amplifiers.
Three Macintosh G3's for experimental control with LabView control software.
2 complete Nonlinear Resonant Ultrasound Spectroscopy (NRUS) experimental set-ups
1 Nonlinear Wave Modulation experimental set-up.
Numerous piezoelectric ceramics, connectors, etc. for experiments.
Numerous samples of damaged and undamaged materials.
Vacuum system and supplies for experiment.
Numerous passive and active wave filters
signal processing software (MatLab and IGOR)
Access to an Origin 2000 (100 parallel processing machine) for modeling

UNITED STATES DEPARTMENT OF COMMERCE
National Institute of Standards and Technology
325 Broadway
Boulder, Colorado 80303-332B

Reply to the attention of:

January 21, 1999

Dr. Yulian Kin
Professor of Mechanical Engineering
Purdue Calumet University
Hammond, IN 46323

Dear Prof. Kin:

I am writing with regard to Dr. Alexander Sutin of the Stevens Institute of Technology and his participation in the NSF proposal entitled "Nonlinear Acoustic Instrumentation for the Detection and Investigation of Fatigue Damage."

In my position as a physicist at the National Institute of Standards & Technology, I am developing new measurement techniques in the field of nonlinear acoustics. My research is aimed primarily at using these techniques for the nondestructive characterization of materials. Dr. Sutin has made several notable contributions to this same field. For instance, he has demonstrated the use of the vibroacoustic method for detecting fatigue damage.

Although I have been aware of his work since I began working in nonlinear acoustics in 1995, I did not meet Dr. Sutin until 1997. Since then, we have maintained contact through personal correspondence and meetings at professional conferences. Based on my interactions with Dr. Sutin, he seems to be an excellent researcher, with strong skills in both the experimental and theoretical areas. He appears eager to meet and overcome technical challenges, and is very enthusiastic about realizing the full potential of nonlinear acoustics for materials characterization. Therefore, in this letter I wish to voice my support for his part in the proposal. I am confident that his performance will be excellent, and that he will work towards accomplishing the objectives to the very best of his ability.

Sincerely yours,

Donna C. Hurley, Ph.D.
Materials Reliability Division
National Institute of Standards & Technology

FORD
George Mozurkewich
Ford Research Laboratory
P. O. Box 2053, Mail Drop 3028
Dearborn, MI 48121-2053

Internet:gmozurke@ford.com
Tel: (313) 845-5038
Fax (313-594-6863

January 22, 1999

Dr. Yulian Kin
Professor of Mechanical Engineering
Purdue University Calumet
2200 169th Street
Hammond, IN 46323-2094

RE: **NSF Proposal entitled "NONLINEAR ACOUSTIC INSTRUMENTATION FOR THE DETECTION AND INVESTIGATION OF FATIGUE DAMAGE"**

Dear Dr. Kin,

I am writing in support of the proposal cited above. Because of my familiarity with Dr. Sutin's work, I arranged for Ford Motor Company to provide him and his colleagues with engine heads, composite plates, and other parts for preliminary experiments. The results of those tests were very impressive.

Consequently, I anticipate that this work will have significant scientific impact in the areas of metallurgy, materials science, and nondestructive evaluation (NDE). Furthermore, I expect that further development of these techniques will in due course become of great economic importance to industry.

As a scientist in the Ford Research Laboratory, I plan to maintain close contact with Dr. Sutlin during the progression and completion of this work, and I hope that his techniques will also prove useful in my own endeavors.

Sincerely,

George Mozurkewich
Senior Technical Specialist
(313) 845-5038

Office of the Chancellor

December 9, 1999

Dr. Spencer T. Wu
Program Manager
Air Force Office of Scientific Research
801 N. Randolph Street, Room 732
Arlington VA 22203-1977

Dear Dr. Wu:

At the request of Dr. Yulian Kin, Professor of Mechanical Engineering at Purdue University Calumet, I am informing you of the University's support of the following project: Quantitative Non-Destructive Evaluation and Reliability Assessment of Aging Aircraft Structure Components. Professor Kin is a respected member of our faculty and maintains a high level of research activity that has been beneficial to him, to the university, and particularly to our students.

My review of the proposal gives me confidence that control instrumentation based on a non-linear acoustical approach will be widely used for quality control in basic university research, in industrial applications, and in fatigue damage assessment in aging structures. Because the proposed project will involve the participation of Professor Kin and will result in specific and commercially available instrumentation, I am sure that both the instrumentation and the theory and practice behind it will be incorporated into our Department of Engineering's curriculum. We look forward to Professor Kin's active role in the design, manufacture, and marketing of the proposed non-linear acoustic instrumentation for reliable damage assessment.

Sincerely,

James Yackel

James Yackel
Chancellor

2200 169th St • Hammond IN 46323-2094 • (219) 989-2203 • Fax: (219) 989-2581

IOWA STATE UNIVERSITY
OF SCIENCE AND TECHNOLOGY

Geological Sciences
253 Science Hall I
Ames, Iowa 50011-3212
515 294-4477
FAX 515 294-6049

Professor Yulian B. Kin
Purdue University Calumet
Engineering Department
Hammond, IN 46323

Dear Dr. Kin:

I am writing in support of the project for the development of Novel Nonlinear Acoustic NDE Instrumentation.

I believe that nonlinear acoustic methods, that have very high sensitivity to crack and damage detection, will be soon widely used to detect and estimate damage in aging structures. The application of Nonlinear Acoustic NDE was so far restricted to laboratory conditions, because of the lack of commercially available instrumentation. The Purdue University Calumet and the University of Illinois intention to develop and market the Nonlinear Acoustics Apparatus is thus very topical and important.

I have many years of experience in both nonlinear acoustics and seismology and would be happy to participate in the creation of related instrumentation and methods. I can donate my time working on the theoretical aspects of materials science involving nonlinear material behavior, including developing crack models.

I am sure that both the instrumentation and the theory will be implemented in the Iowa State University curriculum and fundamental research conducted in our department.

Yours sincerely,

Dr. Igor Beresnev
(515) 294-7529
beresnev@iastate.edu

serSonix Technologies, Incorporated

4615 Post Oak Place, Suite 285
Houston, Texas 77027
phone: 713-355-5855, fax: 713-355-5888
http://www.lasersonix.com

Doctor Yulian Kin
Purdue University Calumet
Engineering Department
Hammond, Indiana 46323

December 23, 1999

Dear Dr. Kin,

I am writing this letter to express our company' intention to support development of the Instrumentation for Nonlinear Acoustic Nondestructive Testing. It is my understanding that Nonlinear Acoustic NDE Technique opens a new opportunity in crack and fatigue detection.

LaserSonix Technologies is a start-up company, recently founded with the aim to develop a new generation of imaging systems with sensitivity and resolution that supersedes specifications of existing imaging modalities. The laser optoacoustic imaging system (LOIS) has two principal types of applications: (1) medical diagnostic imaging and (2) non-destructive testing and evaluation of materials properties. The current goal of LaserSonix is to fabricate and market four systems for the Opto-Acoustic Tomography (OAT): (1) 3D opto-acoustic tomography for breast cancer detection, (2) 2D endoscopy system for characterization of lesions in the human GI tract from oral cavity to colon and rectum, (3) 2D imaging system for characterization of skin lesions, (4) System for characterization of properties of composite materials, ceramics and metals employed in the aircraft industry.

The sensitivity and resolution of Nonlinear Acoustic NDE systems can be dramatically improved with utilization of laser ultrasound generator and wide-band acoustic detectors. LaserSonix is a world leader in manufacturing wide-band acoustic transducers and also has significant experience in laser generation of ultrasound pulses. These two system components would be our contribution in a collaborative project with Smart Material Design, Inc.

We enthusiastically support the development of Nonlinear Acoustic Instrumentation suggested by Smart Material Design and intend to work together on NDE

technique based on laser excitation of probing ultrasonic signal and applications of laser shock as a source of low frequency vibration signal. As a result of our joint efforts, two NDE systems could be developed: (1) Nonlinear Acoustic Imaging System with laser excitation and, possibly, laser detection, and (2) Laser Ultrasound NDE System for quantitative material characterization at a given location. LaserSonix Technologies will assume participation in production and marketing of the developed devices.

The following infrastructure will be employed by LaserSonix Technologies for the joint project with Smart Material Design:

Compact nanosecond YAG-Nd laser
Laser heterodyne probe, Model SH-140
Front-surface opto-acoustic transducer, model FST-10
Tektronix oscilloscope, Model TDS-220 (5 GigaSamples/sec)
The cost of this equipment exceeds $50k.

We estimate an annual labor cost for this research and development as $150k per year.

Look forward for our cooperation.

Sincerely,

Alexander Oraevsky, Ph.D.
CTO

December 1, 1999

Dr. Yulian B. Kin
Smart Material Design, Inc.
3114 Belwood Lane
Glenview, Illinois 60025
fax: 847 729 1813
e-mail: kin@calumet.purdue.edu

RE: QUANTITATIVE NONDESTRUCTIVE EVALUATION AND RELIABILITY ASSESSMENT OF AGING AIRCRAFT COMPONENTS
Principal Investigator: Dr. Alexander Sutin

Dear Dr. Kin,

I am writing in support of the further development of the above-cited project, and commit DRS to fully support you in this project. I understand that Smart Material Design, Inc., Purdue University, and University of Illinois are intending to extend their research in nondestructive characterization of materials and aging structures. Dynamic Resonance Systems, Inc is committed to providing industry with the very best non-destructive testing equipment possible and sees collaboration as a benefit to all.

The personnel at DRS have considerable experience bringing new technologies to market. Bob Gose, the vice chairman of our board of directors, is very active in the day to day and long term operation of DRS and has 40 years experience in the development and utilization of advanced technology. I have been with DRS since the company was founded and have been using Resonant Ultrasound Spectroscopy for 8 years. Data for my PhD research at Colorado State University was taken exclusively with RUS. Since completing my PhD, I have played an active role in developing RUS as a non-destructive testing technology. DRS has been working with Paul Johnson at Los Alamos National Lab to develop non-linear RUS as a viable industrial tool. We would very much like to have DRS included in the development of your product.

I would be happy to discuss details with you in person or by telephone.

Sincerely,

Frank Willis

Frank Willis, PhD
Director of Technologies
DRS
Fwillis@ndtest.com

Equipment / Personnel available at DRS

Large base of installed DRS Resonance Ultrasound Spectroscopy units for both testing and research applications
Microprocessor development kits
Professional PCB layout software
Visual C++ programming
Microprocessor programming and debugging hardware / software
Established marketing organization
Established relationship with vendors / machinists
Extensive inventory of good / defective manufactured components
15 Pentium / Pentium II computers
Dedicated internet access / Web / Email servers
Oscilloscope
Function generator
Multimeters
Digital oscilloscope
Digital scale
Microscope
Surface mount soldering / desoldering equipment
Complete prototyping capabilities
Some machining capabilities
MIG welder including aluminum and stainless steel capabilities
Large color printer / plotter
Color scanner
Digital camera

Staff personnel include:
Scientists, engineers, electronics technicians and marketing / adminstrative.